FUNCTIONAL AND MOLECULAR ANALYSIS OF C2 DOMAINS OF SYNAPTOTAGMIN

A THESIS PRESENTED

BY

SUNITHA. S.S.

TO

THE DIVISION OF MOLECULAR MEDICINE

IN PARTIAL FULFILMENT OF THE REQUIREMENTS

FOR THE DEGREE OF

DOCTOR OF PHILOSOPHY

SREE CHITRA TIRUNAL INSTITUTE FOR
MEDICAL SCIENCES AND TECHNOLOGY
THIRUVANANTHAPURAM – 695 011

DECLARATION

I, **Sunitha. S. S.**, hereby declare that I had personally carried out the work depicted in the thesis entitled **"Functional and Molecular Analysis of C2 Domains of Synaptotagmin"** under the direct supervision of **Dr. Anoopkumar Thekkuveettil**, Scientist E, Division of Molecular Medicine, Biomedical Technology Wing, Sree Chitra Tirunal Institute for Medical Sciences and Technology, Thiruvananthapuram, Kerala, India, except where external help sought and acknowledged.

Sunitha

Sunitha. S. S.

Dr. Anoopkumar Thekkuveetil
Scientist E

Division of Molecular Medicine
Biomedical Technology Wing
Sree Chitra Tirunal Institute for Medical Sciences and Technology
Poojapura, Thiruvananthapuram

CERITIFICATE

This is to certify that Ms. Sunitha. S.S., in the Division of Molecular Medicine of this Institute, has fulfilled the requirements of the regulations relating to the nature and prescribed period of research for the PhD degree of the Sree Chitra Tirunal Institute for Medical Sciences and Technology, Thiruvananthapuram. The work relating to her thesis entitled **"FUNCTIONAL AND MOLECULAR ANALYSIS OF C2 DOMAINS OF SYNAPTOTAGMIN"** was carried out under my direct supervision.

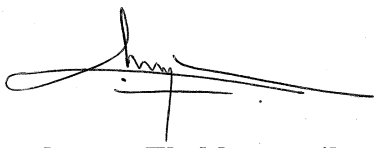

Dr. Anoopkumar Thekkuveettil

The thesis

Entitled

FUNCTIONAL AND MOLECULAR ANALYSIS OF C2 DOMAINS OF SYNAPTOTAGMIN

Submitted by

SUNITHA. S.S.

For

Doctor of Philosophy

of

Sree Chitra Tirunal Institute
for
Medical Sciences and Technology
Thiruvananthapuram

Evaluated and approved

By

Name of the guide

Name of thesis examiners

6/2/09

DR. T. R. RAJU

To my parents.....

CONTENTS

Page

Page

ACKNOWLEDGEMENTS

First of all, I am most grateful to my guide Dr. Anoopkumar Thekkuveettil for supporting me on my thesis and for his constant encouragements over the last years. I thank him for trusting me and giving me the freedom and responsibility in my work. I greatly appreciate his efforts in resolving the scientific problems that I faced. I owe a debt of gratitude for the long interesting scientific discussions we had during these years.

My Doctoral Advisory Committee members gave me quite a lot of directions during these years and I thank Prof. K. Radhakrishnan, Prof. M. D. Nair, Dr. Mira Mohanty and Dr. R.V. Omkumar for their valuable suggestions.

I express my sincere gratitude to The Director, SCTIMST, The Head, BMT Wing and The Registrar, SCTIMST for providing the necessary facilities throughout my PhD work.

I am grateful to Council of Scientific and Industrial Research (CSIR) for providing the fellowship during the PhD work and Societe de Biologie Cellulaire de France (SBCF) for giving the travel grant to attend the Synapse 2006 conference in Paris, France.

I thank Dr. Salini Bhasker and Mr. Jose Jacob for the guidance during initial stages of my research. It is with great pleasure I acknowledge Siddharth Banerjee for his sincere and valuable suggestions and good company throughout this period. I am grateful to Sheeja Liza Easo and Vrinda S. Kumar for their friendship.

I am really lucky to have my long-term close friend, Kathleen Zylbersztejn at Paris. We exchanged different opinions of life, work and future through mails. She gave me the constant encouragement and love during my PhD work as well as during the thesis preparation.

Finally, I want to thank my parents and brother for their loving support and endless care. I warmly thank them for letting me make my own choices and being there whenever I needed. Without them, none of this would have been possible.

Sunitha. S. S.

LIST OF FIGURES

LIST OF TABLES

ABBREVIATIONS

AP-2	adaptor protein-2
ATP	adenosine tri phosphate
bp	base pair
BSA	bovine serum albumin
CaMKII	calmodulin kinase II
CBB	coomassie brilliant blue
CDEI	centromere DNA element I
cyclic AMP	cyclic adenosine mono phosphate
DMSO	dimethyl sulphoxide
DNase	deoxyribonuclease
dNTP	dinucleotide phosphate
DTT	dithiothreitol
EDTA	ethylenediaminetetraacetic acid
FITC	fluorescein isothiocyanate
GABA	γ-amino butyric acid
GFP	green fluorescent protein
Gly	glycine
GST	glutathione s-transferase
H&E staining	harrin haematoxylin staining
HRP	horseradish peroxidase
Hsp 70	heat shock protein 70
IgG	immunoglobulin
IPTG	isopropyl β-D-1-thiogalactopyranoside
$K_2Cr_2O_7$	potassium dichromate
K_2HPO_4	dipotassium hydrogen phosphate
$K_3Fe(CN)_6H_2O$	potassium ferricyanide

kb	kilo base
kDa	kilo Dalton
KIFs	kinesin superfamily proteins
LB broth	Luria Bertani broth
LTD	long term depression
LTP	long term potentiation
Lys	lysine
Met	methionine
MLCK	myosin light chain kinase
MOPS	morpholinopropanesulfonic acid
MW	molecular weight
Na_2HPO_4	sodium phosphate dibasic
$Na_2S_2O_3.\ H_2O$	sodium thiosulphate
NaH_2PO_4	sodium phosphate monobasic
NSF	N-ethylmaleimide-sensitive fusion protein
OD	optical density
OsO_4	osmium tetroxide
PBS	phosphate buffered saline
PL	phospholipids
PMSF	phenyl methyl sulphonyl fluoride
qRT-PCR	quantitative reverse transcriptase polymerase chain reaction
RNase	ribonuclease
RNP	ribonucleoprotein
RP	recovery period
rpm	rotations per minute
s.e.m	standard error of the mean
SDS-PAGE	sodium dodecyl sulphate polyacrylamide gel electrophoresis
SE	*status epilepticus*
SNAP	soluble N-ethylmaleimide sensitive factor attachment protein

SNAP-25	synaptosomal associated protein of 25 kDa
SNAREs	soluble N-ethylmaleimide sensitive factor attachment receptors
SP	seizure period
SPF	soluble protein fraction
STAT6	signal transducer and activator of transcription 6
SV	synaptic vesicle
Syt	synaptotagmin
TE buffer	tris-EDTA buffer
TEM	transmission electron microscopy
TLE	temporal lobe epilepsy
TM	transmembrane
tPA	tissue plasminogen activator
UD plasmid	undigested plasmid
UTR	untranslated region
VAMP	vesicle associated membrane protein
VDCC	voltage-dependent calcium channels

SYNOPSIS

Communication between neurons is mediated through regulated release of neurotransmitters and is essential in all functions of the nervous system, from sensory perception to learning and memory. Synaptic vesicles govern the storage, retrieval and Ca^{2+}- dependent exocytosis of neurotransmitters. A large inventory of proteins present both at the presynaptic membrane and synaptic vesicles control these functions. The major focus of neurobiology in recent years is to understand the molecular and functional role of these proteins in synaptic communication. Alterations in neurotransmitter release could lead to synaptic plasticity as well as diseases like seizure, and it is critical to understand how the synaptic proteins help in facilitating or preventing these changes.

Chapter 1 provides an introduction to the topic being discussed in the thesis. Synaptotagmin I (Syt I) is one of the highly conserved presynaptic membrane proteins regulating Ca^{2+}-dependent neurotransmitter release in neurons. Even though, Syt I in neurons is critical for its proper physiological function, it is not very well understood how the protein level is regulated. Both mRNA and protein of Syt I reach a constant level during the early stages of development independent of synaptic vesicle formation. One of the assumptions is that the Syt I protein synthesis happens at constant rate, often in excess, in developing neurons, which promotes the increase in synaptic vesicle formation and synaptic growth. However, it is not clear whether this hypothesis is correct or an alternate molecular mechanism is involved in its controlled expression. This work attempts to understand the molecular pathways involved in the regulation of Syt I level in

neurons and bring evidences that the Syt I protein level can be attenuated by autoregulation through its sequence-specific interaction with the 3' untranslated region (3'UTR) of its own mRNA.

Chapter 2 gives a broad description of the literature related to the study. Synaptic vesicles, which store neurotransmitters, are budded off from early endosomes. The classical model of synaptic vesicle cycle contains different steps: docking and priming of synaptic vesicles on the presynaptic membrane, exocytosis/fusion resulting in neurotransmitter release and endocytosis, the clathrin-mediated retrieval of synaptic vesicles. Apart from this, alternate pathways like kiss-and-stay and kiss-and-run also exist. The neurotransmitter release is triggered when Ca^{2+} influx into a nerve induces the fusion of synaptic vesicles with the active zone of presynaptic plasma membrane. Syt I is identified as the Ca^{2+} sensor in the synaptic vesicle cycle. In addition, Syt I plays critical role in docking, fusion and recycling of synaptic vesicle. Syt I is continuously synthesized at the cell body and transported directly from the trans-Golgi network to specialized axonal endosomes from which synaptic vesicles originate. Rapid anterograde axonal transport of synaptic proteins allows the newly synthesized synaptic vesicle proteins to reach their target within an hour after synthesis. However, the translational regulation of Syt I protein and the molecular interactions associated with it are poorly understood.

Chapter 3 explains the experimental design of the study including the materials and methods used. Studies using prolonged seizure models have shown significant variations in synaptic plasticity, including changes in the neurotransmitter release

pathway and in the expression levels of synaptic proteins. So seizure was used as a model in this study to estimate the level Syt I protein during hyperactivation of neurons. Pilocarpine was injected in rat to induce seizure and the rats were sacrificed at 4 hour (seizure period-SP) and 24 hour (recovery period-RP) after pilocarpine injection. The expression level of Syt I protein in hippocampus of control, SP and RP rats were checked using western blotting and immunohistochemistry. The synaptic vesicle density during seizure was analyzed with Transmission Electron Microscopy (TEM).

The Syt I RNA level was verified using Northern hybridization, quantitative reverse transcriptase PCR (qRT-PCR) and probe based Microarray analysis. The genes corresponding to Syt I 3' UTR of 360 bp, Syt I full protein coding region, region corresponding to both C2 domains – C2A and C2B and each domain alone were amplified by polymerase chain reaction (PCR). The amplified products were cloned and confirmed by restriction digestion and sequencing reactions. The Syt I 3' UTR clone was used for *in vitro* synthesis of RNA using T7 RNA polymerase. Soluble protein fractions of rat and human brain were prepared by ultracentrifugation. The Syt I, Syt I C2, Syt I C2A and Syt I C2B genes sub-cloned in expression vector and GST fusion recombinant proteins were synthesized. The proteins were purified using MicroSpin affinity columns and confirmed by SDS-PAGE. RNA-protein interactions were further established using electrophoretic mobility shift assay, UV-crosslinking assay, competitive assay and filter binding assay. The translation regulation of Syt I protein was checked by TNT Quick coupled transcription/translation system.

Chapter 4 includes the results obtained from the various experimental aspects of this study, described under separate headings with discussions on each aspect. Pilocarpine induced clinical features analogous to temporal lobe epilepsy in rat. The western blotting result showed that Syt I protein level was downregulated during seizure period and retained back during recovery period. The immunohistochemistry also revealed a significant downregulation of Syt I in the hippocampal CA3 pyramidal region. The TEM analysis indicated that the drastic reduction of Syt I protein is not related with synaptic vesicle density. The constant level of Syt I RNA was confirmed by Northern hybridization, qRT-PCR and Microarray analysis.

The sequence analysis of Syt I mRNA revealed two probable protein binding domains in the 3' UTR of the gene, namely GU repeat and a heptamer sequence "GUCAAUG". This region (Syt I 3'UTR) was PCR amplified, cloned, and used in the study to construct the RNA probe to verify the RNA-protein interactions. The probe showed binding affinity for human and rat soluble protein fraction in the electrophoretic mobility shift assay. The molecular weight of proteins binding with the Syt I 3' UTR RNA was checked by UV-crosslinking assay. A selective set of human brain proteins having molecular weight ranging from 58 and 65 kDa in rat and 31 to 86 kD were binding with the Syt I 3' UTR RNA probe. The Syt I protein, having a molecular weight of 65 kDa, was a plausible candidate. This was confirmed using GST-Syt I recombinant protein, which detected the Syt I 3' UTR RNA with high specificity. Experiments using various RNA constructs proved that the binding affinity was significantly lower in the absence of heptamer or GU repeat sequences underscoring the essential role of both

sequences in this molecular interaction. Among the recombinant protein constructs the ones containing the C2A domain namely, GST-Syt I, GST-C2 and GST-C2A induced RNP complex formation, but GST-C2B did not show significant RNA binding. These results suggested that in Syt I protein, the C2A domain is essential and enough for the RNA recognition. The filter binding assay, however showed difference in kinetics for GST-C2 and GST-C2A protein which could be because of structural variations among the fusion proteins and/or a cooperative role of C2A and C2B in RNA binding. In the *in vitro* translation experiments, the translation efficiency of the 3' UTR-containing clone was reduced ~50% compared to the construct lacking the 3' UTR. This brings the strong evidence that there is a dynamic interaction between Syt I mRNA and protein in the translation machinery and autoregulates the level of Syt I in the cell.

Chapter 5 gives a summary of the whole study and provides the conclusions drawn out. The results of the study indicate that during seizure there is a rapid reduction in Syt I protein level in hippocampus without affecting its gene expression level. Syt I can autoregulate its protein expression effectively by the interaction of 3' UTR RNA with the C2A domain. It is possible that this highly effective regulation of Syt I translation in the brain during seizure could lead to the control of the neurotransmitter release and thus to an extent prevent excitotoxicity. This study assumes significance because it provides novel insights into the translational regulation of Syt I protein in normal as well as hyperacitve neurons.

Chapter 1

INTRODUCTION

1.1. SYNAPTIC TRANSMISSION

The neuronal communication is mediated through the regulated Ca^{2+}-dependent exocytosis of synaptic vesicles at the presynaptic active zone of nerve terminals. Synaptic vesicles, the highly specialized organelles to store and secrete the neurotransmitters, undergo a trafficking cycle to facilitate the continuous synaptic transmission. Recent studies shed light on the better understanding of the different steps involved in regulated neurotransmission. The neurotransmitter release requires the functional assembly of proteins at the synaptic vesicles and presynaptic membrane. The controlled expression of synaptic proteins determines nervous system development as well in the functions of neurons including sensory perception, learning and memory.

1.2. SYNAPTIC PROTEINS

The synaptic functions are governed by the variety of synaptic proteins, including Synaptotagmin (Syt). The gene manipulation studies of synaptic proteins in various model organisms gave insight into the function of each molecule in synaptic transmission (Broadie and Richmond, 2002). The different functions of synaptic

proteins include maintaining the structure and organization of synapse, exocytosis and endocytosis (Brachya, *et al.*, 2006). The organized actions of almost 50-100 synaptic proteins required for the functioning of neurotransmitter release pathway (Augustine, *et al.*, 1999). The variations in their expression pattern can modify the neuronal functions. Moreover, the alterations in the interactions of synaptic proteins involved in neurotransmitter release can modify the synaptic transmission contributing to the conditions like seizure.

1.2.1. Synaptotagmin I: a Ca^{2+} sensor that triggers neurotransmitter release

Synaptotagmin I (Syt I), a presynaptic vesicular protein functions as a putative Ca^{2+} sensor and plays essential role in the Ca^{2+}-dependent neurotransmitter release pathway. It allows the formation of a ternary complex of soluble N-ethylmaleimide sensitive factor attachment receptors (SNAREs), composed of synaptobrevin/VAMP-2, syntaxin and SNAP-25 at the active zone (Lin and Scheller, 2000; Sudhof, 2004). Syt I is one of the members of the large family of C2 domain proteins as it contains two internal repeats that show high similarity to the C2 domain of protein kinase C **(Figure 1A)** (Perin, *et al.*, 1991a). In addition to the highly conserved C2 domains, Syt I contains a single transmembrane domain at the N-terminus and a short conserved C-terminal sequence. The C2 domains, namely C2A and C2B, which upon binding Ca^{2+}, undergo structural changes that enhance its SNARE binding affinity (Davletov and Sudhof, 1994) and allow vesicles to fuse with the plasma membrane (Tang, *et al.*, 2006). The functional domains in the Syt I protein have distinct interaction sites with many binding partners **(Figure 1A and B)**. The biochemical

interaction of Syt I with other molecules has been extensively studied while, how th protein level is maintained in neurons is still poorly understood.

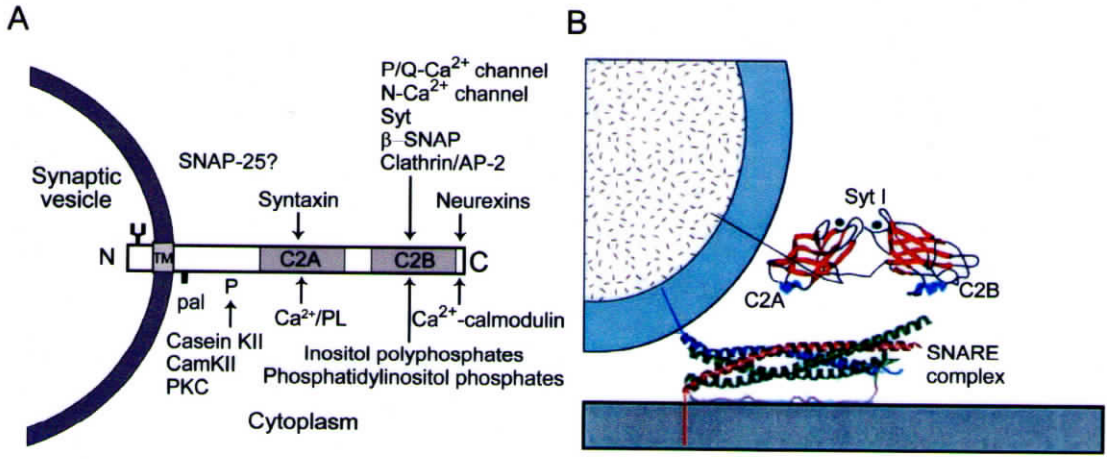

Figure 1: Syt I protein domains have different binding partners. (A) Schematic representation of Syt I domain structure with the interaction sites and major binding partners. C- carboxy terminal, N- amino terminal, TM- transmembrane region, P- phosphorylation site, pal- palmitoylation site and PL- phospholipid. (Adapted from Marqueze, *et al.*, 2000). (B) Schematic representation of the crystal structure of Syt I protein with SNARE complex. (Adapted from Adolfsen and Littleton, 2001).

1.2.2. Functional analysis of Syt I

The disruption of Syt I gene leads to intense deficiency in neuronal transmitter release, emphasizing the crucial role played by Syt I protein in synaptic vesicle exocytosis. The micro-injection of anti Syt I antibodies and protein regions into the living cells resulted in the blockage of vesicle fusion and endocytosis (Bommert, *et al.*, 1993; Fukuda, *et al.*, 1995). Similarly, the gene disruption studies in *C. elegans*, *Drosophila* and mice revealed severe defects in the evoked neurotransmitter release **(Table 1)**. These genetic studies bring evidence that level of Syt I protein has to be maintained very stable in neurons for the proper synaptic functions.

Table 1: Gene manipulation studies of Syt I

Organism	Phenotype	Reference
C. elegans	Defective muscle movement, reduced synaptic vesicle number at synapses	Nonet, *et al.*, 1993 Jorgensen, *et al.*, 1995
Drosophila	Lethal, decrease in neurotransmitter release, increase in spontaneous vesicle fusion	Littleton, *et al.*, 1993 Littleton, *et al.*, 1994 DiAntonio and Schwarz, 1994
Mice	Disruption of fast synchronous fusion	Geppert, *et al.*, 1994

1.2.3. Syt I protein regulation

The expression levels of Syt I mRNA and protein attain a constant level during the early stages of development even before the formation of synaptic vesicles (Daly and Ziff, 1997). It is assumed that in developing neurons the Syt I protein synthesis happens at an excess rate, which enhances the synaptic vesicle formation (Daly and Ziff, 1997) and synaptic growth (Feany and Buckley, 1993). However, the molecular mechanisms underlying the constant expression and regulation of Syt I protein in neurons is not well elucidated.

In addition to the abundant and well studied Syt I protein, the Syt family constitute a large number of isoforms **(Figure 2)**. The expression levels of different Syt isoforms with varying Ca^{2+} sensitivities determine the dynamics of synaptic vesicle fusion.

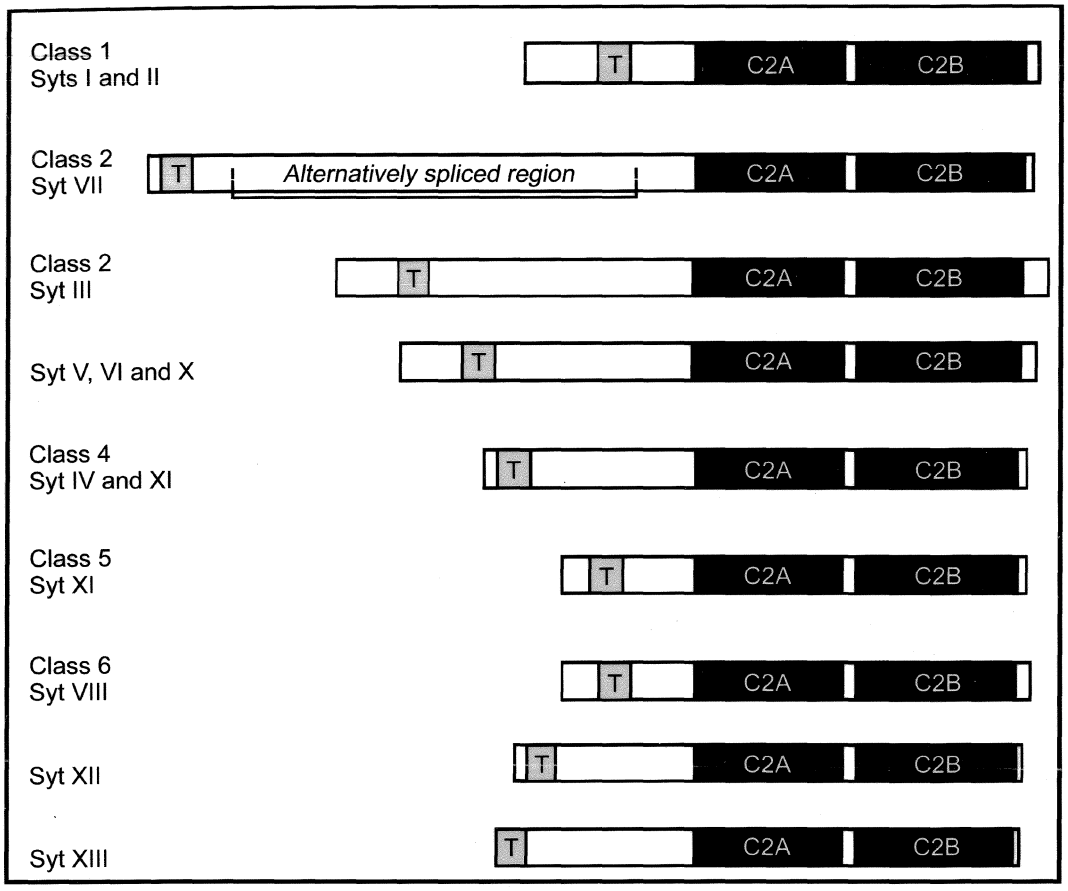

Figure 2: Domain structure of Syt isoforms I-XIII. The closely related isoforms are grouped together. All the isoforms contain the well conserved cytoplasmic domain while the N-terminal region is varied. (Modified from Sudhof, 2002).

Chronic neuronal depolarization results in upregulation of an unusual Syt isoform, Syt IV (Vician, *et al.*, 1995), having low affinity for membrane binding in response to Ca^{2+} influx (Ullrich, *et al.*, 1994). Neurons over expressing Syt IV showed reduction in neurotransmitter release, suggesting a regulation of the excitation-secretion coupling through hetero-dimerization of this isoform with Syt I (Littleton, *et al.*, 1999). However, there are reports suggesting that in *in vivo* Syt IV is localized at the post synaptic terminal and the possibility of hetero-dimerization is implausible

(Adolfsen, *et al.*, 2004). This reopens the question on the regulation of Syt I level at the presynaptic terminal in an activity dependent manner. One possibility could be the translational modification of Syt I. For example, in brain p40 fragment of Syt I corresponding to the extravesicular portion of p65 Syt I has been detected during cellular stress (LaVallee, *et al.*, 1998). This soluble Syt I protein fragment is translated by alternate AUG transcription initiation site at Met113 (Bagala, *et al.*, 2003). Besides, the translation regulation of mRNA usually mediated through the different mechanisms, by the formation of secondary structures like stable stem loops (Myers, *et al.*, 2004) or by the interactions of proteins with the UTRs (Samson, 1998). Understanding the regulation of Syt I translation and transcript distribution in neurons could provide insights into synaptic function.

The main objectives of this study were to find out how Syt I protein expression is maintained at a constant level in neurons, whether Syt I can be regulated in an activity-dependent manner during various neuronal functions and if so what could be molecular mechanisms underlying in the regulatory pathway. To answer these questions better, a systematic study was performed using various molecular biology and biochemical techniques. Firstly, we checked for the activity-dependent regulation of Syt I protein using seizure as a model and found that during seizure there is a drastic reduction in Syt I protein level without altering its mRNA level. This suggests that in neurons the dynamics of synaptic vesicle protein expression can be selectively tuned and linked to the functional neuronal output. On analysis of the human Syt I mRNA sequence two possible protein-binding domains within its 3' UTR were identified: a GU_{15} repeat domain (Gao, *et al.*, 2004) and a GUCAAUG

'heptamer' sequence analogous to the known protein binding CDEI sequence [A/G]TCAC[A/G]TG (Blangy, *et al.*, 1991).

We hypothesized that translation of Syt I can be constantly regulated by RNA-protein interaction to maintain Syt I level at the synapse in an activity dependent manner. We verified whether 3' UTR can recognize proteins and surprisingly found that the Syt I protein can interact with its own mRNA. The *in vitro* translation of Syt I coding region with/without 3' UTR in rabbit reticulocyte lysate revealed that the presence of 3' UTR can effectively downregulate protein expression. The results in this thesis bring evidence that the Syt I level in neurons undergoes autoregulation and this could effectively modulate the neurotransmitter release and synaptic plasticity.

Chapter 2

REVIEW OF LITERATURE

Neurons are the primary component in the nervous system that process and transmit information. The structure of neurons has three distinct morphological parts, dendrites for receiving electrical signals from other neurons, soma for information integration and axon for passing the information to other neurons; dendrites and axons help to form extensive neuronal circuit. Neurons communicate with each other at synapse, the specialized zones of functional contact site between the axon terminal (presynaptic) and dendrites (postsynaptic).

2.1. SYNAPSE – GENERAL STRUCTURE AND FUNCTION

The synapses can generally classify into two types: electrical or chemical synapses, based on the transmission arising at the neuronal terminal (Eccles, 1982). In electrical synapse the transmission occur through direct electrical pulses whereas in chemical synapses the transmission is *via* chemical intermediates called neurotransmitters. The simplest method for one neuron to communicate with another is through electrical synapses by direct electrical interaction, in which the extracellularly generated current formed from the action potential in one neuron transfers to the neighboring neurons. However, most of the neuronal communications depend on chemical transmission. A typical chemical synapse consists of three parts;

presynaptic terminal containing numerous synaptic vesicles filled with neurotransmitters, postsynaptic terminal bearing receptors to bind with neurotransmitters and synaptic cleft separating them (Zhen and Jin, 2004). The chemical transmission allows a single action potential in a presynaptic terminal which can produce a large postsynaptic potential, achieved by the release of thousands to hundreds of thousands of neurotransmitter molecules from presynaptic terminal to the synaptic cleft and bind to postsynaptic receptor molecules within a very short time. This fast response to an action potential made the synapse as a model to study the neuronal function under various conditions like long term potentiation (LTP), seizure, long term depression (LTD) etc (Bliss and Collingridge, 1993). The synapse stabilization and synaptic strength modification allow developmental and activity-dependent plasticity in the brain.

The synapses can be easily identified through electron microscopy by the morphological features; a group of small vesicles docked to a membrane (active zone) opposite to a thickened scaffold (postsynaptic density) **(Figure 3).** Based on the synaptic functions, the chemical synapses can be of two different groups, excitatory and inhibitory. The neurotransmitters in the excitatory neurons are mainly glutamate while the inhibitory neurons contain γ-amino butyric acid (GABA) as the neurotransmitter (Deutch and Roth, 1999). In resting state, a neuron keeps a potential difference of a range -60 to -90 mV across the membrane. Depolarization of the membrane potential above the threshold causes Na^+ ions to influx leading to action potential which propagate along the axon to the presynaptic terminals. This action potential cause the voltage-dependent calcium channels (VDCC) present on the

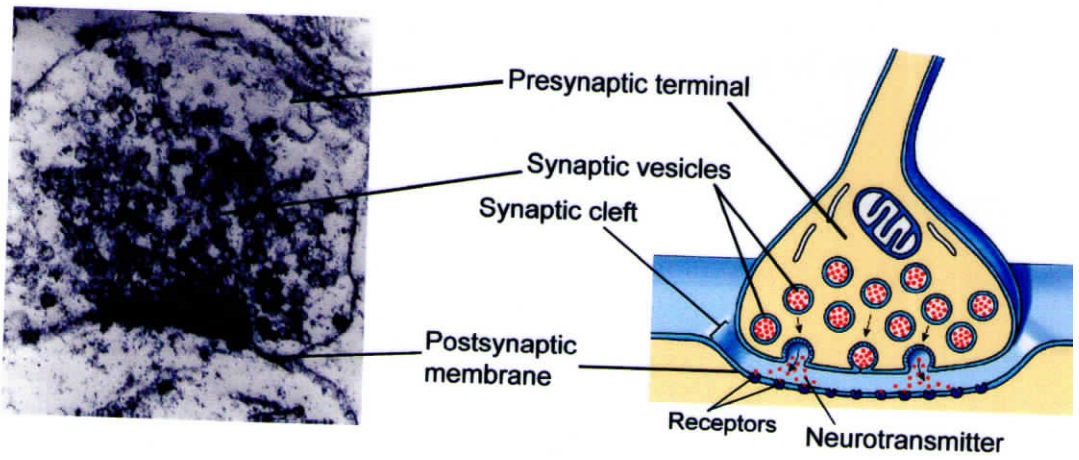

Figure 3: Typical structure of a synapse. Electron micrograph of a neuronal synapse (left) and a schematic illustration (right).

presynaptic membrane to open resulting in the influx of external Ca^{2+} ions (in millimolar range). The brief rise of Ca^{2+} concentration activates the fusion of synaptic vesicles to the presynaptic membrane releasing the neurotransmitters to the synaptic cleft (Katz, 1969). The neurotransmitters diffuse and bind to the ionotropic receptors on the postsynaptic membrane which in turn activate the opening of ligand-gated ion channels on postsynaptic neurons for the influx of ions. Thus the synaptic transmission propagates through the neurons.

2.2. SYNAPTIC VESICLE CYCLE

At the active zone of the nerve terminal the synaptic vesicles fuse with the presynaptic membrane mediating neurotransmitter release, a process called exocytosis. The synaptic vesicles at a synaptic terminal are limited to 100-200 in number, in order to achieve rapid, regulated and repeated rounds of neurotransmitter release (Granseth, *et al.*, 2006). The exocytosis must be followed by efficient retrieval of synaptic vesicles. After exocytosis, the synaptic vesicles undergo

recycling through endocytosis. This trafficking cycle of synaptic vesicles can be divided into 9 sequential steps described as follows: the synaptic vesicles filled with neurotransmitters are clustered and docked at the active zone (step 1, docking); the docked vesicles undergo a maturation process, which is a rate limiting step making the synaptic vesicles competent for the exocytosis on Ca^{2+} arrival (step 2, priming); Ca^{2+} triggered synaptic vesicle membrane fusion with the presynaptic membrane leading to neurotransmitter release (step 3 fusion or exocytosis); internalization of the synaptic vesicle membrane, by clathrin-mediated retrieval (step 4, endocytosis); the recovered vesicles leave the active zone and fuse with the endosome (step 5 and 6); the newly formed vesicles bud-off the endosome (step 7) and are filled with neurotransmitters by active transport determined by electrochemical gradient formed by a proton pump (Schuldiner, *et al.*, 1995) (step 8); matured vesicles translocate and approach the active zone ready for a next round of release (step 9) **(Figure 4)** (Heuser and Reese, 1973; Sudhof, 1995).

In this classical view of the neurotransmitter release, the synaptic vesicles completely fuse with the membrane resulting in the rapid depletion of the synaptic vesicles in the nerve terminal. The presynaptic membrane area progressively enlarges and a synaptic button takes out the surplus of membrane in lateral areas to the active zone by clathrin-mediated endocytosis. These endocytosed vesicles lose the clathrin coat and fuse with the endosome (Heuser and Reese, 1973). The synaptic vesicles are regenerated by budding from the endosomes, reacidify and refill with neurotransmitters. In addition to the classical view of neurotransmitter release, there are views that the synaptic vesicles need not necessarily have to completely merge

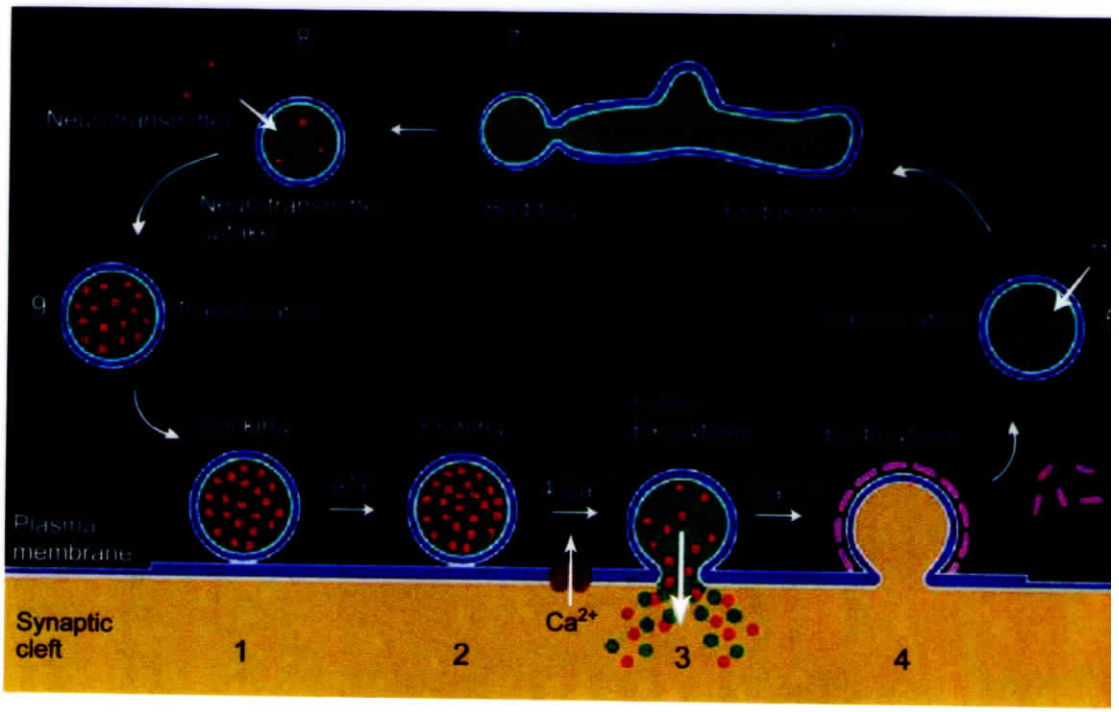

Figure 4: The schematic illustration of the synaptic vesicle cycle. Detailed description is in the text. (Adapted from Sudhof, 1995).

with the active zone but the full fusion occurs during the conditions of maximal stimulation (Ceccarelli and Hurlbut, 1980). The endocytosis and recycling can occur through two alternative pathways, namely kiss-and-stay; kiss-and-run (Fesce, *et al.*, 1994), where the synaptic vesicles will briefly fuse with the membrane under low stimulation conditions and release its contents through a fusion pore. In the kiss-and-stay pathway without undocking from the active site the vesicles are reacidified and refilled with neurotransmitters, making them readily available for a new fusion event whereas in the kiss-and-run pathway, the synaptic vesicles are undocked from the active site and locally recycled to reacidify and refill the neurotransmitters **(Figure 5)**.

These two modes of vesicle recycling differ chiefly in keeping the identity of vesicle during recycling. In kiss-and-run mode the vesicles quickly retrieve from the

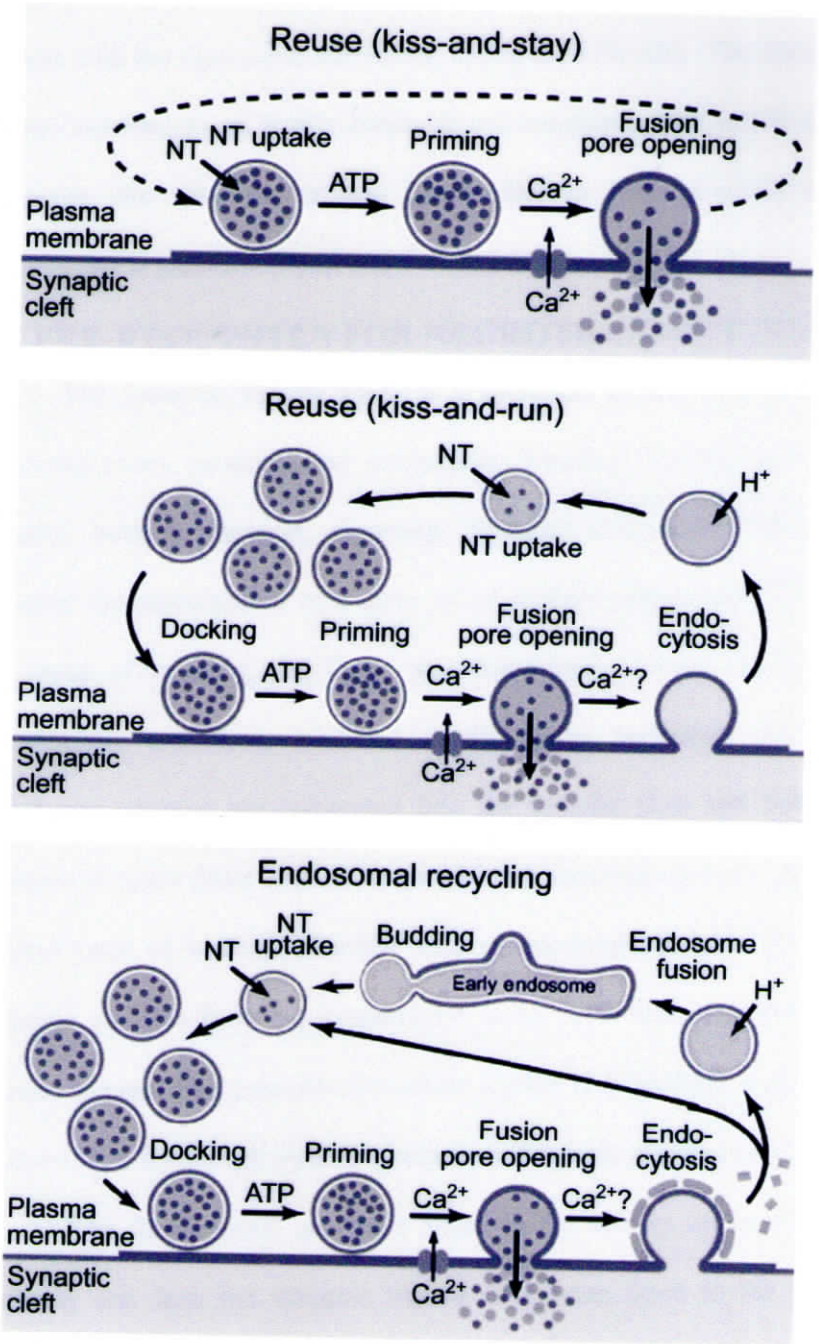

Figure 5: The three possible pathways of synaptic vesicle recycling in neurons. (Adapted from Sudhof, 2004.)

membrane keeping their identity whereas in the classical mode, the vesicle membrane remixes with the endosome membrane losing their identity. The data supporting kiss-and-run mechanism are highly debatable and conflicting (He and Wu, 2007).

Moreover, the time for reusing the vesicle in both classical and kiss-and-run mechanisms is identical (Ryan and Smith, 1995).

2.3. PRE-REQUISITES FOR NEUROTRANSMITTER RELEASE

The synaptic vesicle cycle is a multipart event with each and every step involving many proteins and interactions (Sudhof, 2004). Numerous studies on synaptic vesicle transport, targeting, docking, exocytosis and endocytosis have revealed the participation of a quite lot of proteins (Burre and Volknandt, 2007). In the soma of neurons, the lipids and membrane proteins are synthesized in the endoplasmic reticulum, modified in the Golgi apparatus and the fundamental membrane proteins are integrated into the vesicles (Lin and Scheller, 2000). The synaptic vesicles filled with neurotransmitters are targeted to the active zone, forms a reserve pool of vesicles attached with cytoskeletal elements. The mobilization of synaptic vesicles from the cytoskeleton is an ATP-dependent process in which the protein kinases like calcium/calmodulin kinase II (CaMKII) and myosin light chain kinase (MLCK) phosphorylates synapsin and myosin proteins (Ryan, 1999).

The fundamental questions asked in the studies on neurotransmitter release pathway are: how the synaptic vesicle membrane fuses to the presynaptic plasma membrane and how the synaptic vesicles sense the Ca^{2+} influx signal? For the fusion of the vesicular membrane with the plasma membrane, firstly both the vesicular membrane and presynaptic membrane have to conquer their own electrostatic

counteracting forces to be in close proximity; secondly the close membrane has to be destabilized leading to the formation of the fusion pore (Jahn, *et al.*, 2003). The SNARE proteins present on the membranes of synaptic vesicle (Synaptobrevin – v-SNARE) and presynaptic terminal (Syntaxin and Synaptosomal Associated Protein of molecular weight 25 kDa, SNAP-25 – t-SNAREs) have been suggested to form extraordinarily stable complex called SNARE complex. This complex formation will supply the energy required for membranes to overcome the counteracting force barrier (Fasshauer, *et al.*, 2002). Even though, the formation of SNARE complex can catalyze the fusion of proteoliposomes *in vitro*, this complex formation by purified SNAREs occur as a very slow process (takes minutes) and is not regulated by Ca^{2+}. These observations suggest the need for a Ca^{2+} sensor as well other proteins, which can function in concurrence with SNAREs to facilitate the fast and Ca^{2+} regulated synaptic vesicle exocytosis that happens at synapse (Chapman, 2002).

The Ca^{2+} triggered synaptic vesicle fusion occurs very fast with a maximal rate of 1000-3000 s^{-1} while the latency period between Ca^{2+} influx and fusion is very short calculated as approximately 100 μs (Heidelberger, *et al.*, 1994; Llinas, *et al.*, 1981; Sabatini and Regehr, 1996). This fast exocytosis indicates that synaptic vesicles are already docked before the Ca^{2+} entry. The Ca^{2+} influx should lead to the Ca^{2+} induced conformational changes in the fusion complex ultimately causing vesicle fusion with the presynaptic membrane. In respect to Ca^{2+} entry, the evoked neurotransmitter release can be classified into two: a fast synchronous form and a slower asynchronous form (Hagler and Goda, 2001). The dual nature of this neurotransmitter release gives the possibility of having two distinct Ca^{2+} sensors. The

low affinity Ca^{2+} sensor can trigger a fast release and is supposed to be localized near to the Ca^{2+} channels while the high affinity Ca^{2+} sensor for slow release is possibly located away from the Ca^{2+} channels.

A Ca^{2+} sensor should have the ability to sense and convert a small increase of Ca^{2+} signal into a physiological function, the synaptic vesicle membrane fusion. It should also have the affinity for Ca^{2+} ions. The short delay between Ca^{2+} influx and neurotransmitter release makes it possible that the Ca^{2+} receptor should be the part of fusion complex and to be expected to position either on the synaptic vesicle membrane or presynaptic membrane. The binding of Ca^{2+} should cause changes in the properties of the receptor protein leading to the rearrangement of membrane to provide the fusion (Yoshihara and Montana, 2004). The minimum intracellular Ca^{2+} concentration required for the vesicle exocytosis is 20 μM, with half-maximal fusion rates at 194 μM Ca^{2+} (Heidelberger, *et al.*, 1994). Such high Ca^{2+} concentrations are only expected to have very close to the Ca^{2+} channels (Llinas, *et al.*, 1992). So the fusion complex should be localized near the Ca^{2+} channels in the presynaptic membrane.

2.4. SYT I : A Ca^{2+} SENSOR AT PRESYNAPTIC TERMINAL

The discovery that neuronal exocytosis is activated by Ca^{2+} initiated a search for presynaptic Ca^{2+} sensor. Syt I, a presynaptic protein, appear to be the most likely candidate for the sensor of Ca^{2+} at the nerve terminal for the synchronous release as its sequence revealed that it has two Ca^{2+} binding domains similar to those present in protein kinase C (Perin, *et al.*, 1990; Perin, *et al.*, 1991a). Consequently, Syt I was found to bind divalent cations with the required specificity and concentrations to have

a role in neurotransmitter release (Brose, *et al.*, 1992; Davletov and Sudhof, 1993). The C2A and C2B domains of Syt I can bind with 3 and 2 Ca^{2+} ions respectively with low affinities (Rizo and Sudhof, 1998) **(Figure 6A and B)**.

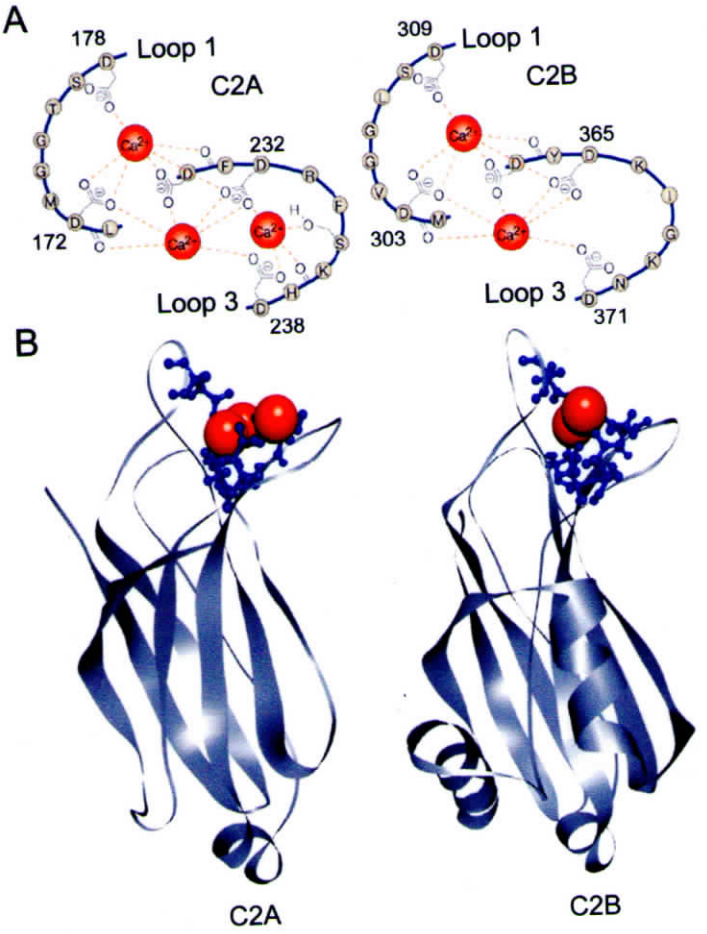

Figure 6: Syt I structure showing the C2 domains (A) Schematic drawing shows the interaction between the Ca^{2+} ions and amino acids in the C2A and C2B domains. (B) Three dimensional structure of the C2A and C2B domains in Ca^{2+} binding state. Red balls represent Ca^{2+} ions. (Adapted from Chapman, 2002).

Additionally, Syt I undergo a conformational change after the Ca^{2+} binding (Davletov and Sudhof, 1994). The other features of Syt I to act as a Ca^{2+} sensor include its binding ability for phospholipids in a Ca^{2+} dependent manner (Brose, *et al.*, 1992; Perin, *et al.*, 1990), Ca^{2+} dependent or independent binding with SNARE complex (Chapman, *et al.*, 1995; Ernst and Brunger, 2003; Rickman and Davletov, 2003) and Syt I self oligomerization (Chapman, *et al.*, 1996; Sugita, *et al.*, 1996; Wu, *et al.*, 2003). The interactions of Syt I with phospholipid and SNARE as well the self oligomerization was found to occur on a millisecond scale (Bai, *et al.*, 2004b; Davis, *et al.*, 1999). All these biochemical interactions can occur sequentially or simultaneously to function as a Ca^{2+} sensor during synaptic neurotransmission. Furthermore, the interaction between Syt I and the Ca^{2+} channel (in the plasma membrane) can be the best way for keeping synaptic vesicles in their correct place (Charvin, *et al.*, 1997). The biochemical properties of Syt I to act as a Ca^{2+} sensor has been correlated to physical function by various experiments by altering the Syt I protein.

Knockout mice without functional Syt I showed loss of the fast component of Ca^{2+} triggered neurotransmitter release (Geppert, *et al.*, 1994) while the knock-in mice having mutated Syt I C2A domain did not show alterations in synaptic transmission (Fernandez-Chacon, *et al.*, 2001). *Drosophila* Syt I mutants resulted in the disruption of evoked neurotransmitter release (DiAntonio and Schwarz, 1994; Littleton, *et al.*, 1993). The asynchronous release of synaptic vesicle in Syt I mutant revealed that Syt I is needed to convert the slow asynchronous release into fast synchronous release (Yoshihara and Littleton, 2002). The mutants that disrupt the

functions of SNARE proteins also showed reduction in evoked neurotransmitter release (Yoshihara, *et al.*, 1999). So the phenotype that is the decreased transmission alone could not prove Syt I as a Ca^{2+} sensor, instead the reduced transmission in Syt I mutants can be due to defects in any of the other synaptic vesicle cycle stages.

The specific role of Syt I as Ca^{2+} sensor further elucidated by checking the Ca^{2+} cooperativity in Syt I mutants. The mammalian neuromuscular junction has a fourth order cooperativity for the Ca^{2+} dependent transmitter release (Dodge and Rahamimoff, 1967), which is conserved in *Drosophila* neuromuscular junction also. This high order cooperativity demands the requirements for Ca^{2+} sensor for the vesicle fusion (Yoshihara and Montana, 2004). The *Drosophila* AD1 mutant with no C2B domain in Syt I showed the destruction of Ca^{2+} cooperativity of synchronous release indicating Syt I function as the Ca^{2+} sensor for the synchronous release (DiAntonio and Schwarz, 1994). Additionally in *Drosophila* the abolishment of Syt I function using photoinactivation technique resulted in decrease of Ca^{2+} cooperativity (Marek and Davis, 2002). In mice, the Ca^{2+} cooperativity was distorted by mutating one of the Ca^{2+} binding sites of Syt I C2A domain (Stevens and Sullivan, 2003). Contradicting this data, the mutation of Ca^{2+} binding sites showed no change in Ca^{2+} cooperativity in other studies (Fernandez-Chacon, *et al.*, 2001; Mackler, *et al.*, 2002; Robinson, *et al.*, 2002). The kinetic measurements of Syt I for Ca^{2+} sensitivity and speed of response also satisfied with the requirement for synaptic vesicle fusion (Davis, *et al.*, 1999). Even though, Syt I protein has the essential biochemical characteristics to act as a Ca^{2+} sensor for neurotransmission, the comprehensive mechanisms have to be identified by which Syt I function as a cooperative fast

synchronous release sensor (Yoshihara and Montana, 2004).

2.5. FUNCTIONS OF SYT I IN EXOCYTOSIS

2.5.1. Role of Syt I in docking

The Syt I protein is suggested to have roles in vesicle docking at the plasmamembrane (Chieregatti, *et al.*, 2004; Schiavo, *et al.*, 1997). On morphological analysis of *Drosophila* Syt I null mutants, it was revealed that there is a slight overall reduction in the number of synaptic vesicles and a marked reduction in the number of docked vesicles (Reist, *et al.*, 1998) indicating the function of Syt I in facilitating docking step. The AD3 mutant flies, harboring a single substitution mutation resulting in disruption of Ca^{2+} sensing ability (DiAntonio and Schwarz, 1994), did not shown any defects in synaptic vesicle docking but exhibited physiological deficits (Littleton, *et al.*, 2001). The C-terminal of Syt I, in particular the WHXL motif, plays a crucial role in the synaptic vesicle docking at the active zone of the synapse (Fukuda, *et al.*, 2000b). The synaptic vesicles dock very close proximity of the presynaptic Ca^{2+} channels to experience very high local Ca^{2+} concentrations, a function modulated by Syt I protein by directly interacting with Ca^{2+} channels (Catterall, 1999).

2.5.2. Role of Syt I in uncoupling the fusion clamp

Genetic studies in *Drosophila* and *Xenopus* demonstrated that Syt I inhibits spontaneous fusion (Littleton, *et al.*, 1994; Morimoto, *et al.*, 1998). Syt I can control vesicle fusion by avoiding constitutive fusion until Ca^{2+} influx (Sudhof and Rizo, 1996). Various studies have been carried out to find the molecules that can regulate the SNARE-dependent vesicle fusion. Complexins were identified as one among them, which associate with the assembled SNARE complex but not with individual

SNARE proteins (McMahon, *et al.*, 1995; Pabst, *et al.*, 2002). Over-expression or microinjection of complexins resulted in the reduced neurotransmitter release suggesting the role of these proteins as a negative regulator (Itakura, *et al.*, 1999; Ono, *et al.*, 1998). Besides complexin knocking out also caused impairment of synchronous neurotransmitter release (Reim, *et al.*, 2001). The phenotypes exhibited by complexin and Syt I mutants are matching indicative of the direct or indirect cooperative role of these proteins in Ca^{2+} evoked exocytosis (Geppert, *et al.*, 1994; Reim, *et al.*, 2001). Complexin acts as a "clamp" blocking vesicle fusion while Syt I can relieve the "clamp" in presence of Ca^{2+} allowing fusion (Giraudo, *et al.*, 2006). The complexin binding turn on the SNARE complex into a hemifusion arrest and Ca^{2+} bound Syt I displaces the complexin from the metastable SNARE complex resulting in full fusion (Schaub, *et al.*, 2006; Tang, *et al.*, 2006).

2.5.3. Role of Syt I in synaptic vesicle fusion

Even though in the absence of Syt I the exocytotic membrane fusion continues, it does not take place quickly or synchronously in response to stimulation. Syt I mediate the rate-limiting steps in vesicle exocytosis by its specific interactions with phospholipids and SNAREs (Bai, *et al.*, 2004b; Fernandez-Chacon, *et al.*, 2001; Fukuda, *et al.*, 1995). The Ca^{2+} binding to the acidic residues in the flexible loops of Syt I C2A and C2B domains leads to the partial penetration of these loops into the lipid bilayers that containing anionic phospholipids like phosphatidyl serine and phosphatidylinositol 4, 5- biphosphate (Bai, *et al.*, 2002; Bai, *et al.*, 2004a; Chapman and Davis, 1998). It was reported that upon Ca^{2+}-dependent phospholipid binding Syt I can form heptameric rings through the C2B mediated oligomerization (Wang and

Chong, 2003). However, later studies show evidence that Syt I cannot form oligomers upon Ca^{2+}-dependent phospholipid binding, but can induce Ca^{2+}-dependent vesicle clustering by simultaneously interacting with two membranes of vesicles bringing them into close proximity (Arac, *et al.*, 2006). The mutations in Syt I which selectively impaired the Syt I-phospholipid interaction resulted in decreased neurotransmitter release (Fernandez-Chacon, *et al.*, 2001; Li, *et al.*, 2006) while the mutations that increase phospholipid binding caused enhanced neurotransmitter release (Rhee, *et al.*, 2005). These studies illustrate the importance of Ca^{2+}-dependent phospholipid binding of Syt I in vesicle exocytosis.

In addition to phospholipid binding, Ca^{2+} binding causes Syt I to form complexes with individual SNARE proteins, namely Syntaxin and SNAP-25 or with SNARE complex itself (Banerjee, *et al.*, 1996; Bowen, *et al.*, 2005; Rickman, *et al.*, 2004; Schiavo, *et al.*, 1997). The single amino acid substitution in Syt I (D232N), which selectively augmented its SNARE binding property, resulted in the enhancement of neurotransmitter release (Pang, *et al.*, 2006). Similarly, the mutations that caused the selective disruption of Syt I binding to t-SNARE destabilized the fusion pore resulting in reduced rate of secretion (Bai, *et al.*, 2004b). The Syt I interaction with the SNARE complex can act both as a positive and negative regulator of synaptic vesicle exocytosis.

The proposed scenario for the function of Syt I during exocytosis is that at resting Ca^{2+} concentrations, Syt I weakly interacts with phospholipids and t-SNAREs in the plasma membrane, but bound to the synaptic vesicle protein SV2 through its C2B domain (Bajjalieh, 1999; Lazzell, *et al.*, 2004). This conformation can stabilize

the SNARE complexes, strengthening a hemi-fused state, thereby hindering nor stimulated exocytosis. The Ca^{2+} influx inhibits its interaction with SV2 whil stimulates the C2B mediated dimerization and organize the SNARE complexes nea the Ca^{2+} entry. At high Ca^{2+} concentrations, Syt I binds with membrane phospholipic leading to the rapid penetration of the Ca^{2+} binding loops of Syt I into the membran favoring its affinity for interaction with t-SNARE proteins. This will result in th disturbance of the hemi-fused state or alter the conformation of SNARE comple promoting the complete fusion **(Figure 7)** (Bajjalieh, 1999; Tucker and Chapman 2002). Immediately after vesicle fusion, α-SNAP dislocates Syt I for N ethylmaleimide-sensitive fusion protein to disassemble the SNARE complex (Sollne *et al.*, 1993).

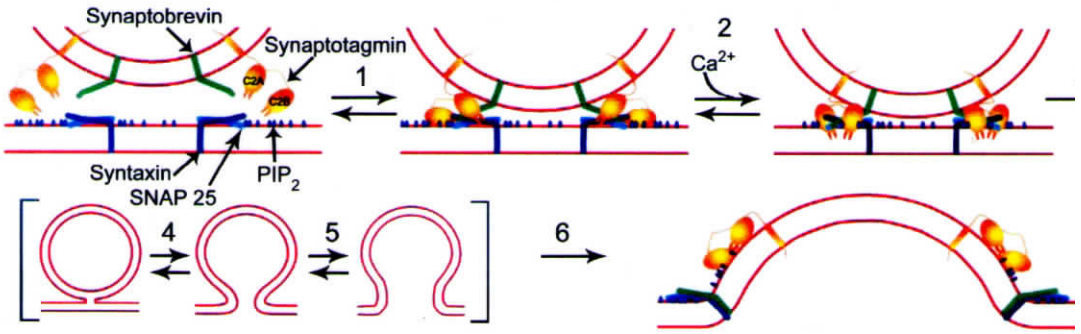

Figure 7: Model showing the function of Syt I in exocytosis. (Adapted from Tucker and Chapman, 2002).

2.6. FUNCTIONS OF SYT I IN ENDOCYTOSIS

Following to the exocytosis, the synaptic vesicles are retrieved by a clathrin dependent endocytosis, the only mechanism by which the used vesicles are recycle to the releasable vesicle pool (Mousavi, *et al.*, 2004; Murthy and De Camilli, 2003

In order to maintain the vesicle pool and preserve the morphology of plasma membrane, the rate of synaptic vesicle endocytosis must be adjusted to match the rate of exocytosis (Jarousse and Kelly, 2001). The vesicle retrieval from presynaptic membrane is mediated by AP-2, a class of adaptor protein, which can bind to synaptic vesicle membrane to activate the assembly of clathrin for endocytosis. The biochemical study exposed a high affinity interaction between AP-2 and the C2B domain of Syt I (Zhang, *et al.*, 1994). In addition, a striking reduction of synaptic vesicles was observed at nerve terminals of Syt I deficient *C. elegans* (Jorgensen, *et al.*, 1995). Similarly a kinetic insufficiency of endocytosis was noticed in Syt I knock out mice hippocampal neurons (Nicholson-Tomishima and Ryan, 2004).

Thus, Syt I nucleates the formation of clathrin-coated vesicles by acting as a synaptic plasma membrane docking site for the AP-2 complex. The AP-2 binding site was determined to be the polybasic site ($K_{326, 327}$) in C2B domain of Syt I (Chapman, *et al.*, 1998). Besides AP-2, this polybasic site is identified as the binding site for multiple molecules like inositol polyphosphates (Fukuda, *et al.*, 1994) and Ca^{2+} channels (Kim and Catterall, 1997; Sheng, *et al.*, 1997). Interestingly the same site is involved in the oligomerization of Syt I (Chapman, *et al.*, 1996; Desai, *et al.*, 2000; Sugita, *et al.*, 1996) and this oligomer formation becomes a pre-requisite for AP-2 binding (Grass, *et al.*, 2004). Further more, one of the binding partners for Syt I C2A domain is phosphatidylinositol-4, 5-bisphosphate (Tucker, *et al.*, 2003) which is also crucial for the clathrin-mediated endocytosis (Krauss, *et al.*, 2003). All these evidences strongly support the critical role played by the Syt I in the endocytotic process. In synapse, the exoctyosis and endocytosis pathways are strongly coupled

and Syt I might be acting as the key regulator for coupling these pathways by playing central roles.

2.7. SYNAPTOTAGMIN ISOFORMS

Syt constitutes a large family of synaptic proteins, with sixteen different isoforms, associated with vesicular trafficking in both vertebrates and invertebrates (Adolfsen and Littleton, 2001; Fukuda, 2003a; Fukuda, 2003b; Sudhof, 2002). A detailed analysis of the Syt members has been carried out to understand the evolution of the gene family (Craxton, 2001; Craxton, 2004). The phylogenetic tree of the human Syt isoforms was created using ClustalW to get a broad picture of the evolutionary relationship within the protein family **(Figure 8)**.

The Syt proteins have a characteristic intravesicular N-terminal transmembrane domain and C-terminal C2 domains (C2A and C2B) (Perin, *et al.*, 1991a). The N-terminal domain contains divergent amino acid residues while the cytoplasmic region is well conserved. The transmembrane and C2 domains are separated by a variable length central linker (spacer domain). The various Syt genes have distinct patterns of tissue distribution, developmental profiles and biochemical functions. Majority of Syt isoforms (Syt I-V and IX-XI) are widely distributed in the brain, still some isoforms (Syt VI-VIII) are detected in the non-neuronal tissues like heart, kidney and intestine (Marqueze, *et al.*, 2000). In the brain itself, the Syt isoforms show differential subcellular localization which is a topic of debate (Chapman, 2002) **(Table 2)**.

Syt proteins can form a hierarchy of exocytotic Ca^{2+} sensors with distinct Ca^{2+} affinities (Sudhof, 2002). The presynaptic membrane associated Syt isoforms

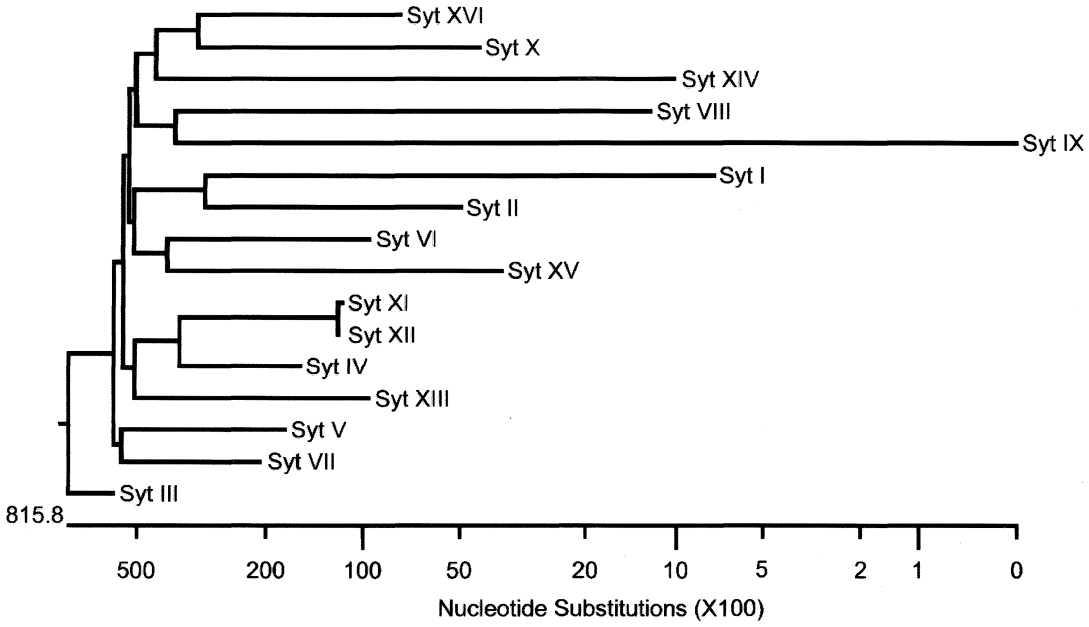

Figure 8: The phylogenetic tree of human Syt isoforms I-XVI is shown. Multiple sequence alignment was made by Megalign and phylogenetic tree was drawn by ClustalW (PAM250) using Lasergene 6 software. (Accession numbers: Syt I - NP_005630.1, Syt II - NP_796376.2, Syt III - NP_115674.1, Syt IV - NP_065834.1, Syt V - NP_003171.1, Syt VI - NP_995320.1, Syt VII - NP_0041912, Syt VIII - NP_612634.3, Syt IX - NP_783860.1, Syt X - NP_945343.1, Syt XI - BAA07527, Syt XII - NP_689493.2, Syt XIII - NP_065877.1, Syt XIV - NP_694994.1, Syt XV - NP_852660.1 and Syt XVI - CAE85114).

represent high affinity Ca^{2+} sensors involved in slow Ca^{2+}-dependent exocytosis, whereas the vesicular Syt I isoforms function as low affinity Ca^{2+} sensors specialized for fast Ca^{2+}-dependent exocytosis (Sudhof, 2002). However, unlike Syt I, most of the Syt isoforms cannot bind Ca^{2+} and phospholipids. In Syt IV and XI, the Ca^{2+} binding

Table 2: Distribution of Syt isoforms

Syt isoform	Species	Expression pattern	Subcellular localization
Syt I	human, rat, mouse, *Drosophila*, *C. elegans*	neuronal	synaptic vesicles
Syt II	human, rat, mouse	neuronal, mast cells, pancreatic cells	synaptic vesicles, lysosomes of mast cells
Syt III	rat, mouse	neuronal, pancreatic cells	presynaptic plasma membrane, secretory granules in β-cells
Syt IV	rat, mouse, *Drosophila*, *C. elegans*	neuronal	postsynaptic vesicle, Golgi apparatus
Syt V	rat, mouse, *Drosophila*	neuronal, kidney, adipose tissue, lung, heart	unknown
Syt VI	human, rat, mouse	ubiquitous	excluded from synaptic vesicles
Syt VII	human, rat, mouse, *Drosophila*, *C. elegans*	ubiquitous	unknown
Syt VIII	human, mouse	ubiquitous	unknown
Syt IX	human, rat, mouse, *Drosophila*	ubiquitous	unknown
Syt X	rat, mouse	neuronal	unknown
Syt XI	human, rat, mouse	neuronal	unknown

Adapted from Adolfsen, 2001

site of the C2A domain is abolished by evolutionarily conserving an amino acid substitution mutation (Dai, *et al.*, 2004; von Poser, *et al.*, 1997). Similarly in the Syt isoforms Syt VIII, XII and XIII, the aspartate and glutamate residues in the top loops of the C2A and C2B domains, critical for Ca^{2+} binding, are absent (Sudhof, 2002). All the Syt isoforms maintained Syntaxin and AP2 binding indicating a role in synaptic vesicle fusion and endocytotic events (Li, *et al.*, 1995; Zhang, *et al.*, 1994). The various functions of Syt family members include neuronal exocytosis, hormonal secretion, plasma membrane repair, lysosomal fusion, neurite outgrowth and the sperm acrosome reaction during fertilization (Marqueze, *et al.*, 2000). The Syt isoforms are differentially expressed and the synaptic vesicle fusion kinetics can be altered by the changes in the ratio of expression level of each isoform (Wang, *et al.*, 2001).

2.8. SYNAPTOTAGMIN OLIGOMERIZATION

The Ca^{2+}-dependent or -independent homo- and hetero-oligomerization is a well conserved characteristic feature of the majority of Syt isoforms (Fukuda, *et al.*, 1999). The Ca^{2+}-independent oligomerization is mediated through the region just downstream of the transmembrane domain (Perin, *et al.*, 1991a) whereas the Ca^{2+}-depedent oligomerization is contributed by the C2B domain (Chapman, *et al.*, 1998; Damer and Creutz, 1996; Sugita, *et al.*, 1996). The Ca^{2+}-independent oliogmers can be either SDS-resistant (stable) or SDS-sensitive (unstable) (Fukuda, *et al.*, 2001). The cysteine cluster present at the interface between the transmembrane and linker domain is essential for the SDS-resistant Ca^{2+}-independent homo- and hetero-oligomerization, in addition, the number of cysteine residues decide the

oligomerization potency of the different isoforms (Fukuda, *et al.*, 2001). The SDS-sensitive oligomers are formed by the interaction of the spacer domain in a Ca^{2+}-independent manner (Fukuda, *et al.*, 2001).

The C2B domains of the different Syt isoforms can undergo Ca^{2+}-driven conformational changes and form homo- or hetero-oligomers in response to rapid increase in Ca^{2+} ions (Desai, *et al.*, 2000). The Syt oligomerization is essential for the neurotransmitter release as the interruption of Ca^{2+}-mediated oligomer formation resulted in the impairment of exocytosis (Fukuda, *et al.*, 2000a; Littleton, *et al.*, 2001). However, there are controversies regarding the Ca^{2+}-dependent oligomerization of recombinant C2B domain proteins, where the RNase/high salt treatment abolished its oligomerization properties (Ubach, *et al.*, 2001; Wu, *et al.*, 2003). Still, the studies on oligomerization by co-immunoprecipitation (Osborne, *et al.*, 1999) and gel filtration chromatography (Ubach, *et al.*, 2001) demonstrated that the native Syt isoforms can undergo Ca^{2+}-triggered oligomerization.

Based on the Ca^{2+}-dependent and -independent oligomerization properties of Syt I-XI, the isoforms are classified into four groups: Syt III, V, VI and X belonging to group A which have strong homo- and hetero-oligomerization irrespective of the presence of Ca^{2+}; Syt I, II, VIII and XI form the group B which show moderate homo-oligomerization in spite of the presence of Ca^{2+}; Syt IV and Syt IX are grouped as C with no homo-oligomerization or weak Ca^{2+}-dependent oligomerization respectively and Syt VII is in group D with unique Ca^{2+}-dependent homo-oligomerization (Fukuda and Mikoshiba, 2000) **(Figure 9)**. The synaptic function can be modulated by the hetero-oligomerization of Syt isoforms with distinctive Ca^{2+} sensing properties

creating a variety of Ca^{2+} sensors.

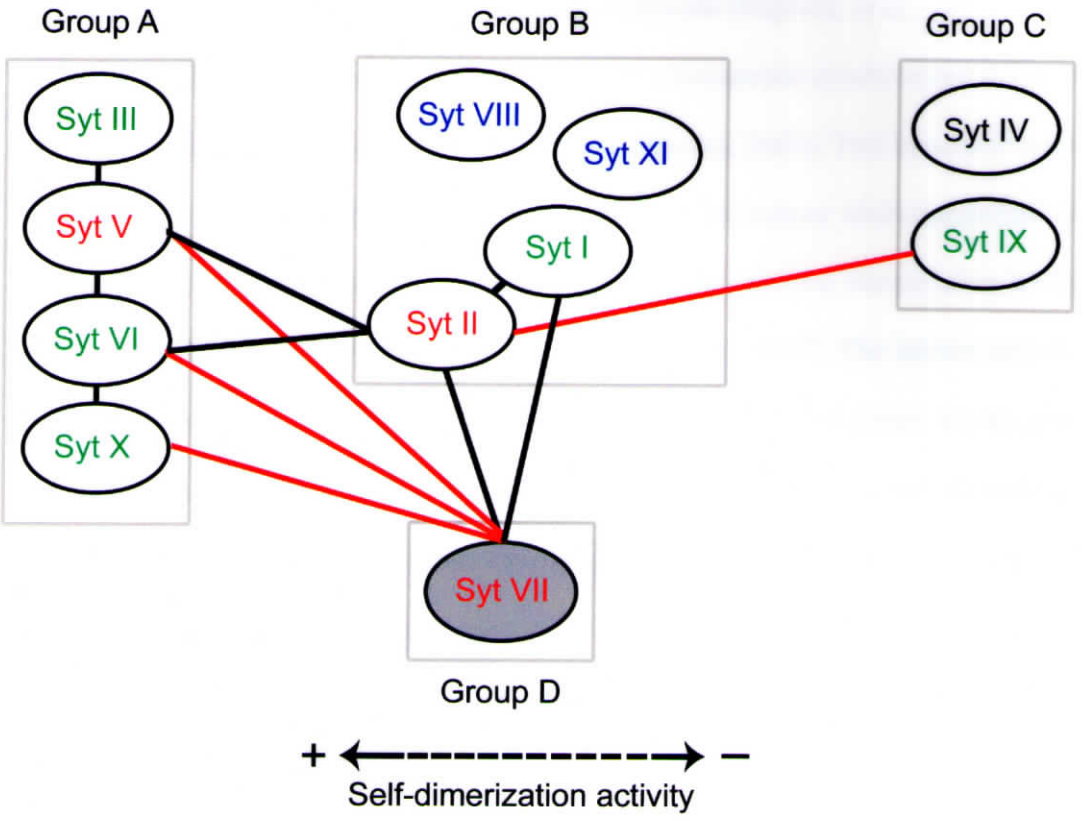

Figure 9: Grouping of Syt isoforms I-XI on the basis of Ca^{2+}-dependent and -independent oligomerization properties. Isoforms that show strong or weak Ca^{2+}-dependent homo-oligomerization mediated by C2B domain are indicated by red or green letters respectively. Syt VII is further shaded because it shows robust Ca^{2+}-dependent oligomerization. Isoforms that do not essentially show hetero-oligomerization are indicated by blue letters. An isoform that does not fundamentally show homo-oligomerization is indicated by black letters. Lines indicate the hetero-oligomerization of two molecules. Hetero-oligomerization that was activated by Ca^{2+} is coloured in red. (Adapted from Fukuda and Mikoshiba, 2000).

2.9. SEIZURE AND SYNAPTOTAGMIN

Epilepsy is one of the most frequent neuronal disorders affecting approximately 1.5% of the human population worldwide (Majores, *et al.*, 2004). It is a chronic condition of recurrent seizures induced by spontaneous synchronized firing of a large population of neurons (McKeown and McNamara, 2001). This hyperactivation of neurons may arise through the hyper-secretion of excitatory neurotransmitter or hypo-secretion of inhibitory neurotransmitter that alters synaptic transmission levels in excitatory and inhibitory pathways (Engel and Pedley, 1997). The seizure activity is resulted in the transcriptional activation of the immediate early genes whose gene products can control the expression of downstream genes (Sheng and Greenberg, 1990). There is a great need to understand the reasons for the development of seizures to treat human epilepsy. Animal models of epilepsy serve to study the molecular mechanisms of hyperexcitability and pharmacoresistance (Majores, *et al.*, 2004). *Status epilepticus* (SE) is a condition of increased neuronal activity induced in experimental models by the application of chemicals like kainic acid or pilocarpine or by electrical stimulation called kindling (Ben-Ari and Cossart, 2000; Mello, *et al.*, 1993; Sutula, 2001).

Two isoforms of Syt family, namely Syt IV and X, undergo rapid up-regulation following neuronal depolarization (Babity, *et al.*, 1997; Vician, *et al.*, 1995). The Syt X gene is expressed in the neurons undergoing delayed cell death and the role played by this gene is not well defined, though it is speculated to modulate the neurotransmitter release during excitotoxic neuronal activation (Babity, *et al.*, 1997). The Syt IV isoform is particularly interesting because of its less affinity for

Ca^{2+} by a substitution mutation, making it not efficient for Ca^{2+}-mediated interactions (von Poser, *et al.*, 1997). Earlier it was believed that the high level of Syt IV in neurons during hyperexcitability can be a protective mechanism by its hetero-oligomerization with Syt I forming a part of Ca^{2+} sensor to regulate neurotransmission (Ferguson, *et al.*, 1999; Littleton, *et al.*, 1999; von Poser, *et al.*, 1997). Besides, in PC12 cells, the over-expression of Syt IV resulted in the inhibition of evoked secretion reducing the Ca^{2+} stimulated release (Machado, *et al.*, 2004). However, the later studies questioned the neuroprotective role played by Syt IV isoform since it was localized at the postsynaptic terminal and hence its hetero-oligomerization with Syt I is unlikely (Adolfsen, *et al.*, 2004). Moreover, there are reports that the up-regulation of Syt IV unaltered the fast neurotransmission, giving no evidence for the inhibitory effect with regard to basal release probability, Ca^{2+}-dependent release, short term plasticity and fusion pore kinetics (Robinson, *et al.*, 2002; Ting, *et al.*, 2006).

2.10. SYT I PROTEIN TRAFFICKING

Synaptic transmission necessitate the appropriate targeting of proteins to the synaptic vesicles and the assembly of synaptic terminals, however, the mechanisms fundamental for the presynaptic protein organization in the synapses are not well elucidated (Ziv and Garner, 2004). Irrespective of the functional synapse formation, Syt I level enhances during synaptogenesis (Lou and Bixby, 1995) and attains a constant rate (Daly and Ziff, 1997). In mature neurons, Syt I protein is exclusively present on synaptic vesicle localized at the presynaptic terminal and it is unlikely that the protein synthesis (or translation of mRNA) to occur at the presynaptic terminal (Hirokawa, 2006), though there are reports suggesting possible translation machinery

in the axons (Koenig and Giuditta, 1999). Besides, there are reports that Syt I i continuously synthesized from mRNA localized at the cell body and transporte directly from the trans-Golgi network to specialized axonal endosomes from whic the synaptic vesicles originate (Mundigl, *et al.*, 1993). One of the Kinesin superfamil proteins, KIF1A, facilitate the anterograde transport of synaptic vesicle precurso containing Syt I as well as other synaptic vesicle proteins (Hirokawa and Takemura 2005) **(Figure 10)**.

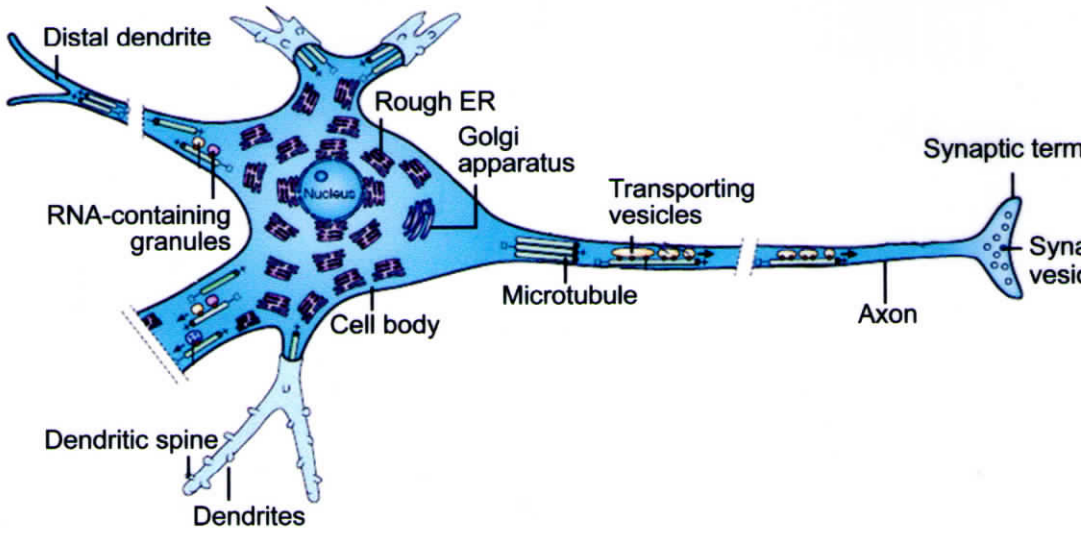

Figure 10: A neuron showing extensions of several dendrites and a single axon from the cell body. The KIFs transport synaptic vesicle precursors to axon terminal (marked as transporting vesicles). Adapted from Hirokawa and Takemura, 2005.

The rapid anterograde axonal transport of synaptic proteins allows the newl synthesized synaptic vesicle proteins to reach their target within an hour aft synthesis (Ferguson, *et al.*, 1999). Alternate mechanisms may exist for the sorting Syt I protein to synaptic vesicles. A structural element, WHXL motif conserve across Syt isoforms, present at the C-terminal domain of Syt I is critical for protei

targeting to neurite terminals (Krasnov and Enikolopov, 2000). There are also reports on the Syt I protein sorting through the mechanisms of palmitoylation and glycosylation of particular regions within the protein. The palmitoylation of the cysteine cluster at the junction between transmembrane and cytoplasmic domain is required for the targeting of Syt I to the synaptic vesicle pool at the presynaptic terminal (Kang, *et al.*, 2004). The glycosylation of N-terminal sequence can also help in the internalization and trafficking of Syt I during synaptic vesicle recycling (Han, *et al.*, 2004). The variety of mechanisms for the Syt I trafficking indicate that the protein level has to be highly regulated in neurons.

Chapter 3

MATERIALS AND METHODS

3.1. COMPETENT CELL PREPARATION ($CaCl_2$ METHOD)

The competent cells were prepared according to the standard protocol (Sambrook and Russel, 2001). 100 ml of LB broth (Luria Bertani Broth, Miller, Himedia, India) was inoculated with 2 ml of over-night bacterial culture (DH5α or XL1 Blue) and incubated at 37°C with shaking at 250 x rpm till OD reaches 0.3. The cells were kept on ice for 10 minutes and then centrifuged at 1600 x g for 10 minutes at 4°C. The LB medium was decanted and pellet was resuspended in 20 ml of ice cold 0.1 M $CaCl_2$ and centrifuged at 1100 x g for 10 minutes at 4°C. The solution was decanted and the cells were resuspended in 4 ml of 0.1 M $CaCl_2$, 140 µl of DMSO was added, swirl mixed and kept on ice for 15 minutes. An additional volume of 140 µl of DMSO was added to the solution, swirl mixed, aliquoted to microfuge tubes (200 µl each) and stored at -80°C. The transformation efficiency of the cells was checked for each batch of competent cell. A fresh stock of competent cells was prepared on every 2 months.

3.2. ELECTROCOMPETENT CELL PREPARATION

The standard protocol was followed for the preparation of electrocompetent cells (Sambrook and Russel, 2001). 250 ml of the LB broth was inoculated with 2 ml of over-night bacterial culture (XL1 Blue) and incubated at 37°C with shaking at 250 x rpm till OD reaches 0.5. The cells were chilled on ice for 10 minutes. Centrifuged at 4500 x g for 15 minutes at 4°C and removed the LB broth. The cells were resuspended in 250 ml of 10% glycerol, centrifuged at 4500 x g for 15 minutes at 4°C. This step was repeated with 125 ml and 10 ml volumes of 10% glycerol. Finally the cells were resuspended in 0.5 ml of 10% glycerol and aliquoted to microfuge tubes (40 µl each) and stored at -80°C. A fresh stock of competent cells was prepared on every 2 months.

3.3. TRANSFORMATION

The frozen competent cells prepared by $CaCl_2$ method were thawed at 37°C for 1 minute and immediately placed on ice for 10 minutes. To 50 µl of the competent cells, plasmid DNA or ligation mixture were added and kept on ice for 15 minutes. The cells were then subjected to heat shock by incubating at 42°C for 90 seconds and rapidly transferred to an ice bath to chill for 2 minutes. LB broth (950 µl) was added to the tube and the cells were grown at 37°C for 90 minutes with mixing at 300 x rpm. As a control the competent cells without any plasmid DNA were plated on a plain LB plate (to check the viability of cells after heat shock) and on a LB plate with appropriate antibiotic (to check contamination in the competent cells). Similarly, 50-200 µl of the transformed cells (test) were plated on to the LB plates with appropriate antibiotic. The plasmids containing β-galactosidase were transformed in competent

cells and plated on to the LB plate with antibiotics and X gal-IPTG for blue-white selection (the transformed colonies with plasmid alone will appear blue in colour, while the colonies with plasmid containing insert will appear white in colour). The plates were kept in room temperature until the liquid has been absorbed (15-20 minutes). The plates were incubated at 37°C for over-night.

3.4. ELECTROPORATION

The electrocompetent cells (40 µl) were thawed at 37°C for 1 minute and placed on ice for 10 minutes. To a cooled bacterial electroporation cuvette (Gene pulser cuvettes, Bio-Rad, USA) 25 ng of the DNA (1-2 µl of ligation mixture) and the electrocompetent cells were added and incubated on ice for 1 minute. The electroporation apparatus (MicroPulser, Bio-Rad, USA) was set in EC2 mode (for *E coli*, 0.2 cm cuvette) to deliver an electrical pulse of 2.5 kV. The electroporation cuvette was placed in the chamber slide and delivered the pulse. The electroporation cuvette was removed immediately from the chamber slide and 1 ml of LB broth was added. The cells were transferred to a microfuge tube and grown at 37°C for 1 hour with mixing at 300 x rpm. The cells were plated on LB-agar plate as mentioned above.

3.5. PLASMID ISOLATION

The basic protocol was followed for the plasmid preparation (Sambrook and Russel, 2001).

STE buffer

Tris-HCl, pH 8.0	-	10 mM
NaCl	-	0.1 M

EDTA, pH 8.0	-	1 mM

Alkaline lysis solution I (GTE buffer)

Glucose	-	50 mM
Tris-HCl, pH 8.0	-	25 mM
EDTA, pH 8.0	-	10 mM

Alkaline lysis solution II

NaOH	-	0.2 N
SDS	-	1%

Alkaline lysis solution III

5 M potassium acetate	-	60 ml
Glacial acetic acid	-	11.5 ml
Deionized water	-	28.5 ml

Tris-saturated Phenol, pH 8.0

The molecular biology grade phenol was distilled, saturated with Tris-Cl and the pH was adjusted to 8.0

Chloroform-isoamyl alcohol (24:1)

Chloroform	-	24 ml
Isoamyl alcohol	-	1 ml

3.5.1. Small-scale plasmid isolation (Mini preparation)

A single colony of transformed bacteria was inoculated in 5 ml LB medium containing the appropriate antibiotic for over-night at 37°C with vigorous shaking. 1.5 ml of over-night bacterial culture was centrifuged at 10,000 x g for 2 minutes at 4°C. The pellet was resuspended in 0.25 volume of STE buffer and centrifuged at 10,000 x

g for 2 minutes at 4°C. The pellet was resuspended in 100 µl of GTE buffer by vigorous vortexing and kept at room temperature for 5 minutes. To this solution 200 µl of the alkaline lysis solution II was added, mixed gently by inverting the tubes for 10 times and placed on ice for 15 minutes. To the tube 150 µl of alkaline lysis solution III was added, mixed gently by inverting the tubes for 10 times and kept on ice for 10 minutes. The tube was centrifuged at 10,000 x g for 5 minutes at 4°C. The clear supernatant was transferred to a fresh microfuge tube. An equal volume of Tris-saturated phenol (pH 8.0) and chloroform-isoamyl alcohol mix (24:1) was added to the tube and mixed vigorously. The microfuge tube was centrifuged at 10,000 x g for 5 minutes at 4°C and the aqueous phase was transferred to a fresh tube. The step was repeated with equal volume of chloroform-isoamyl alcohol, mixed vigorously and centrifuged at 10,000 x g for 5 minutes at 4°C. The aqueous phase was transferred to a microfuge tube and the plasmid DNA was precipitated by adding 0.2 volume of 3 M sodium acetate (pH 4.8) and one volume of isopropanol. The tube was kept at -80°C for 30 minutes and centrifuged at 10,000 x g for 15 minutes at 4°C. Isopropanol was removed by decantation and the pellet was washed with 500 µl of 70% ethanol and air dried, before dissolving in appropriate volume of deionized water or TE buffer .

3.5.2. Large-scale plasmid isolation (Maxi preparation)

A single colony of transformed bacteria was inoculated in 50 ml of LB media with appropriate antibiotics and grown over-night at 37°C. The bacterial culture was centrifuged at 10,000 x g for 5 minutes at 4°C in a 50 ml round bottom tube. The pellet was resuspended in 20 ml of STE buffer and centrifuged at 10,000 x g for 5 minutes. The pellet was resuspended in 1.8 ml of GTE buffer, by vortexing and kept

at room temperature for 5 minutes. 4 ml of alkaline lysis solution II was added, mixed the solution gently by inverting and the tube was placed on ice for 15 minutes. To the tube 2 ml of alkaline lysis solution III was added and kept on ice for 10 minutes. The solution mixture was centrifuged at 10,000 x g for 30 minutes at 4°C and the supernatant was filtered through 4-ply gauze. To the supernatant one volume of isopropanol was added and kept at -80°C for 30 minutes. The tube was centrifuged at 10,000 x g for 15 minutes at 4°C. The pellet was collected and dissolved in 300 µl of deionized water. This plasmid DNA was further purified by phenol:chloroform extraction as mentioned in the small scale plasmid DNA isolation protocol.

3.6. GENOMIC DNA ISOLATION FROM BRAIN TISSUE

DNA was extracted according to the basic protocol (Sambrook and Russel, 2001).

10 X Phosphate Buffered Saline (10 X PBS)

NaCl	-	80 g
Na_2HPO_4	-	9.9 g
KCl	-	2.2 g
K_2HPO_4	-	2 g

Dissolved in deionized water, adjusted pH to 7.4 and made up to 1 litre.

DNA extraction buffer

Tris-HCl, pH 8.0	-	10 mM
EDTA, pH 8.0	-	100 mM
SDS	-	0.5%
DNase free RNase	-	20 µg/ml

100 mg human brain tissue (from National Brain Bank, Bangalore, India) was

washed thoroughly with 1X PBS for 5 times. The tissue was homogenized in 1.2 ml of extraction buffer and incubated at 37°C for 1 hour in a microfuge tube. To this homogenate 13.5 µl of proteinase K (14.8 mg/ml) was added and incubated at 50°C for over-night. The mixture was cooled to room temperature and added equal volume of Tris-saturated phenol (pH 8.0) and continued incubation at room temperature for 40 minutes. The tube was centrifuged at 5,000 x g for 15 minutes at room temperature, collected the aqueous layer. The phenol extraction was repeated with 10 minutes incubation and the aqueous layer was treated with 1:1 ratio of phenol and chloroform-isoamyl alcohol mix (24:1) at room temperature for 10 minutes. The aqueous layer was collected after centrifuging at 5,000 x g for 15 minutes at room temperature. Equal volume of chloroform-isoamyl alcohol mix was added to the aqueous layer and incubated at room temperature for 10 minutes and centrifuged at 5,000 x g for 10 minutes. The genomic DNA was precipitated from the aqueous layer using 0.2 V of 10 M ammonium acetate and one volume of isopropanol by keeping at -80°C for 1 hour. The DNA pellet was obtained by centrifuging at 13,000 x g for 30 minutes at room temperature. The pellet was washed with 70% ethanol, dried and dissolved in appropriate volume of deionized water.

3.7. RNA ISOLATION

3.7.1. Guanidium thiocyanate method

The RNA isolation was performed using a single step method (Chomczynski and Sacchi, 1987).

Solution D

Guanidium thiocyanate - 4 M

Sodium citrate, pH 7.0	-	25 mM
SDS (w/v)	-	0.5%
β-mercaptoethanol	-	100 mM

Water saturated phenol

The molecular biology grade phenol was distilled, saturated with distilled water and the pH was adjusted to 5.0 – 6.0.

Chloroform-isoamyl alcohol (49:1)

Chloroform	-	49 ml
Isoamyl alcohol	-	1 ml

Rat brain hippocampus tissue (approximately 100 mg) was homogenized in 1 ml of solution D keeping on ice. To the homogenized tissue 100 µl of 2 M sodium acetate (pH 4.0), 1 ml of water saturated phenol and 200 µl of chloroform-isoamyl alcohol were added and mixed thoroughly after the addition of each reagent by inversion. The final suspension was shaken vigorously for 10 seconds and cooled on ice for 15 minutes. The solution was centrifuged at 10,000 x g for 20 minutes at 4°C and the RNA containing aqueous phase was transferred to a fresh tube. To this solution 1 ml of isopropanol was added and kept for precipitation at -20°C for 1 hour. The RNA was pelleted by centrifugation at 10,000 x g for 20 minutes at 4°C and dissolved in 300 µl of solution D. The RNA was again precipitated with 1 volume of isopropanol as mentioned in the previous step. The pellet was washed with 75% of ethanol, air dried and dissolved in deionized water by keeping at 65°C for 10 minutes. The RNA samples were aliquoted and stored at -80°C till experimentation.

3.7.2. Tri-reagent method

Rat brain hippocampus tissue (approximately 100 mg) was homogenized in 1 ml of Tri-reagent (Sigma, USA) keeping on ice. The homogenate was centrifuged at 12,000 x g for 10 minutes at 4°C. The supernatant was transferred to fresh tube and kept at room temperature for 5 minutes. To the tube 200 µl of chloroform was added, shook vigorously for 15 seconds and incubated at room temperature for 10 minutes. It was centrifuged at 12,000 x g for 15 minutes at 4°C. The aqueous phase was transferred to a fresh tube and added 50 µl of isopropanol, stored at room temperature for 5 minutes and centrifuged at 12,000 x g for 10 minutes at 4°C. The supernatant was transferred to a fresh tube and 450 µl of isopropanol was added and kept the tubes at room temperature for 10 minutes for RNA precipitation. The tube was centrifuged at 12,000 x g for 10 minutes at 4°C and decanted the supernatant. The RNA pellet was washed with 1 ml of 75% ethanol by centrifuging at 7500 x g for 5 minutes. The pellet was air dried and dissolved in deionized water by keeping at 60°C for 10 minutes. The aliquoted RNA samples were stored at -80°C till experimentation.

3.7.3. RNA gel electrophoresis

10 X MOPS electrophoresis buffer

MOPS, pH 7.0	-	0.2 M
Sodium acetate	-	20 mM
EDTA, pH 8.0	-	10 mM

RNA gel- loading buffer

Deionized formamide (v/v)	-	95%
Bromophenol blue (w/v)	-	0.025%
Xylene cyanol (w/v)	-	0.025%

EDTA, pH 8.0	-	5 mM
SDS (w/v)	-	0.025%

RNA (2-4.5 µl) was denatured in the presence of 2 µl of 10 X MOPS buffer, 3.5 µl of formaldehyde (37-41% w/v) and 10 µl of formamide by incubating at 65°C for 8 minutes and immediately chilled on ice for 2 minutes. After adding 1 µl of ethidium bromide (10 mg/ml) and 2 µl of RNA gel loading buffer, the sample was electrophoresed on 1% agarose-formaldehyde (2.2 M) gel. The voltage was initially set to 100 V till the sample enters into the gel, then the electrophoresis was performed at 40 V till the bromophenol blue reached bottom of the gel.

3.8. MICROBRADFORD ASSAY

For the quantitation of proteins the standard assay was followed (Bradford, 1976).

Bradford reagent

Coomassie brilliant blue G-250	-	10 mg
Absolute alcohol	-	5 ml
85% Phosphoric acid	-	10 ml

The solution was diluted to 100 ml with deionized water and filtered through Whatman filter paper. It was protected from light and stored at 4°C.

For the standard graph 2, 4, 6, 10, 15 and 20 µl of BSA protein (1 mg/ml) was taken and made up to 100 µl with deionized water. To this solution 1 ml of Bradford reagent was added and measured the absorbance at 595 nm using Biophotometer (Eppendorf, Germany). The standard graph was plotted against protein concentration versus the absorbance. The absorbance of test proteins were also measured in a

similar manner and the protein concentration was calculated from the standard graph.

3.9. SDS-PAGE

1 X SDS gel-loading buffer

Tris-HCl, pH 6.8	-	50 mM
SDS	-	2%
Bromophenol blue	-	0.1%
Glycerol	-	10%
β-mercaptoethanol	-	5%

Coomassie staining solution

Coomassie brilliant blue R-250	-	0.25 g
Methanol	-	45%
Glacial acetic acid	-	10%
Distilled water	-	45%

Destaining solution

Methanol	-	45%
Glacial acetic acid	-	10%
Distilled water	-	45%

The proteins were separated by electrophoresis on a denaturing SDS-polyacrylamide gel. Before loading on the SDS-PAGE gel the proteins were incubated with 1 X SDS gel-loading buffer for 10 minutes in boiling water bath. The proteins were analyzed on 10 or 12% resolving gels, with a stacking gel of 5%. Protein marker of medium range - 97.4, 66, 43, 29, 20.1 and 14.3 kDa (Bangalore Genei, India) was loaded in each gel. The gels were stained with Coomassie staining solution to visualize the protein bands. The gels were immersed in staining solution

for 15-30 minutes and destained with repetitive changes of fresh destaining solution with shaking till the protein bands were visible. The gels were documented using gel documentation system (Kodak Digital Science 1D, USA or Uvitec, UK) and by drying the gel in a gel dryer (Bio-Rad, USA).

3.10. SILVER STAINING OF PROTEIN GELS

Methanol- acetic acid solution

Methanol	-	45%
Acetic acid	-	12%

Ethanol-acetic acid solution

Ethanol	-	10%
Acetic acid	-	5%

$K_2Cr_2O_7$ solution

0.3 M $K_2Cr_2O_7$	-	1 ml
HCl	-	20 µl

Made up to 100 ml with deionized water.

Silver nitrate solution (1.2 M)

Silver nitrate	-	204 mg

Dissolved in 100 ml of deionized water

Developing solution

Sodium carbonate	-	11.87 g (0.28 M)
40% Formaldehyde	-	0.2 ml

Made up to 400 ml with deionized water

Farmer's reducer

0.074 g/ml $K_3Fe(CN)_6.H_2O$	-	1 ml

0.24 g/ml $Na_2S_2O_3$. H_2O - 4 ml

Made up to 100 ml with deionized water

The protein gels with less concentration of proteins were visualized by the silver staining method (Tsang, *et al.*, 1983). The whole protocol was carried out at room temperature, keeping the gel in constant motion using a shaker. The gel was placed in 100 ml of methanol-acetic acid solution for 30 minutes; washed using 100 ml of ethanol-acetic acid solution for 10 minutes for 3 times. The gel was transferred to 100 ml of $K_2Cr_2O_7$ solution for 5 minutes and washed 4 times for 30 seconds with 100 ml of deionized water. The gel was exposed to 100 ml of silver nitrate solution for 30 minutes. After removing the silver nitrate solution, the gel was quickly rinsed twice with 100 ml of developing solution. Fresh developing solution was added and the gel was developed till the desired bands and back ground were seen. The reaction was stopped by removing the developing solution and by adding 200 ml of 1% acetic acid. To reduce the back ground colour, the gel was exposed to Farmer's reducer and was repeatedly washed with deionized water to remove the traces of Farmer's reducer. The gels were documented using gel documentation system (Kodak Digital Science 1D, USA or Uvitec, UK) and by drying the gel in a gel dryer (Bio-Rad, USA).

3.11. BRAIN LYSATE PREPARATION

Homogenization buffer

Tris-HCl pH 7.5	-	50 mM
Glycerol	-	25%
KCl	-	50 mM
EDTA, pH 8.0	-	0.1 M

DTT	-	0.5 mM
PMSF	-	1 mM
Aprotinin	-	5 μg/ml

Human brain hippocampal tissue (from National Brain Bank, Bangalore, India) and rat hippocampus were homogenized in ice-cold buffer using an electronic homogenizer (Ultra Turrax T8, IKA Labortechnik, Germany) at a maximum speed of 25,000 L/minute for 30 seconds at 4°C. The homogenization was repeated three to four times with an interval of 1 minute. The homogenate was centrifuged for 5 minutes at 1700 x g and the pellet was discarded. The supernatant was centrifuged for 1 hour at 100,000 x g at 4°C. The supernatant (SPF) and pellet were stored at -80°C until experimentation. The membrane proteins may release into solution because the high speed homogenization for ~ 2 minutes disrupts the membrane integrity of organelles.

3.12. BRAIN PHOSPHOLIPID PREPARATION

The phospholipids were extracted according to a modified protocol of Folch (1942). Rat brain tissue (100 mg) was homogenized in 380 μl of acetone and allowed to precipitate by keeping at room temperature for 30 minutes. The solution was centrifuged at 16,000 x g for 5 minutes at room temperature and the precipitate was resuspended in chloroform. After incubating at room temperature for 30 minutes the solution was centrifuged at 16,000 x g for 5 minutes at room temperature and the supernatant was collected. The solvent was removed under vacuum and the phospholipids were resuspended in RNA-protein binding buffer (see section 3.28) by bath sonication at 7°C with 3 strokes for 30 seconds and with intermittent vortexing.

3.13. INDUCTION OF SEIZURE IN RATS

All animal experiments were carried out with the approval of Institutional Animal Ethics Committee. Male Wistar rats weighing 180-200 g were injected with a single dose of pilocarpine (380 mg/kg, i.p.), which induced *status epilepticus* (SE; 3-4 hours duration) in all rats. To reduce the peripheral muscarinic effects, the animals were preconditioned with atropine (0.04 mg/kg s.c. 20 minutes prior to pilocarpine injection). The animal behavior was monitored and the characteristic signs of SE (Walz, *et al.*, 1999) were noticed. Age-matched rats were injected with saline instead of pilocarpine. Diazepam (5 mg/kg, i.p.) was administered 1 hour after pilocarpine injection to terminate the convulsions. Animals were sacrificed at 4 hours (seizure period, SP) and 24 hours (recovery period, RP); hippocampi were removed. The hippocampi from saline injected rats were used as control. All himpocampi were stored at -80°C till experimentation.

3.14. SYT I POLYCLONAL ANTIBODY DEVELOPMENT

Electro-elution buffer

Tris base	-	25 mM
Glycine	-	192 mM
SDS	-	0.1%

The crude bacterial lysate containing GST-Syt I protein (see section 3.26) was electrophoresed on a 12% polyacrylamide gel. The band corresponding to the molecular weight of GST-Syt I protein (73.5 kDa) was cut out. The protein extraction was performed in electro-elution buffer for 10 hours at room temperature using electro-eluter (Bio-Rad, USA). In order to remove the SDS from the protein, the

solution was precipitated with 4 volumes of cold acetone at -80°C, over-night. The precipitate was washed with 80% acetone and dissolved in 1X PBS. To cleave Syt I protein from the GST tag, Thrombin (10 U) digestion was carried out over-night at 22°C with mixing. The digestion product was then resolved on a 12% polyacrylamide gel; the band corresponding to Syt I protein (47.5 kDa) was cut out and electro-eluted as mentioned above.

The basic methods were adapted for raising antibody (Harlow and Lane, 1988). The eluted Syt I protein was mixed with equal volume of Freund's complete adjuvant and intramuscularly injected to New Zealand White rabbit and 3 more booster doses were given with an interval of 28 days. After the 4^{th} booster dose the animal was sacrificed and total proteins were precipitated from the blood serum by saturated ammonium sulphate precipitation. The precipitated protein was dissolved in 1X PBS and dialyzed to remove the salt. The crude serum protein was fractionated by passing through Protein A-CL agarose column (Bangalore Genie, India). The column was washed using 10 column volumes of the following solutions, 2 M urea, 1 M LiCl and 100 mM Glycine, pH 2.5 and finally equilibrated with 10 mM Tris-Cl, pH 8.0. Before passing through the column, the pH of the crude serum protein was adjusted to 8.0 by adding 1/10 volume of 1 M Tris-Cl, pH 8.0. The column was washed with 10 column volumes of 10 mM Tris-Cl, pH 8.0, eluted the antibody with 100 mM Glycine, pH 3.0 and collected 500 µl each in tubes containing 50 µl of 1 M Tris-Cl, pH 8.0. The solution was mixed thoroughly to make the pH of the antibody solution back to pH 8.0. The absorbance of eluted antibody was measured at 280 nm and the peak fractions were pooled together. The antibody solution was dialyzed

against 1X PBS for 24 hours at 4°C. The Syt I antibody dilutions were standardized by dot blot assay.

3.15. WESTERN BLOTTING AND IMMUNOSTAINING OF BLOTS

Western transfer buffer

Tris-base	-	48 mM
Glycine	-	39 mM
SDS	-	0.039%
Methanol	-	20%

Blocking buffer

ECL advance blocking powder	-	2%
Tween 20	-	0.1%

Dissolved in 1X PBS, pH 7.4

Wash buffer

10 X PBS, pH 7.4	-	100 ml
Tween 20	-	0.1%

Made up to 1 litre with deionized water

The control and SP rat hippocampi (50 mg) were homogenized in 1X PBS (150 µl) using electronic homogenizer (Ultra Turrax T8, IKA Labortechnik, Germany) and the homogenate was centrifuged at 10,000 x g for 30 minutes at 4°C. The pellet was discarded and the total protein in the supernatant was quantified by microBradford method. Equal concentration of proteins (10 µg) were resolved on a 12% polyacrylamide-SDS gel and transferred to a nitrocellulose membrane by wet transfer method (Mini Trans-blot, Bio-Rad, USA) at 100 V for 2 hours at 4°C or at

100 V for 1 hour at room temperature using the western transfer buffer. The blots were washed with 1X PBS for 15 minutes (twice).

Immunostaining was performed using ECL advance western blotting detection kit (GE healthcare, UK) protocol. Briefly, blocking was performed for 1 hour at room temperature in blocking buffer. The membrane was rinsed with two changes of wash buffer. Polyclonal rabbit Syt I and synapsin antibodies (Sigma, USA) were used with the dilutions of 1:20,000 and 1:500, respectively. The blocking buffer was used as the diluent for all the antibodies. Syt I antibody incubation was for 1 hour at room temperature and the Synapsin incubation was for over-night at 4°C. After primary antibody incubation the membranes were rinsed with two changes of wash buffer and washed for 15 minutes (once) and for 5 minutes (3 times). The membranes were incubated in HRP conjugated goat anti rabbit IgG secondary antibody (1:200,000) for 1 hour at room temperature and washings were performed as mentioned above. The signals were detected by ECL advance western blotting detection reagents by mixing solution A and B in 1:1 ratio and incubating the membranes for 5 minutes at room temperature in dark. Excess detection reagent was drained off by holding the membrane gently with forceps and touching the edge against tissue paper. The membranes were wrapped in cling film and scanned using phosphor imager (FLA5100, Fujifilm, Japan) in chemiluminescence mode. The signal intensities of the bands were analyzed using MultiGauge software (Fujifilm, Japan).

3.16. IMMUNOHISTOCHEMISTRY

Buffered formalin (10%)

37-40% formalin	-	100 ml
NaH_2PO_4	-	4 g

Na_2HPO_4 - 6.5 g

Made up to 1 litre with distilled water.

Control rats and SP rats were deeply anesthetized and physiological saline containing heparin was injected through ascending aorta for 1 minute followed by perfusion fixation with buffered formalin for 20 minutes. The brain was removed, sliced and fixed over-night in buffered formalin. The brain slices were washed thoroughly by keeping inside a processing cassette and continuous stirring for 30 minutes in 1 liter distilled water. The slices were dehydrated by passing through a series of ethanol and finally in xylene.

50% ethanol	-	45 minutes
70% ethanol	-	45 minutes
95% ethanol	-	45 minutes
100% ethanol	-	45 minutes (2 times)
Xylene	-	15 minutes (2 times)

The slices were placed in molten paraffin wax at 60°C for 1 hour (repeated twice) and then paraffin embedded in the processing cassette at room temperature for 30 minutes and at 4°C for over-night. 5 micron sections were taken using microtome (Leica RM 2125RT, Germany) and set on egg ovalbumin coated slides.

3.16.1. H & E staining

To confirm the quality of the tissue sections, the sections were hematoxylin and eosion (H&E) stained. The sections were deparaffinized and hydrated before staining.

Xylene	-	15 minutes

90% isopropanol	-	2 minutes
70% isopropanol	-	2 minutes
Distilled water	-	2 minutes

The sections were put in Harrin haematoxylin stain for 15 minutes, rinsed with deionized water, added 1-2 drops of acid alcohol and dipped in Scott's tap water. Dehydrated in 70% isopropanol for 1 minute and Eosin stained for 1 minute. After washing with distilled water, the sections were dehydrated in 100% isopropanol for 2 minutes, cleared in xylene for 15 minutes and mounted in DPX for 1 hour. The sections were viewed under microscope.

3.16.2. Immunostaining

For immunohistochemistry, the slices were deparaffinized and rehydrated by passing through a series of solutions.

Xylene	-	5 minutes (3 times)
100% alcohol	-	3 minutes (2 times)
95% alcohol	-	3 minutes (2 times)
80% alcohol	-	3 minutes
50% alcohol	-	3 minutes
1 X PBS	-	3 minutes (2 times)

The sections were incubated in boiling citrate buffer pH 6.0 for 1 hour to retrieve the antigen epitopes, allowed to cool in the same buffer itself and then kept in 150 mM Glycine for 15 minutes. The sections were blocked using 10% rabbit non-immune serum for 30 minutes, washed (all the washings were performed using 1X PBS containing 0.05% Tween 20 for 5 minutes, 3 times) and incubated with 1:500

diluted polyclonal Rabbit Syt I antibody for over-night at 4°C. FITC conjugated Goat anti rabbit IgG (1:200 dilution) used as the secondary antibody, incubated for 30 minutes at room temperature. Finally the sections were washed, mounted using 10% glycerol and scanned using the phosphor imager (FLA 5100, Fujifilm, Japan) at 473 nm, 700 V, FITC mode, 25 micron.

3.17. NORTHWESTERN BLOTTING

TNED buffer

Tris-HCl, pH 7.5	-	10 mM
NaCl	-	50 mM
EDTA, pH 8.0	-	0.1 M
DTT	-	1 mM

Pre-hybridization buffer

Non-fat milk powder	-	5%
Tris-HCl, pH 7.5	-	50 mM
NaCl	-	50 mM
EDTA, pH 8.0	-	0.1 M
DTT	-	1 mM

The Northwestern protocol was adapted from Zehner, *et al.*, (1997). SPF (10 µg) and pellet fraction of human brain lysate were electrophoresed on a 12% polyacrylamide denaturing gel. For refolding the denatured proteins, the gel was incubated in TNED buffer for 10 minutes, replaced fresh buffer and continued incubation for 20 minutes. The nitrocellulose membrane was soaked in Western transfer buffer without SDS for 20 minutes. The transfer was carried out at 100 V for 1 hour at room temperature; the membrane was washed twice with 1X PBS for 10

minutes and allowed to dry. The blot was made wet with TNED buffer and placed in pre-hybridization buffer for over-night at 4°C. The blot was briefly rinsed and washed with TNED buffer for 10 minutes at room temperature. The denatured RNA was mixed with TNED buffer and hybridized with the blot for 2½ hours at room temperature followed by washing for 10 minutes at room temperature (3 times). The bots were air dried and exposed to IP plates and scanned using phosphor imager (FLA5100, Fujifilm, Japan).

3.18. TRANSMISSION ELECTRON MICROSCOPY (TEM)

Phosphate buffer, pH 7.4 (0.1 M)

1M Na_2HPO_4 - 77.4 ml

1M NaH_2PO_4 - 22.6 ml

Made up to 1 litre with distilled water.

3.18.1. Fixation

Frozen hippocampal tissue from control, SP and RP rats were cut into 1 mm^3 size. The tissues were fixed in 3% gluteraldehyde in phosphate buffer and stored at 4°C. The tissues were washed with four changes of phosphate buffer at 4°C for 10 minutes each. Thereafter the tissues were post-fixed in 1% OsO_4, which acts as a fixative cum primary stain, for 2 hours at 4°C, again washed with four changes of phosphate buffer for 15 minutes and finally rinsed in distilled water for 5 minutes.

3.18.2. Dehydration

The tissues were dehydrated in the ascending grades of acetone.

50% acetone - 10 minutes in cold (2 times)

70% acetone - 10 minutes in cold (stored over-night at 4°C)

70% acetone - 10 minutes at room temperature

90% acetone - 10 minutes at room temperature (2 times)

100% acetone - 10 minutes at room temperature (2 times)

Dry acetone - 10 minutes

Following dehydration the samples were cleared in Propylene oxide for 10 minutes.

3.18.3. Infiltration

Infiltration of tissues with Epon Polybed 812 resin (Polysciences Inc., USA) was performed by keeping it in varying ratios of Propylene Oxide and resin.

Propylene Oxide: Resin in 3:1 ratio for 1½ hours

Propylene Oxide: Resin in 1:1 ratio for 1½ hours

Propylene Oxide: Resin in 1:3 ratio kept over-night in vacuum

Pure resin for 1 - 2 hours in vacuum

3.18.4. Embedding

The tissues were embedded in silicone molds containing Polybed 812 resin mixed with dodecenyl succinic anhydride (DDSA – Hardener), Nadic methyl anhydride (NMA -Hardener) and Dimethylaminomethyl phenol (DMP - Accelerator) in appropriate ratios as per the kit instructions (Polysciences Inc., USA). The molds were placed in an oven at 60°C for 3 days for polymerization of the resin blocks.

3.18.5. Ultra-thin sectioning

Ultra-thin sections of 50-70 nm thickness were cut using a diamond knife (Diatome®) and sections were taken on to the shiny side of the copper grid (300 mesh size).

3.18.6. Staining

The ultra thin sections were stained in Uranyl acetate, by immersing the grids with the section side up, for 2 hours; thereafter washed in methanol–water mixture of 100%, 80 % and 50 %. The sections were then stained for 10 minutes in Lead citrate in 0.1 N NaOH (prepared in CO_2 free water) by floating the grids on the drop of the stain with the section side facing down in a CO_2-free petri dish (placing NaOH pellets). The grids were then washed in four changes of distilled water and air dried.

3.18.7. Viewing

The sections were viewed under the electron microscope (Model Hitachi H-600, Japan) at an accelerating voltage of 75 kV with 40,000X magnification and photographed (Kodak Ilford film, USA).

3.19. NORTHERN HYBRIDIZATION

20 X SSC

Sodium chloride	-	175.3 g
Sodium citrate	-	27.6 g

Dissolved in 800 ml deionized water, adjusted pH to 7.0 and made up to 1 litre.

Northern prehybridization/hybridization buffer

Sodium phosphate, pH 7.2	-	0.5 M
SDS (w/v)	-	7%
EDTA, pH 7.0	-	1 mM

Denatured RNA samples (10 µg) from control, SP and RP rats were electrophoresed. The gel was rinsed in deionized water, soaked in 5 gel volumes of

0.05 N NaOH for 20 minutes, transferred in 10 gel volumes of 20 X SSC for 40 minutes and transferred to positively charged nylon membrane (Amersham Biosciences, USA) using wet transfer method (Sambrook and Russel, 2001). The gel was placed on a Whatman paper wick, saturated with 20 X SSC by capillary action on a platform in inverted position. The wet nylon membrane was placed carefully on the gel without trapping any air bubbles. It was overlaid with a wad of 10-15 Whatman filter paper pre-soaked in 2 X SSC and above which placed a dry stack of filter paper. Appropriate weight was placed on top of the filter paper stack and the whole assembly was wrapped tightly with cling film and kept undisturbed for over-night to allow the capillary transfer. The transfer unit was dislodged and well positions were marked on the nylon membrane before removing from the assembly. The membrane was washed in 6 X SSC at room temperature for 5 minutes and allowed to dry for 30 minutes. The membrane was fixed by UV-irradiation at 254 nm for 2 minutes and stored at room temperature protected from light.

α-^{32}P-labeled Syt I coding region RNA probe was synthesized by *in vitro* transcription using T7 RNA polymerase (see section 3.23). The membrane was incubated in prehybridization/hybridization buffer at 68°C for 2 hours. Hybridization was carried out at 68°C for over-night using Syt I RNA probe (1:500 diluted), which was denatured by heating at 99°C for 10 minutes and immediately chilled on ice before adding to fresh hybridization buffer. The blots were washed with 1 X SSC, 0.1% SDS at room temperature for 10 minutes (once) and with 0.5 X SSC, 0.1% SDS at 68°C for 10 minutes (3 times). The blots were exposed to imaging plate for 8-16 hours and scanned using phosphor Imager (FLA5100, Fujifilm, Japan). The blots

were deprobed and hybridized with β-actin RNA under similar conditions mentioned above.

3.20. QUANTITATIVE REVERSE TRANSCRIPTASE PCR (qRT-PCR)

5X Reaction buffer

Tris-Cl, pH 8.3	-	50 mM
KCl	-	50 mM
$MgCl_2$	-	4 mM
DTT	-	10 mM

7.6 µg of RNA isolated from control, SP and RP rat hippocampi were used to reverse transcribe β-actin (internal control) and Syt I genes using Revert Aid M-MuLV reverse transcriptase enzyme (MBI Fermentas, Canada) and gene specific primers. In reverse transcriptase reaction, the RNA was denatured at 70°C for 5 minutes in the presence of reverse primer and immediately chilled on ice. After adding 4 µl of 5 X reaction buffer, 2 mM dNTP mix and ribonuclease inhibitor (15 U), the reaction was continued at 37°C for 5 minutes. Finally 100 U of reverse transcriptase enzyme was added and incubated at 42°C for 1 hour. The reaction was stopped by keeping at 70°C for 10 minutes.

The resulting cDNA were analyzed by qRT-PCR (DNA Engine OPTICON 2-MJ Research, Bio-Rad, USA) using the 2X PCR Master Mix for SYBR-Green I assays (Eurogentec, Belgium). The analysis was performed using MJ Opticon Monitor Analysis Software version 3.1 (Bio-Rad, USA).

PCR conditions:

Syt I		β-actin	
94°C 10 minutes		94°C 10 minutes	
94°C 30 seconds	40 cycles	94°C 30 seconds	40 cycles
50°C 30 seconds		58°C 30 seconds	
72°C 2 minutes		72°C 2 minutes	
72°C 15 minutes		72°C 15 minutes	

Table 3: qRT-PCR primers

Gene	Primers	PCR product size
β-actin	5' GCCAACCGTGAAAAGATGAC-3' (Forward) 5'-AGCCACCAATCCACACAGAGTA-3' (Reverse)	691 bp
Syt I	5'- ATCTCCAGAGCGCTGAGAAAG-3' (Forward) 5'- AAAGGCTTCGTTTTCCCTTTAC-3' (Reverse)	503 bp

The relative expression level of mRNA was determined from the threshold cycle (C_T, obtained from the software analysis) for amplification using $2^{-\Delta\Delta C}{}_T$ method (Livak and Schmittgen, 2001).

$\Delta\Delta C_T = (C_{T\ test} - C_{T\ control})_{\text{at time T}} - (C_{T\ test} - C_{T\ control})_{\text{at time 0}}$

$C_{T\ test}$ - Threshold value for Syt I amplification

$C_{T\ control}$ - Threshold value for β-actin amplification

Time T - SP or RP (epileptic rat)

Time 0 - Non-epileptic rat control

3.21. MICROARRAY ANALYSIS

The mRNA from rat hippocampi during SP, RP and control were isolated using oligoTex mRNA purification kit (Qiagen, Germany). The microarray experiment was conducted using Applied Biosystem Expression array system (Applied Biosystem, USA). Digoxigenin labeled cRNA were synthesized using RT-IVT kit and screened using Rat Genome Survey Microarray slide (Applied Biosystems, USA) as per the manufacturer's instructions. The signals were detected using chemiluminescence detection kit and 1700 microarray analyzer. Data analysis was carried out using 'R' (www.r-project.org) and Spotfire DecisionSite for Microarray Analysis (Spotfire Inc. USA). Fold changes of Syt isoforms, other synaptic protein genes and seizure and stress associated genes mRNA expression in SP and RP were calculated from the signal intensities compared to the control.

3.22. CLONING OF GENE FOR THE SYNTHESIS OF RNA CONSTRUCTS

PCR buffer (1X)

Tris-HCl, pH 8.8	-	10 mM
KCl	-	50 mM
Nonidet P40	-	0.08%

Cohesive end ligation buffer (1X)

Tris-HCl, pH 7.4	-	50 mM
$MgCl_2$	-	10 mM
DTT	-	20 mM
BSA	-	50 µg/ml
ATP	-	1 mM

3.22.1. Syt I 3' UTR RNA construct

To generate pTZ57R/T-Syt I 3' UTR plasmid, a region containing GT repeats and Heptamer sequence (GTCAATG) was PCR amplified (Robocycler Gradient 96, Stratagene, USA) using genomic DNA isolated from human brain cortex tissue.

Components of PCR mixture: Forward and reverse primers, 2 mM dNTP mix, 2 mM $MgCl_2$, PCR buffer, 2 U of Taq DNA polymerase (MBI Fermentas, Canada) and genomic DNA as template.

PCR condition:

94°C 10 minutes

94°C 1 minute
58°C 1 minute
72°C 1 minute
} 35 cycles

72°C 30 minutes

Table 4: Syt I 3' UTR PCR primers

Gene	Primers	PCR product size
Syt I 3' UTR	5'-CATAGCCACAAAACAGAATAGC-3' (Forward) 5'-CAAACTCTAATGTGCAAACC-3' (Reverse)	360 bp

The purified PCR product was cloned in pTZ57R/T vector (MBI Fermentas, Canada) by ligation reaction using cohesive end ligation buffer at 22°C for over-night. The presence of the gene and orientation were confirmed by restriction digestions (Eco R1, Eco R1-Bam H1) and sequencing. The sequence was deposited in GenBank (Accession No. DQ448032). Syt I 3' UTR gene was released from the reverse clone

of pTZ57R/T-Syt I 3' UTR plasmid by restriction digestion with Pvu II enzyme and used for the *in vitro* transcription of Syt I 3' UTR RNA. For synthesizing the reverse Syt I 3' UTR RNA (as negative control in RNA-protein interaction), the direct clone in pTZ57R/T was selected.

The Syt I 3' UTR smaller fragments namely, Syt I_{1-171}, Syt I_{1-101}, Syt I_{94-360} and Syt $I_{102-302}$ fragments were prepared from digestion of either the Syt I 3' UTR PCR product or pTZ57R/T-Syt I 3' UTR plasmid.

3.22.2. Syt I_{1-171} RNA construct

The pTZ57R/T-Syt I 3' UTR plasmid was digested with Pvu II fragment to release the Syt I 3' UTR fragment. The eluted Pvu II fragment was digested with Apa L1 enzyme. This Pvu II-Apa L1 fragment of size 421 bp was used for the *in vitro* transcription of Syt I_{1-171} RNA.

3.22.3. Syt I_{1-101} RNA construct

The purified Syt I 3' UTR PCR product was digested with Ple I enzyme and two fragments (259 bp and 101 bp) were obtained. The 101 bp fragment was gel eluted and end-filled with Taq DNA polymerase by incubating at 72°C for 20 minutes. The reaction mixture contained 2.5 mM dNTP mix, 2 mM $MgCl_2$, 1 X PCR buffer and 2 U of Taq polymerase. The DNA was ligated into pTZ57R/T vector. The presence of gene was confirmed by double digestion with Eco R1 and Sal I enzymes and the orientation of the gene was confirmed by sequencing reaction. The reverse clone of pTZ57R/T-Syt I_{1-101} was linearized with Xba I for the *in vitro* transcription of Syt I_{1-101} RNA fragment.

3.22.4. Syt I_{94-360} RNA construct

The purified Syt I 3' UTR PCR product was digested with Hinf I enzyme and two fragments (267 bp and 93 bp) were obtained. The 267 bp fragment was gel eluted, end-filled with Taq polymerase and cloned in pTZ57R/T vector as mentioned above. The presence of gene and orientation in the vector was confirmed by Apa L1 digestion and the reverse clone was linearized with Xba I for synthesizing Syt I_{94-360} RNA fragment by *in vitro* transcription.

3.22.5. Syt $I_{102-302}$ RNA construct

The purified Syt I 3' UTR PCR product was digested with Ple I enzyme and two fragments (259 bp and 101 bp) were obtained. The 259 bp fragment was gel eluted, end-filled with Taq DNA polymerase and cloned in pTZ57R/T vector; then, 200 bp gene fragment was sub-cloned in pGEMT vector (Promega, USA) and confirmed the presence and orientation of gene by Apa L1 and Rsa I digestions. The direct clone in pGEMT vector was Sal I linearized and used for the *in vitro* transcription of RNA.

3.22.6. β-actin RNA construct

As a negative control RNA for protein binding, the β-actin RNA was used. For this the gene was amplified by RT-PCR from rat brain cortex RNA (for the PCR primers and conditions see section 3.20) and cloned in pTZ57R/T vector. The presence and orientation of gene in pTZ57R/T vector was confirmed by restriction digestions, the reverse clone was linearized with Eco R1 and used for the *in vitro* synthesis of β-actin RNA.

3. 23. *IN VITRO* TRANSCRIPTION OF RNA

Transcription buffer (1X)

Tris-HCl pH 7.9	-	40 mM
$MgCl_2$	-	6 mM
DTT	-	10 mM
NaCl	-	10 mM
Spermidine	-	2 mM

The labeled Syt I 3' UTR, Syt I_{1-171}, Syt I_{1-101}, Syt I_{94-360}, Syt $I_{102-360}$, β-actin and reverse Syt I 3' UTR RNAs were synthesized by *in vitro* transcription using T7 promoter with α-^{32}P-UTP in presence of transcription buffer, 10 mM NTP (ACG), 0.1 µl of 20 mM BSA, 30 U RNase inhibitor by T7 RNA polymerase (20 U/µl, MBI) enzyme for 2 hours at 37°C. The reaction was continued for 1 hour after adding 2 µl of 0.5 mM UTP. The reaction was stopped by treating the transcribed RNA with 5U of RNase free DNase I enzyme (MBI Fermentas, Canada) for 30 minutes at 37°C. The *in vitro* transcribed RNA probes were further purified by passing through NucleoSpin RNA isolation column (Macherey-Nagel, Germany) or Perfect RNA column (Eppendorf, Germany). The synthesis of unlabeled RNA probes were performed in a similar manner except that radioactive UTP was not included in the reaction mixture.

3.24. CLONING OF SYT I GENE CONSTRUCTS

Syt I gene corresponding to the full coding region was amplified from Wistar rat brain hippocampus RNA by RT-PCR (GeneAmp PCR System 9700, Applied Biosystems, USA).

Reverse transcription condition	PCR condition	
70°C 5 minutes	94°C 10 minutes	
37°C 5 minutes	94°C 30 seconds	30 cycles
42°C 1 hour	50°C 30 seconds	
70°C 10 minutes	72°C 2 minutes	
	72°C 15 minutes	

Components of PCR mixture: Forward and reverse primers, 2 mM dNTP mix, 2 mM $MgCl_2$, PCR buffer, 2 U of Taq DNA polymerase (MBI Fermentas, Canada) and cDNA from RT reaction.

Table 5: Syt I PCR primers

Gene	Primers	PCR product size
Syt I	5'-TGAACCAAAAATGGTGAGTGC-3' (Forward) 5'-AAAGGCTTCGTTTTCCCTTTAC-3' (Reverse)	1284 bp
Syt I C2	5'-TGGATGACGATGCTGAAACC-3' (Forward) 5'-AAAGGCTTCGTTTTCCCTTTAC-3' (Reverse)	929 bp
Syt I C2A	5'-TGGATGACGATGCTGAAACC-3' (Forward) 5'-GGCCAAAATCCACGGTGTTC-3' (Reverse)	406 bp
Syt I C2B	5'-ATCTCCAGAGCGCTGAGAAAG-3' (Forward) 5'-AAAGGCTTCGTTTTCCCTTTAC-3' (Reverse)	503 bp

The PCR product was purified by gel extraction and cloned in pTZ57R/T vector. Plasmid was isolated and the presence of the gene insert was confirmed by restriction digestions. The regions corresponding to Syt I C2, Syt I C2A and Syt I

C2B were amplified from this clone by PCR (conditions as above) and cloned in pTZ57R/T vector and confirmed by restriction digestions. The pTZ57R/T-Syt I, pTZ57R/T-Syt I C2A and pTZ57R/T-Syt I C2B clones were also verified by sequencing reaction.

3.25. SUB-CLONING OF SYT I GENE CONSTRUCTS FOR PROTEIN EXPRESSION

3.25.1. Sub-cloning of Syt I, Syt I C2A and Syt I C2B

1. Released Syt I/Syt I C2A/Syt I C2B genes from respective plasmids by Xba I-Hind III double digestion
2. Cloned at Xba I-Hind III site of pUC19 vector (MBI Fermentas, Canada)
3. Released Syt I/Syt I C2A/Syt I C2B gene from respective plasmids by Eco R1-Sal I double digestion
4. Cloned at Eco R1-Sal I site of pGEX4T1 vector (Amersham Biosciences, USA)

3.25.2. Sub-cloning of Syt I C2

1. Released Syt I C2 gene from pTZ57R/T-Syt I C2 plasmid by Eco R1-Sal I double digestion
2. Cloned at Eco R1-Sal I site of pGEX4T1 vector

The presence of insert in all the plasmids was confirmed by restriction digestion. The plasmids were also sequenced to confirm the sequence and the reading frame in the pGEX4T1 expression vector.

3.26. RECOMBINANT PROTEIN EXPRESSION AND PROTEIN LYSATE PREPARATION

3.26.1. Small-scale expression of the recombinant proteins

The Syt I gene clones in pGEX4T1 (pGEX4T1-Syt I, pGEX4T1-Syt I C2, pGEX4T1-Syt I C2A and pGEX4T1-Syt I C2B) as well pGEX4T1 (empty expression vector as positive control) were transformed into BL 21 cells, a strain defective in Omp T and Lon protease production, for the GST-fusion protein expression. A single colony was inoculated in 5 ml cultures (LB medium containing 70 μg/ml ampicillin) and incubated at 37°C for over-night. From each of the over-night culture, 100 μl was inoculated in 5 ml LB medium containing 70 μg/ml ampicillin. The cultures were incubated at 37°C until cells reach an absorbance of 0.5 OD at A_{600}. 1 ml of each uninduced culture (zero hour aliquot) was transferred to microfuge tubes and stored at 4°C. The remaining culture was induced by adding 1 mM IPTG and incubated at 37°C for 3 hours. At various time points during the IPTG induction period (1, 2 and 3 hours), 1 ml aliquots of the culture was transferred to microfuge tubes, measured OD at A_{600} and stored at 4°C. These aliquots were centrifuged at 10,000 x g for 2 minutes at room temperature to pellet down the bacterial cells. The pellet was resuspended in 100 μl of 1 X SDS gel-loading buffer, denatured at 99°C for 10 minutes and immediately chilled on ice for 2 minutes. The tubes were centrifuged at 10,000 x g for 2 minutes at room temperature. The volume corresponding to 0.3 OD of the sample was electrophoresed on 10-12% polyacrylamide-SDS gel.

3.26.2. Large-scale expression of the recombinant proteins

For large-scale expression of Syt I -C2, -C2A and -C2B proteins, pGEX4T1-

Syt I C2, pGEX4T1-Syt I C2A and pGEX4T1-Syt I C2B clones were transformed in BL21 cells cultured over-night. 2 ml from this culture was inoculated into 100 ml of LB medium containing 70 μg/ml ampicillin and incubated at 37°C in an orbital shaker. After reaching 0.5 OD, 1 ml aliquot was transferred and stored as zero hour culture. 1 mM IPTG was added to the media and allowed the bacteria to grow for 3 hours. From the IPTG induced culture 1 ml aliquot was transferred and stored as 3 hour culture for SDS-PAGE analysis. The remaining bacterial culture was centrifuged at 10,000 x g for 5 minutes at 4°C. The pellet was washed twice with 1X PBS and resuspended in 1 ml of 1X PBS. Lysozyme was added to a final concentration of 1 mg/ml and kept on ice for 30 minutes. The lysozyme-treated cell suspensions were subjected to freeze-thaw lysis; the tubes were frozen in liquid N_2 for 20 seconds and immediately thawed in warm water (37°C). The freeze-thaw cycle was repeated for 10 times. The highly viscous lysate was treated with RNase free DNase I enzyme (MBI Fermentas, Canada) at room temperature until it was no longer viscous. The lysate was centrifuged at 15,000 x g at 4°C for 15 minutes and the clear supernatant was transferred to fresh tubes.

For the large-scale expression of GST-Syt I protein, 5 ml of the over-night culture was inoculated into 250 ml of LB medium containing 70 μg/ml ampicillin. IPTG induction, lysozyme treatment, freeze-thaw lysis, DNase treatment and centrifugation steps were followed as above. As the GST-Syt I protein was highly insoluble and formed inclusion bodies, the pellet was treated with 3 M urea solution for over-night at 8°C with continuous mixing. The lysate was centrifuged at 15,000 x g at 4°C for 15 minutes and the clear supernatant was transferred to fresh tubes.

The protein concentration in the supernatant was measured by MicroBradford assay. The presence of GST fusion proteins in this soluble fraction was confirmed by SDS-PAGE analysis by the electrophoresis of lysates along with 0 hour and 3 hour 0.3 OD samples.

3.27. PURIFICATION OF RECOMBINANT GST FUSION PROTEIN

Elution buffer

Glutathione	-	10 mM
Tris-HCl, pH 8.0	-	50 mM

The recombinant GST-fusion proteins were purified either using Glutathione Sepharose 4B MicroSpin columns (Amersham Biosciences, USA) with microcentrifuge-based purification or GSTrap HP columns by affinity chromatography with AKTA purifier (Amersham Biosciences, USA).

3.27.1. Microcentrifuge based purification

The resin in Glutathione Sepharose 4B MicroSpin column was resuspended by vortexing gently. The cap was loosened one-fourth turn and snapped off the bottom closure. The column was placed into a 1.5 ml microcentrifuge tube, spun at 800 x g for 1 minute and discarded the storage buffer. The bottom cap was replaced and 600 µl of the protein lysate (passed through 0.45 µm filter) was added to the column. The column was mixed gently at room temperature for 10 minutes to allow the binding of GST-fusion proteins to the Glutathione Sepharose 4B matrix. The column was centrifuged at 800 x g for 1 minute and the flow-through was discarded. The

Glutathione Sepharose 4B matrix was washed with 600 µl of 1X PBS for 2 times. Added 100-200 µl of Glutathione elution buffer and incubated at room temperature for 10 minutes. The purified GST-fusion protein was obtained by centrifuging the columns at 800 x g for 1 minute. The eluted protein was confirmed by SDS-PAGE.

3.27.2. Affinity chromatography

The GSTrap HP 1 ml columns, which can withstand a maximum backpressure of 0.3 MPa were used. The binding buffer (1X PBS), elution buffer and the protein lysate were filtered by through a 0.45 µm filter. Unicorn 5.10 software (GE Healthcare, USA) was used for controlling the chromatography with AKTA purifier. The chromatography program is shown **(Figure 11)**.

Briefly in the chromatography method, the column was equilibrated with 5 column volumes of binding buffer (Pump A1), sample was injected, washed with 5 column volumes of binding buffer, eluted with 5 column volumes of elution buffer (Pump B1), peak fractions at A_{280} were collected and column was re- equilibrated with binding buffer. The eluted protein was confirmed by SDS-PAGE.

3.28. ELECTROPHORETIC MOBILITY SHIFT ASSAY

RNA-protein binding buffer (2X)

Tris-HCl pH 7.5	-	40 mM
KCl	-	100 mM
$MgCl_2$	-	10 mM
DTT	-	2 mM
Glycerol	-	20%
BSA	-	200 µg/ml

Base: Volume, Unit : ml

Main method

0.00 Base CV, 1 {ml}, Any
0.00 Alarm_Pressure Enabled, 0.3 {MPa}
0.00 Block Equilibriation
0.00 Base same as Main
0.00 Pump A Inlet A1
0.00 Injection valve Load
0.00 Outlet valve Waste F1
0.00 Flow 1 {ml/min}
5.00 End_Block
5.00 Block Sample_inject
5.00 Base same as Main
5.00 Flow 0.5 {ml/min}
5.00 Auto Zero UV
5.00 Injection valve Inject
6.50 End_Block
6.50 Block Wash
6.50 Base same as Main
6.50 Injection valve Load
6.50 Flow 1 {ml/min}
11.50 End_Block
11.50 Block Elution
11.50 Base same as Main
11.50 Flow 0.5 {ml/min}
11.50 Auto Zero UV
11.50 Pump B Inlet B1
11.50 Gradient 100 {%B}, 0.00 {base}
11.50 Outlet valve F2
11.50 Fractionation 12 mm, 0.5 {ml}, First Tube, Volume
16.50 End_Block
16.50 Block Re-equilibriation
16.50 Base same as Main
16.50 Flow 1 {ml/min}
16.50 Outlet valve Waste F1
16.50 Fractionation Stop
16.50 Pump A Inlet A1
16.50 Gradient 0.0 {%B}, 0.00 {base}
21.50 End_Block
21.50 End_Method

Figure 11: Chromatography program for the affinity purification of GST-C2 and GST-C2B proteins using GSTrap HP columns with AKTA purifier (GE Healthcare, USA)

6X gel-loading buffer

Bromophenol blue	-	0.09%
Xylene cyanol FF	-	0.09%
Glycerol	-	60%
EDTA	-	60 mM

5 X TBE

Tris base	-	54 g
Boric acid	-	27.5 g
0.5 M EDTA, pH 8.0	-	20 ml

Made up to 1 litre with deionized water.

The electrophoretic mobility shift assay was performed according to the earlier reports (Setzer, 1999). *In vitro* transcribed 5-7 ng α-^{32}P-labeled RNAs were denatured (by heating at 99°C for 10 minutes and immediately chilling on ice for 2 minutes), incubated with 1 μg of human brain lysate (soluble fraction) or purified recombinant protein in the presence of RNA-protein binding buffer for 30 minutes at 37°C. The reactions were stopped by adding 6X gel loading dye and the samples were electrophoresed on a 7% polyacrylamide-TBE native gel. The gel was pre-run at 50 V for 1 hour and run at 100 V till the bromophenol dye front started running out of the gel. The gel was rinsed with deionized water, dried and exposed to X-ray film (Kodak, India) or imaging plate. The imaging plates were analyzed using phosphor imager (FLA5100, Fujifilm, Japan).

3.29. UV CROSS-LINKING ASSAY

The SPF was incubated with labeled Syt I 3' UTR RNA at 37°C for 30 minutes in binding buffer (mentioned above). UV cross-linking assay was carried out

as described earlier (Hanna, *et al.*, 1999). Briefly, the RNA-protein complex was UV cross-linked at 254 nm for 20 minutes (in ice cold conditions). 100 mM DTT was added and incubated at room temperature for 5 minutes in dark. The reaction mixtures were treated with RNase (100 ng) at 37°C for 15 minutes. The samples were resolved on a 12% SDS-polyacrylamide gel and analyzed using phosphor imager (FLA5100, Fujifilm, Japan). Protein molecular weight markers were used to estimate the relative molecular mass.

3.30. COMPETITIVE ASSAY

The specificity of RNA-protein interaction was checked by competitive assay. The RNA-protein binding assay was performed in the presence of increasing concentrations of unlabeled RNA as competitor. For SPF 25, 50, 100 and 200% of unlabeled transcript were used. The unlabeled probe concentrations for GST-Syt I were 10, 25, 50 and 100%. Both labeled and unlabeled RNA were denatured at 99°C for 10 minutes; the solution was cooled on ice and then protein was added in the reaction mix. After incubating at 37°C for 30 minutes, the samples were resolved on 5% non-denaturing gel as mentioned in the electrophoretic mobility shift assay and analyzed.

3.31. FILTER-BINDING ASSAY

The association of proteins to RNA and binding kinetics were checked by filter binding assay (Hall KB, 1999). RNA-protein interactions were performed with GST-C2 (0-160 pMol) and GST-C2A (0-230 pMol) with Syt I 3' UTR RNA as mentioned in electrophoretic mobility shift assay. The RNP complex was filtered through a sandwich of nitrocellulose membrane (Hybond-C Extra, Amersham

Biosciences USA) and nylon membrane (Hybond-N^+, Amersham Biosciences USA) using a slot blot manifold (Amersham Biosciences, USA) under vacuum. The wells were washed twice with 1 ml of RNA-protein binding buffer (twice). The membranes were dried and exposed to imaging plate for appropriate time. The imaging plates were scanned using phosphor imager (FLA5100, Fujifilm, Japan). The band intensities on the Nylon membranes were measured by densitometric analysis using MultiGauge software (Fujifilm, Japan). The bound probe concentration to the protein was calculated by subtracting the normalized probe intensity in nylon membrane in presence of protein from the total probe added (normalized intensity from zero protein in nylon membrane).

3.32. *IN VITRO* TRANSLATION ASSAY

Syt I coding region and Syt I coding region with 3' UTR (360 bp) DNA in pGEMT vector were used as DNA templates for TNT Quick Coupled Transcription / Translation Systems (Promega, USA) in the presence of T7 RNA Polymerase and S^{35} Methionine (1000 Ci/mmole).

For pGEMT-Syt I clone, the gene was released from pTZ57R/T-Syt I plasmid by Eco R1-Sal I double digestion and cloned in pGEMT vector. The Syt I 3' UTR fragment was ligated to the immediate downstream of the full length coding region of Syt I gene in pGEMT vector. The Syt I 3' UTR (360 bp) fragment was released from pTZ57R/T-Syt I 3' UTR plasmid by double digestion with Sac I and Sal I enzymes. The pGEMT-Syt I plasmid was linearized with Sal I enzyme and partially digested with Sac I enzyme. The eluted Syt I 3' UTR fragment was ligated to the Sal I-Sac I digested pGEMT-Syt I. The plasmids were confirmed by restriction digestions.

For *in vitro* translation assay both the plasmids were linearized with Sal I enzyme. Equal concentrations of DNA (750 ng) were used in the translation assay and PCR enhancer was also included. The reaction was performed in a 10 µl volume with 65% of TNT T7 Quick Master Mix (Promega, USA) at 30°C for 90 minutes. The synthesized protein products were denatured by incubating at 70°C for 10 minutes and electrophoretically resolved through a 12% SDS-polyacrylamide gel. The gel was then fixed, dried and exposed to imaging plate for appropriate time. The imaging plates were scanned using phosphor imager (FLA5100, Fujifilm, Japan).

Chapter 4

RESULTS AND DISCUSSION

4.1. REGULATION OF SYT I PROTEIN LEVEL DURING SEIZURE

Studies using prolonged seizure models have shown significant variations in synaptic plasticity, including changes in the neurotransmitter release pathway and in the expression levels of synaptic proteins. Seizure is an excellent model to study gene expression variation (Sandberg, *et al.*, 2000). Administration of pilocarpine, a muscarinic agonist, induces clinical features analogous to temporal lobe epilepsy (TLE) and *status epilepticus* (SE) in rats (Cavalheiro, *et al.*, 1991; Porter, *et al.*, 2006; Rice and DeLorenzo, 1998). Studies have shown that pilocarpine can induce gene expression changes similar to the ones observed in human TLE (Becker, *et al.*, 2003; Kato, *et al.*, 1999). SE induces excessive neurotransmitter release within a short interval of time and Syt I is one of the primary responder to the exocytotic pathway. We checked the level of Syt I protein during seizure in hippocampi of animals at seizure period (SP) and recovery period (RP) by western blotting. Equal concentrations of protein were loaded for the western blotting **(Figure 12A)**, the blots were immunostained with Syt I antibody and antibody against synapsin, another synaptic vesicle protein (Sudhof, 2004) which was used as internal control. There was

a 62±0.12% reduction in Syt I level observed during SP, while the Syt I level recovered to 79±0.6% during RP, both compared to expression of Syt I in control rat hippocampus **(Figure 12B and D)**. However, the level of synapsin did not change significantly under similar conditions **(Figure 12C and D)**.

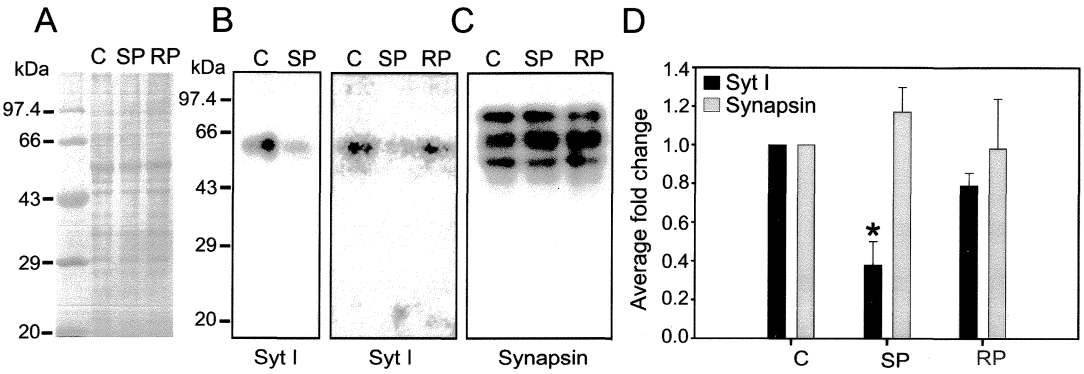

Figure 12: During seizure Syt I protein expression is downregulated (A) SDS-polyacrylamide gel (12%) showing equal concentration of control [C], SP and RP protein loaded. (B and C) Syt I and synapsin were detected using rabbit polyclonal antibodies in hippocampal protein extracts of SP, RP and control rats (n=3 per group). Anti-synapsin (Sigma-Aldrich, USA) detected, in addition to the expected 80 and 77 kDa bands, a cross-reacting lower-molecular-weight band in all three samples. (D) The graph shows fold-change in expression levels of Syt I and synapsin; the Syt I level was significantly reduced in SP relative to the control (*, $P<0.001$). Results are given as mean ± s.e.m.

Syt I protein reduction was evident in immunohistochemical analysis also. Immunohistochemistry of rat brain sections from control and SP rats showed approximately 90-95% reduced Syt I expression during SP; this downregulation was greatest in the hippocampal CA3 pyramidal region **(Figure 13)**.

a 62±0.12% reduction in Syt I level observed during SP, while the Syt I level recovered to 79±0.6% during RP, both compared to expression of Syt I in control rat hippocampus **(Figure 12B and D)**. However, the level of synapsin did not change significantly under similar conditions **(Figure 12C and D)**.

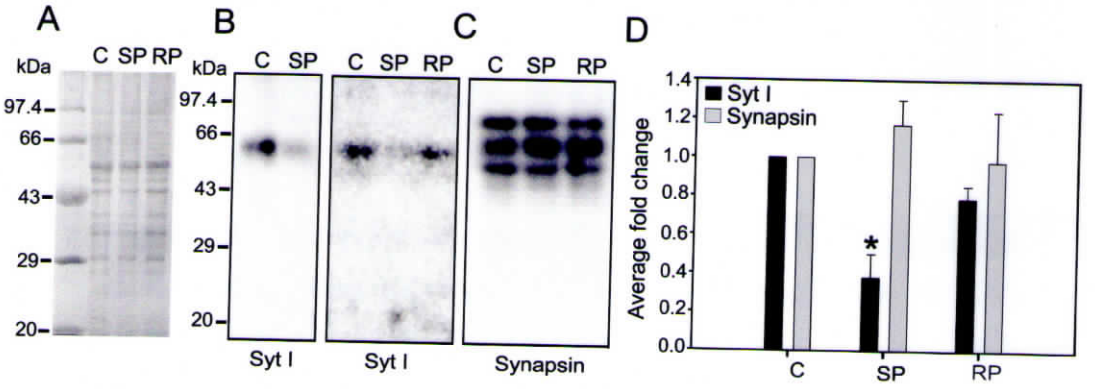

Figure 12: During seizure Syt I protein expression is downregulated (A) SDS-polyacrylamide gel (12%) showing equal concentration of control [C], SP and RP protein loaded. (B and C) Syt I and synapsin were detected using rabbit polyclonal antibodies in hippocampal protein extracts of SP, RP and control rats (n=3 per group). Anti-synapsin (Sigma-Aldrich, USA) detected, in addition to the expected 80 and 77 kDa bands, a cross-reacting lower-molecular-weight band in all three samples. (D) The graph shows fold-change in expression levels of Syt I and synapsin; the Syt I level was significantly reduced in SP relative to the control (*, $P<0.001$). Results are given as mean ± s.e.m.

Syt I protein reduction was evident in immunohistochemical analysis also. Immunohistochemistry of rat brain sections from control and SP rats showed approximately 90-95% reduced Syt I expression during SP; this downregulation was greatest in the hippocampal CA3 pyramidal region **(Figure 13)**.

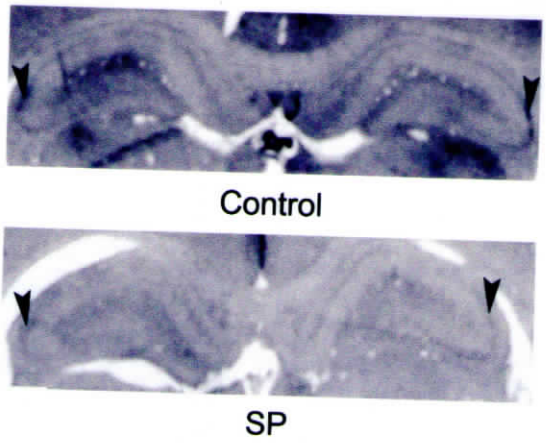

Figure 13: The immunohistochemical analysis using Syt I polyclonal antibody shows dramatic reduction in Syt I level especially in the CA3 pyramidal region of the hippocampus (arrow heads) during SP. This figure is a representation of three independent experiments.

The decrease in Syt I protein level cannot be related to synaptic vesicle density levels because seizure do not reduce the aggregate synaptic vesicle distribution pattern at the synapses (Crowder, *et al.*, 1999) and the constant level of synapsin also suggested the same. The number of active zones and synaptic vesicle density in hippocampal tissue samples of control, SP and RP rats were reconfirmed using Transmission Electron Microscopy (TEM). The synaptic vesicle density was calculated from TEM images and the data showed no significant variation in vesicle density in all the three samples **(Figure 14A-D)**. This observation suggested that the alteration in Syt I level might directly correlate with physiological changes within cells.

It is likely that this regulation of Syt I translation in the brain during seizure could lead to the control of the neurotransmitter release and thus to an extent prevent

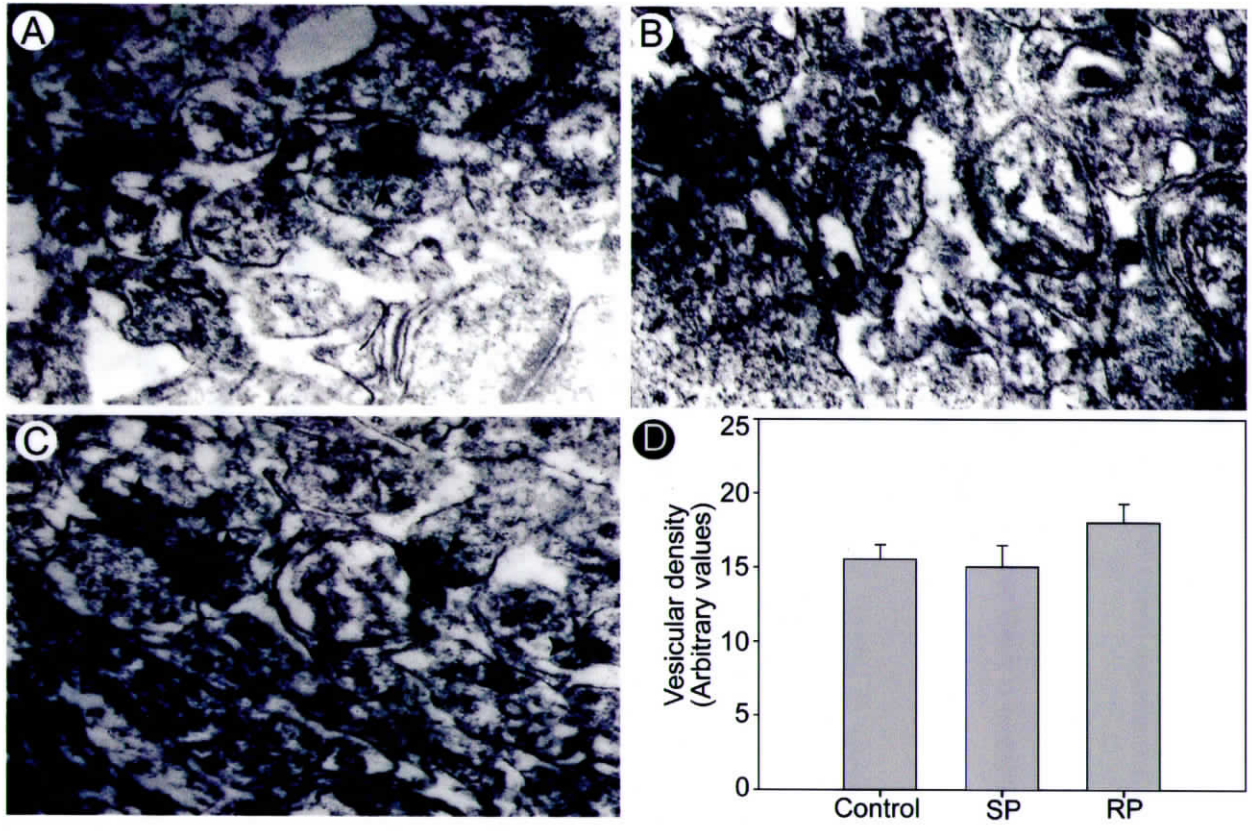

Figure 14: The number of active sites did not show reduction in seizure induced rodent models. Representative TEM images (40,000 X magnification) showing active sites (marked by arrow heads) in (A) control, (B) SP and (C) RP rat brain hippocampus tissue. (D) Graph showing the vesicle density of control, SP and RP. Data derived from 10-15 TEM images from 3 independent experiments, mean±s.e.m. The area of active sites measured using MultiGauge software (Fujifilm, Japan).

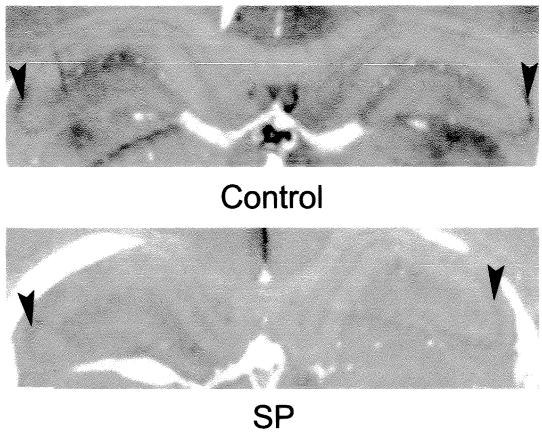

Figure 13: The immunohistochemical analysis using Syt I polyclonal antibody shows dramatic reduction in Syt I level especially in the CA3 pyramidal region of the hippocampus (arrow heads) during SP. This figure is a representation of three independent experiments.

The decrease in Syt I protein level cannot be related to synaptic vesicle density levels because seizure do not reduce the aggregate synaptic vesicle distribution pattern at the synapses (Crowder, *et al.*, 1999) and the constant level of synapsin also suggested the same. The number of active zones and synaptic vesicle density in hippocampal tissue samples of control, SP and RP rats were reconfirmed using Transmission Electron Microscopy (TEM). The synaptic vesicle density was calculated from TEM images and the data showed no significant variation in vesicle density in all the three samples **(Figure 14A-D)**. This observation suggested that the alteration in Syt I level might directly correlate with physiological changes within cells.

It is likely that this regulation of Syt I translation in the brain during seizure could lead to the control of the neurotransmitter release and thus to an extent prevent

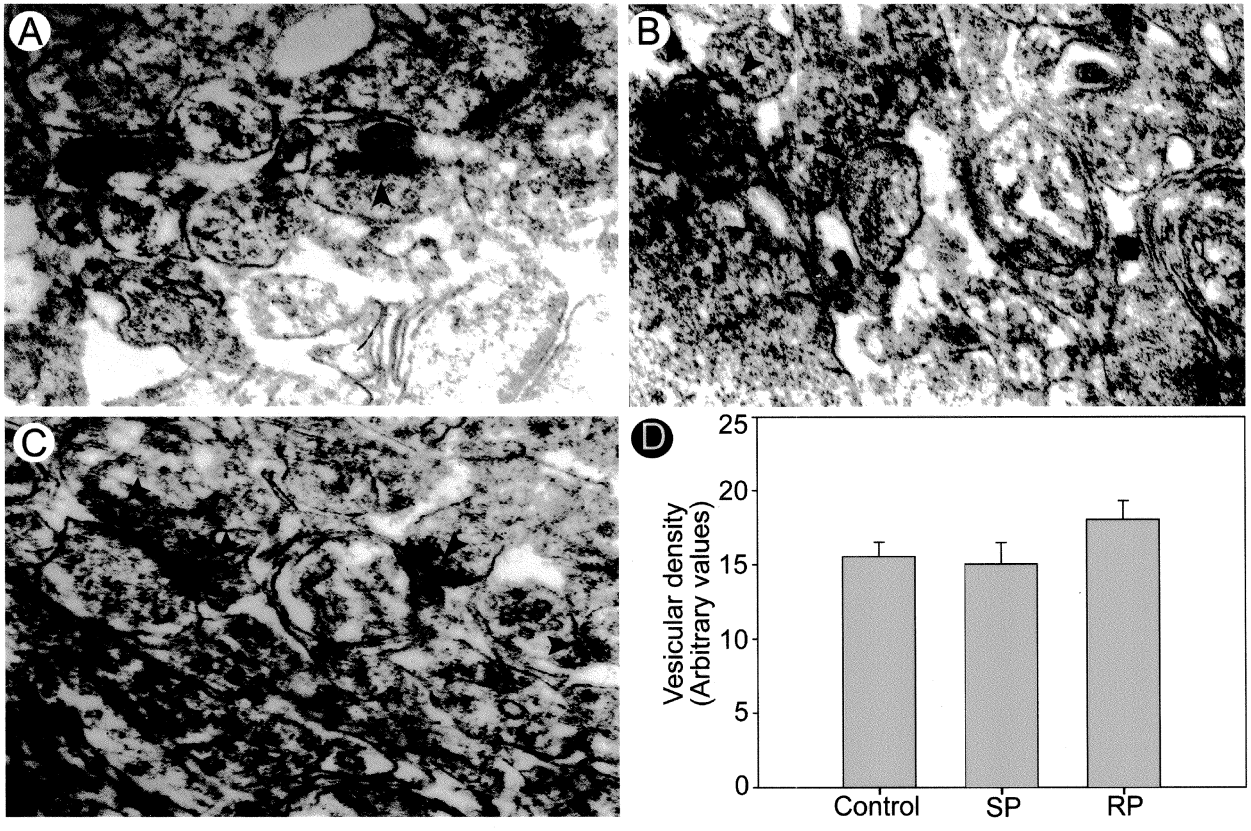

Figure 14: The number of active sites did not show reduction in seizure induced rodent models. Representative TEM images (40,000 X magnification) showing active sites (marked by arrow heads) in (A) control, (B) SP and (C) RP rat brain hippocampus tissue. (D) Graph showing the vesicle density of control, SP and RP. Data derived from 10-15 TEM images from 3 independent experiments, mean±s.e.m. The area of active sites measured using MultiGauge software (Fujifilm, Japan).

excitotoxicity. Our result corroborates with the decrease in Syt I level observed in mesial TLE patients (Yang, *et al.*, 2006). This dramatic reduction in Syt I level during SP, despite its half life of ~8 hours (Daly and Ziff, 1997), could be because of alternate transcription start point Met113 resulting in p40 Syt I (Bagala, *et al.*, 2003) or its hypersensitivity to proteolysis resulting in p39 Syt I (Perin, *et al.*, 1991a). However, the Syt I antibody failed to detect these forms of Syt I in our western blots **(Figure 12B)** probably because it was raised against full length p65 (Syt I). However, constant synthesis of Syt I (Mundigl, *et al.*, 1993) should have compensated the proteolytic loss of existing proteins unless there is instability of mRNA.

4.2. EXPRESSION LEVEL OF SYT I mRNA DURING SEIZURE

Chronic neuronal depolarization results in upregulation of two unusual Syt isoforms: Syt IV, with low affinity for membrane binding in response to Ca^{2+} influx (Littleton, *et al.*, 1999) and Syt X, with unknown function (Babity, *et al.*, 1997). However, there are data suggesting that Syt I mRNA level did not vary significantly during hyperactivation of neurons (Mahata, *et al.*, 1992). To confirm this we verified variations in the Syt I mRNA expression levels during SP and RP compared to the control using techniques like northern hybridization, qRT-PCR and microarray analysis.

4.2.1. Northern hybridization

Northern hybridization was carried out using total RNA from SP, RP and control hippocampus tissue. The RNA was quantitated by UV and equal amount from each sample were resolved on 1% agarose gel **(Figure 15A)** and transferred to nylon membrane. To analyze the Syt I mRNA level during different seizure periods

compared to control, β-actin level was used as an internal control. Hybridizations performed in high stringent conditions (see materials and methods). The results showed a steady state level of Syt I RNA in all the three conditions **(Figure 15B)**.

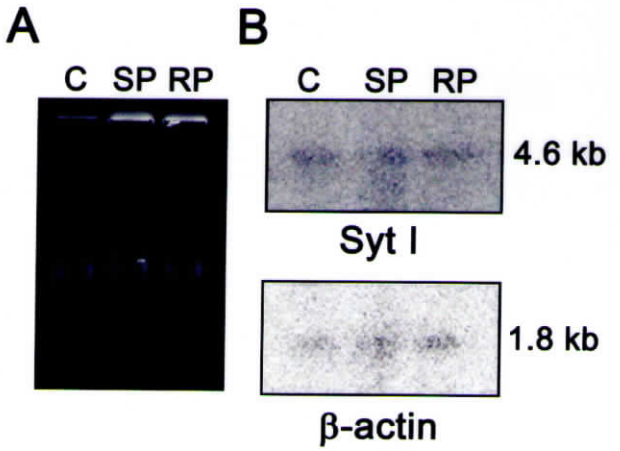

Figure 15: Syt I mRNA level remained constant during seizure. (A) 1% agarose-formaldehyde gel showing equal concentrations of RNA. (B) Representative northern blot of Syt I mRNA in control [C] rats and rats in SP and RP (n=2 per group). The blots were reprobed for β- actin (internal control).

4.2.2. Quantitative Reverse Transcriptase PCR (qRT-PCR)

qRT-PCR analysis was carried out to estimate the expression of Syt I mRNA level in SP and RP using $2^{-\Delta\Delta C}{}_T$ method with β-actin as internal control (Livak and Schmittgen, 2001). The β-actin level was used to normalize the RNA level in the reaction. The $2^{-\Delta\Delta C}{}_T$ value for SP was 1.02±0.16 (n=5) and for RP was 0.7±0.09 (n=4) indicating no obvious change in Syt I mRNA level **(Table 6 and Figure 16A and B)**.

compared to control, β-actin level was used as an internal control. Hybridizations performed in high stringent conditions (see materials and methods). The results showed a steady state level of Syt I RNA in all the three conditions **(Figure 15B)**.

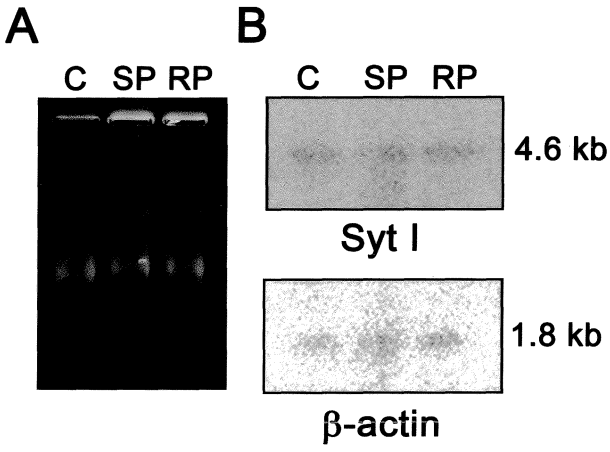

Figure 15: Syt I mRNA level remained constant during seizure. (A) 1% agarose-formaldehyde gel showing equal concentrations of RNA. (B) Representative northern blot of Syt I mRNA in control [C] rats and rats in SP and RP (n=2 per group). The blots were reprobed for β- actin (internal control).

4.2.2. Quantitative Reverse Transcriptase PCR (qRT-PCR)

qRT-PCR analysis was carried out to estimate the expression of Syt I mRNA level in SP and RP using $2^{-\Delta\Delta C}{}_T$ method with β-actin as internal control (Livak and Schmittgen, 2001). The β-actin level was used to normalize the RNA level in the reaction. The $2^{-\Delta\Delta C}{}_T$ value for SP was 1.02±0.16 (n=5) and for RP was 0.7±0.09 (n=4) indicating no obvious change in Syt I mRNA level **(Table 6 and Figure 16A and B)**.

Table 6: Data analysis using $2^{-\Delta\Delta C}{}_T$

Sample	C_T β-actin	C_T Syt I	$\Delta\Delta C_T$	$2^{-\Delta\Delta C}{}_T$
Control	14.56	12.59	0.17	0.89
SP	13.71	11.91		
Control	23.50	16.97	-0.04	1.028
SP	23.73	17.16		
Control	23.22	16.28	0.03	0.979
SP	23.41	16.50		
Control	16.15	13.06	0.72	0.61
SP	16.15	13.78		
Control	9.91	11.83	-0.69	1.61
SP	11.09	12.32		
Average $2^{-\Delta\Delta C}{}_T$ for SP – **1.020** and standard error – ±**0.16**				
Control	23.22	16.28	0.92	0.529
RP	24.40	18.38		
Control	14.77	12.77	0.84	0.559
RP	13.00	11.84		
Control	12.03	12.54	-0.24	0.847
RP	12.80	13.55		
Control	14.77	12.77	0.25	0.84
RP	13.23	11.48		
Average $2^{-\Delta\Delta C}{}_T$ for RP – **0.7** and standard error –± **0.09**				

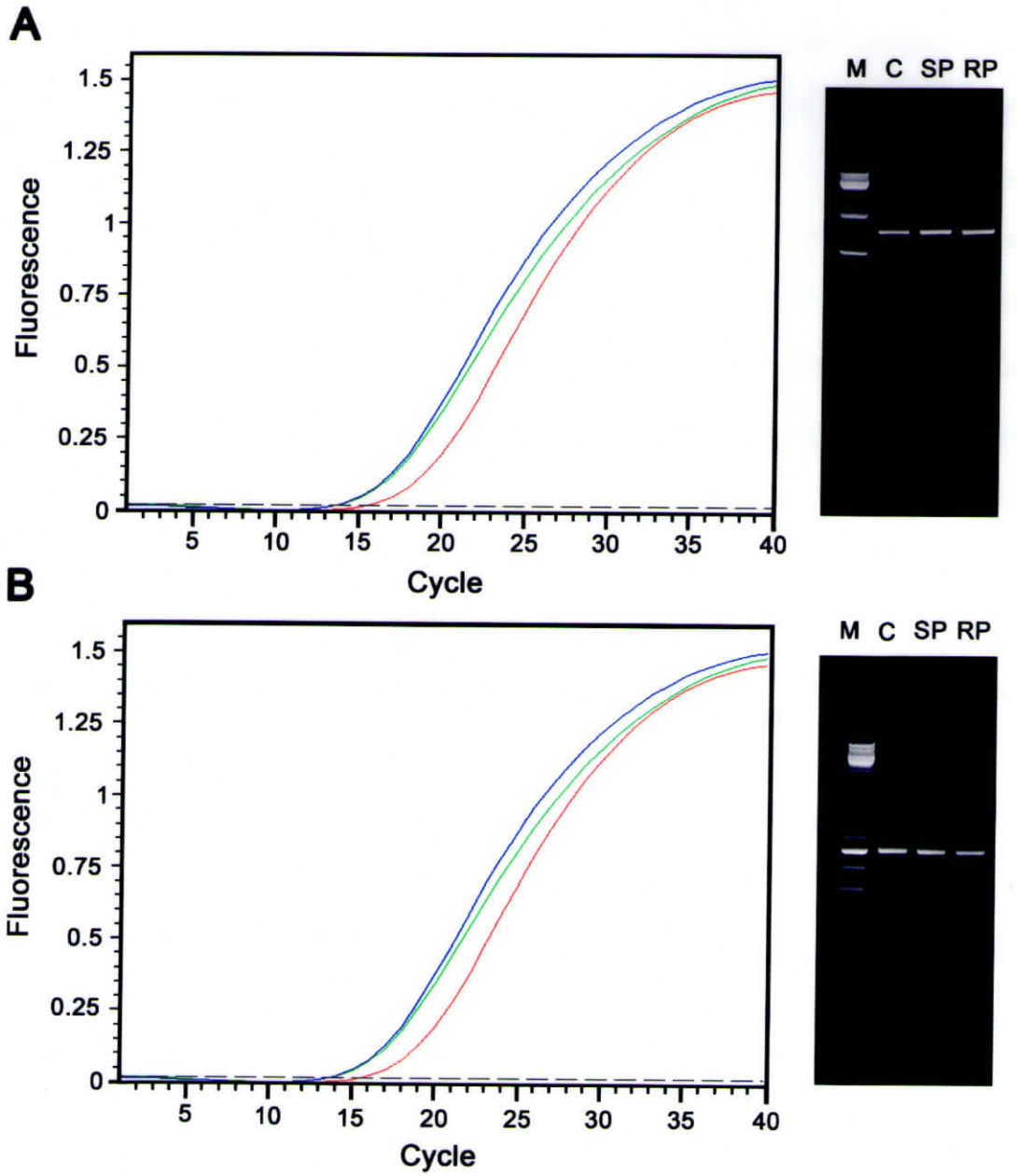

Figure 16: The florescence graph of quantitative RT-PCR for β-actin (A) and Syt I gene (B). Equal concentration of RNA, isolated from control (red line), SP (green line) and RP (blue line) were used for analyzing the expression variation of Syt I gene in reference to β-actin. The threshold line is shown as dotted line. The PCR products are loaded on the gel. The amplified product size for β-actin and Syt I gene is 691 bp and 503 bp respectively.

4.2.3. Microarray analysis

The mRNA levels of Syt isoforms during seizure were estimated and compared with the control using probe-based Microarray analysis. The fold changes were plotted for Syt isoforms, synaptic vesicle protein and seizure associated genes. The isoform, Syt IV scored the maximum mRNA expression variation (4 fold) in seizure induced hippocampus, while Syt I showed less than two fold increases in expression **(Figure 17)**. The mRNA expression variation in the hippocampus was in the order Syt IV>Syt XII> Syt V> Syt VI> Syt III > Syt I > Syt XV > Syt XI >Syt XIII. Three Syts (II, VII and VIII) showed downregulation. The transcripts of the proteins associated with SV fusion (Syntaxin 1B2, Syntaxin 1a and SNAP-25) as well as the seizure associated genes (tissue plasminogen activator - tPA, Rab 3a, Rim 1 and Neurexin 2 were analyzed to get a representative picture on how these genes behave at SP and RP compared to control in pilocarpine induced seizure. Among the reported seizure induced genes, tPA showed a significant three-fold increase during SP and a four-fold increase during RP, while Rim 1 showed a two-fold change during SP. Changes in Rab3a, and Neurexin transcripts were not significant **(Figure 17)**. tPA is directly involved in excitotoxicity induced neurodegeneration and mutant mice lacking this serine protease are less susceptible to pharmacologically induced seizures (Tsirka, *et al.*, 1995). The major genes which showed more than 2 fold increase included the stress induced genes like Hsp70, and c-fos **(Figure 17)**.

Our results correlated closely with earlier report on the constant expression level of Syt I mRNA (Mahata, *et al.*, 1992; Tocco, *et al.*, 1996). The stability of Syt

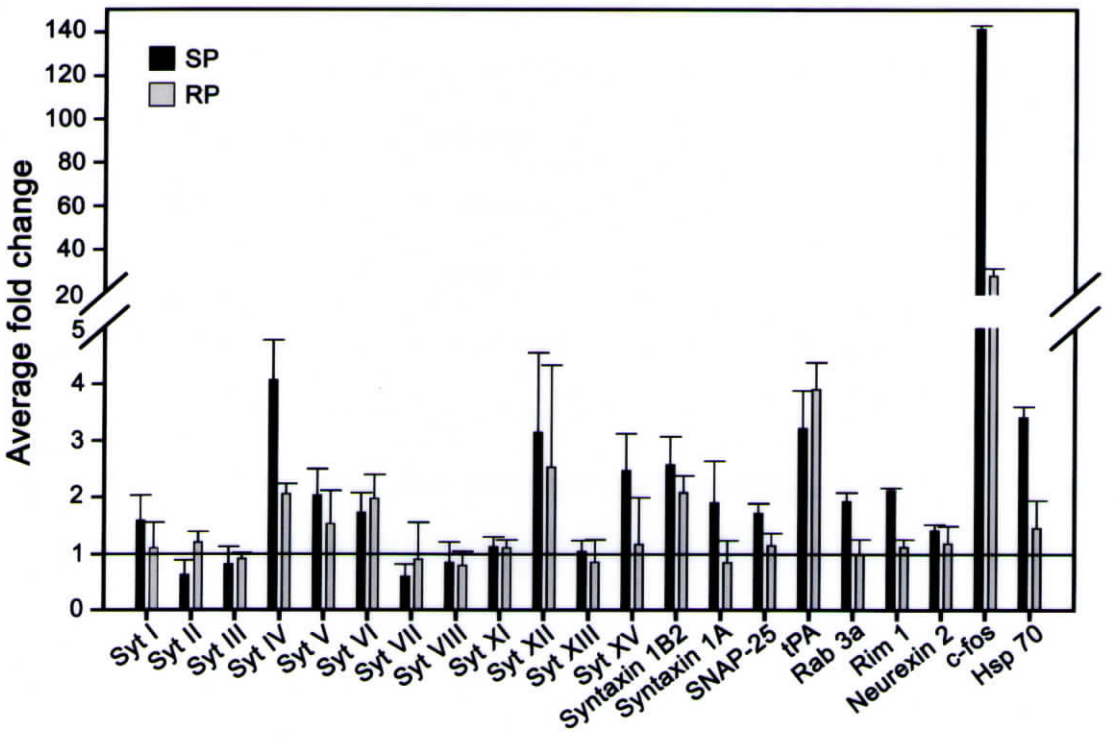

Figure 17: Microarray analysis shows a few isoforms of Syt, but not Syt I, undergo transcriptional regulation during seizure. Fold change in mRNA expression levels of Syt isoforms in rats during SP relative to the control shows Syt IV undergo a four fold increase during seizure while Syt I level remains constant (less than 2 fold increase). Syt XII was another isoform which showed an increase in mRNA expression during seizure besides the known seizure associated genes like tPA and Rim I and stress induced genes like Hsp 70 and c-fos. The expression variations of selected synaptic vesicle proteins were also shown. Data derived from two independent experiments from unpooled brain samples from SP, RP and control rats. Results are given as mean ± range.

mRNA suggested that the observed reduction in protein level during neuronal hyperactivation could be due to an alternative activity dependent regulatory mechanism(s) for Syt I protein expression in neurons.

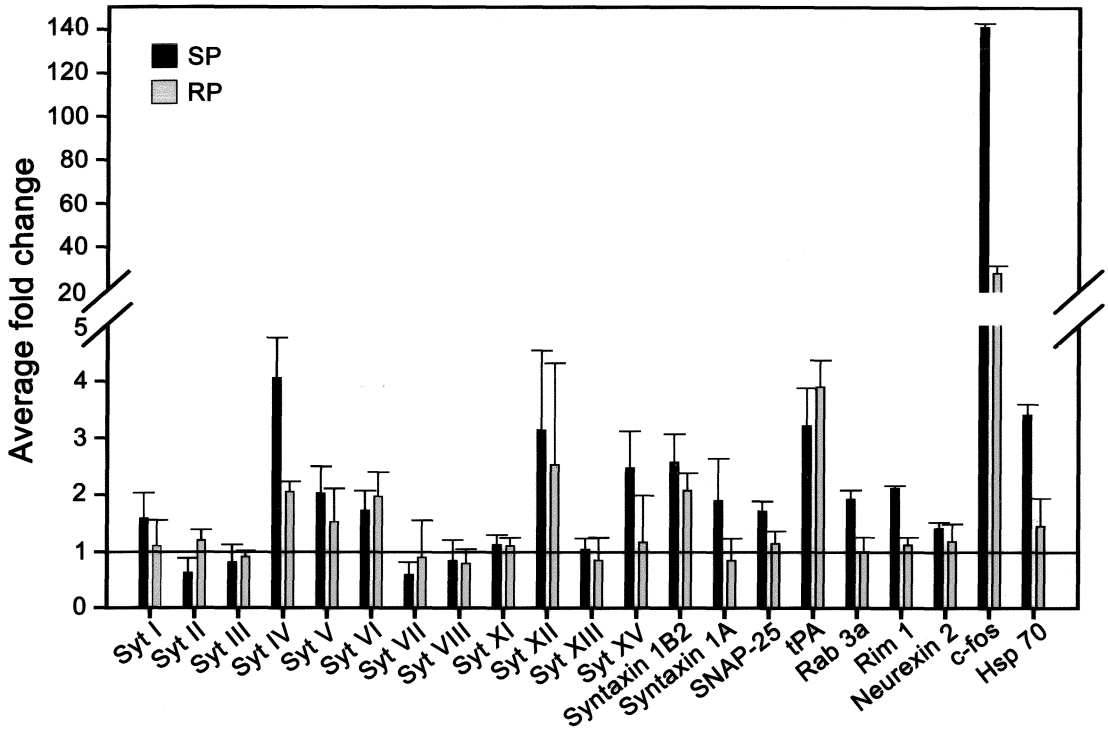

Figure 17: Microarray analysis shows a few isoforms of Syt, but not Syt I, undergo transcriptional regulation during seizure. Fold change in mRNA expression levels of Syt isoforms in rats during SP relative to the control shows Syt IV undergo a four fold increase during seizure while Syt I level remains constant (less than 2 fold increase). Syt XII was another isoform which showed an increase in mRNA expression during seizure besides the known seizure associated genes like tPA and Rim I and stress induced genes like Hsp 70 and c-fos. The expression variations of selected synaptic vesicle proteins were also shown. Data derived from two independent experiments from unpooled brain samples from SP, RP and control rats. Results are given as mean ± range.

mRNA suggested that the observed reduction in protein level during neuronal hyperactivation could be due to an alternative activity dependent regulatory mechanism(s) for Syt I protein expression in neurons.

4.3. PROTEIN BINDING MOTIFS IN SYT I 3' UTR RNA

The translation regulation of mRNA can occur through various mechanisms, including formation of stable stem loop secondary structures (Myers, *et al.*, 2004) or protein interactions at the UTRs (Samson, 1998). The 5' and 3' UTRs of eukaryotic mRNAs are involved in post transcriptional regulation that modulates nucleocytoplasmic mRNA transport, translation efficiency, subcellular localization and stability (Wilkie, *et al.*, 2003). The role of 3' UTR in the autoregulation of translation machinery has been proved in various models (Abe, *et al.*, 1996; Lyubimova, *et al.*, 1999). We hypothesized that one of the reasons for the strong reduction in Syt I level could be due to the selective translational regulation of Syt I by RNA-protein interaction. To explore such a possibility we examined Syt I mRNA sequences for motifs that could function as binding or recognition sites for RNA-protein interaction.

The coding region as well as the 5' and 3' UTR of Syt I are highly conserved across human and rat. The 3' UTR shows almost 84% homology between these two species (Perin, *et al.*, 1991b). The 3' UTR is more interesting because there are two possible protein-binding domains within the Syt I 3' UTR: GT repeat domain (Gao, *et al.*, 2004) and GTCAATG - named as 'Heptamer' sequence, which is a modified oligonucleotide similar to the known protein binding sequence GTCA***C***ATG (Blangy, *et al.*, 1991) **(Figure 18)**. Moreover the promoter region of Syt I is not well defined. The GT repeat region in human shows a variable number of repeats (15-22 GTs) while in rat the repeat is not well conserved (Perin, *et al.*, 1991b). As we were specifically interested in identifying the reason for translational blockage of Syt I, we

suspected that the probable protein interacting motifs could be one of the major factors for such a control mechanism. Because the GT repeats are degenerated in rodents, we amplified the region covering the GT repeats and heptamer sequence from human and cloned to use as a probe for potential interactions.

```
Human CATAGCCACAAAACAGAATAGCACCTGTCTGTACATATTTACAAAGCTAAAATAATGGCT 60
Rat   CAAAGCCACAAACCAGAATAGCATCTGTCTGTCTGTACCTGCAAAGCCAAAGCCATG-CT 59

Human TCACTCTTATATTTGAGGAAGCAACTGAACAGGAGTCAATGATTTCATATTACTGCATAT 120
Rat   TCGCTCTTACAGTCAAGGAAGCAA-TGAACAGGAGCCAATGCGTTCCTACCACTGCATCT 118

Human AGAATAACAACAAGGTG-----TTCCGTGTGTGTGTGTG----------------TGTGT 159
Rat   AGCATAGCTTCATGGTGGTGTTCTCTGTGTGTGCGTGTGCAAGCGTGAAAGTGTATGCAC 178

Human GTGTGTGTGTGTG-----CACATTTGTTTGGGGATGGGGGAGAAGAAGCTAAG--GGGAG 212
Rat   GTGTGTATGTGTGGTGCATGCCTTTGTTTGGGGTTAGGGTGGGGGAGGAGGAGCTGAGGG 238

Human AAGTCAACATTTATGAAATATTGCCTGACTATTTAAAAAGAAAAAAGTAGCTCTCCATTA 272
Rat   AAGTCAGCGTTTCTGAAATATTGCCTGCCTGTTTAAACAGAAAATTATAGCTCTCCATTG 298

Human TCACCTTTATACAAAATGTACATCCTGTGAATTCTGTTCCAGATTTCACACCTACAATAA 332
Rat   TCACATTTATATAAAACGTGCAACCTGGGAATTCTGATCCGGATTTCACCCCAATATTGA 358

Human TTCCAAAAGGTTTGCACATTAGAGTTTG 360
Rat   TTCCAAAA-------------------- 366
```

Figure 18: Homology between human and rat Syt I 3' UTR. Pair-wise alignment of human and rat Syt I 3' UTR RNA using ClustalW (360 bp region used in RNA-protein interaction). The heptamer sequence and GT repeat region are highlighted. In rat sequence, the GT repeat is degenerated.

4.3.1. Cloning of Syt I 3' UTR

Syt I 3' UTR was PCR amplified (360 bp) using genomic DNA extracted from human and cloned in pTZ57R/T vector **(Figure 19A-C)**. The presence of the gene

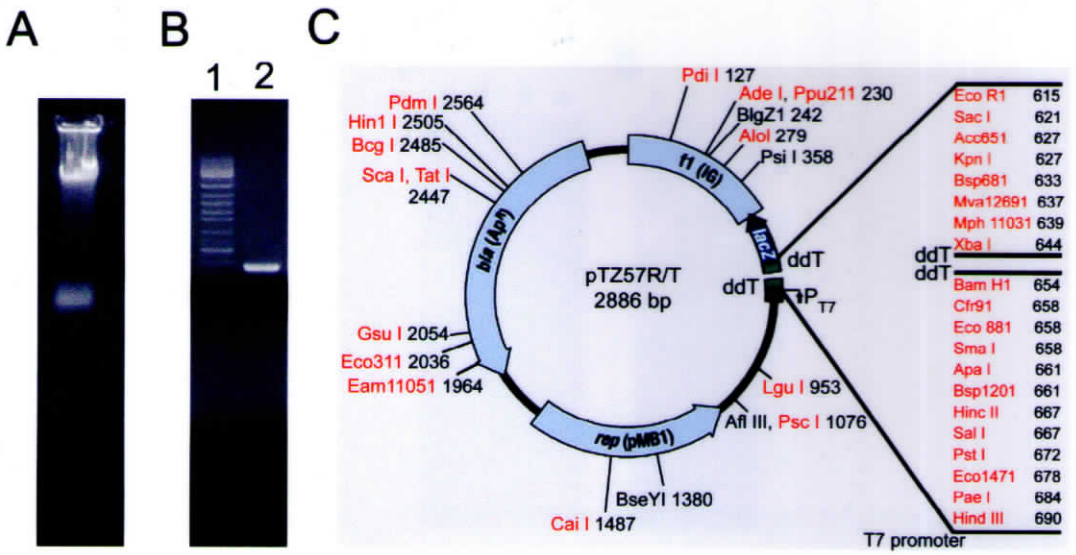

Figure 19: Cloning of Syt I 3' UTR containing Heptamer and GT repeat sequence. (A) Ethidium bromide stained 0.7% gel showing genomic DNA. (B) PCR amplified Syt I 3' UTR (360 bp) is shown in lane 2. Lane 1 represent marker (GeneRuler™ DNA ladder mix, MBI Fermentas) as a standard. (C) The map of pTZ57R/T vector showing restriction enzyme sites and multiple cloning sites.

was confirmed by Eco R1 digestion and Eco R1-Bam H1 double digestion **(Figure 20A and Table 7)**. Sequencing revealed that the 3' UTR clone contained 15 GT repeats **(Figure 21)**. The sequence was deposited in GenBank (Accession No DQ448032). The Syt I 3' UTR fragment was released by Pvu II digestion from a reverse clone in pTZ57R/T vector **(Figure 20B)** which contain the T7 promoter sequence upstream of the Syt I 3' UTR. Sy I 3' UTR RNA was *in vitro* transcribed from this fragment using T7 RNA polymerase. The RNA was purified using RNA purification column and used as a probe to verify its protein binding ability.

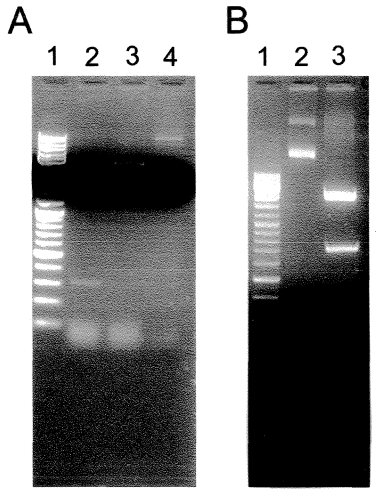

Figure 20: Syt I 3' UTR was cloned in pTZ57R/T vector and confirmed by restriction digestions (A) The plasmid was digested with Eco R1-Bam H1 (lane 2) and Eco R1 (lane 3). In lane 1 and 4, marker (GeneRuler^{TM} DNA ladder mix, MBI Fermentas) and undigested (UD) plasmid are loaded respectively. (B) Pvu II digestion of pTZ57R/T-Syt I 3' UTR plasmid is shown in lane 3. The eluted Pvu II fragment containing the gene and T7 promoter is used for *in vitro* transcription of RNA. UD plasmid is loaded in lane 2.

Table 7: Restriction digestion of pTZ57R/T-Syt I 3' UTR

Clone/Gene	Restriction enzymes	Expected products	Lane No.
pTZ57R/T-Syt I 3' UTR	Eco R1-Bam H1	2.8 kb, 307 bp and 94 bp	A-2
	Eco R1	3.2 kb and 94 bp	A-3
	Pvu II	2.5 kb and 735 bp	B-3

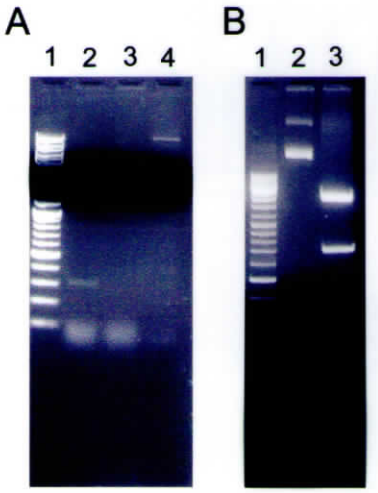

Figure 20: Syt I 3' UTR was cloned in pTZ57R/T vector and confirmed by restriction digestions (A) The plasmid was digested with Eco R1-Bam H1 (lane 2) and Eco R1 (lane 3). In lane 1 and 4, marker (GeneRuler^{TM} DNA ladder mix, MBI Fermentas) and undigested (UD) plasmid are loaded respectively. (B) Pvu II digestion of pTZ57R/T-Syt I 3' UTR plasmid is shown in lane 3. The eluted Pvu II fragment containing the gene and T7 promoter is used for *in vitro* transcription of RNA. UD plasmid is loaded in lane 2.

Table 7: Restriction digestion of pTZ57R/T-Syt I 3' UTR

Clone/Gene	Restriction enzymes	Expected products	Lane No.
pTZ57R/T-Syt I 3' UTR	Eco R1-Bam H1	2.8 kb, 307 bp and 94 bp	A-2
	Eco R1	3.2 kb and 94 bp	A-3
	Pvu II	2.5 kb and 735 bp	B-3

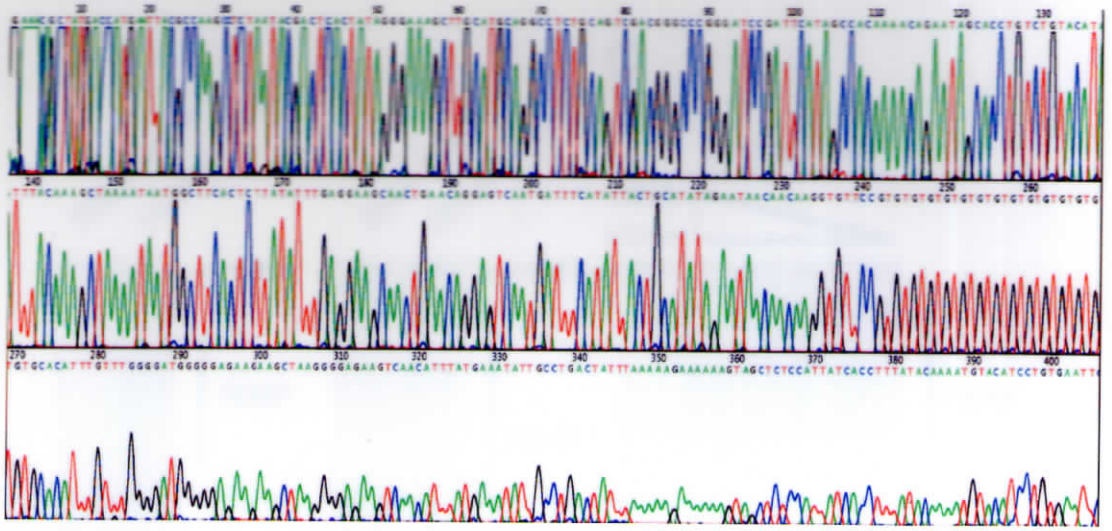

Figure 21: Sequencing data of the human Syt I 3' UTR showing 15 GT repeats. The GT repeat number varied from 15-22 in human population.

4.4. SYT I 3' UTR mRNA RECOGNIZES PROTEINS AND FORMS RNP COMPLEX

Soluble protein fractions (SPF) of human and rat temporal cortex tissue were incubated with the Syt I 3' UTR RNA probe to allow ribonucleoprotein (RNP) complex formation and was evaluated by electrophoretic mobility shift assay. Strong RNP complexes were formed between SPF and the Syt I 3' UTR RNA **(Figure 22A and B)**. The band intensity showed a linear relation with the human SPF protein concentration **(Figure 22C)**. To determine the specificity of the RNA-protein interaction competitive assay was performed with increasing concentrations of unlabeled Syt I 3' UTR probe for binding with human SPF. The formation of bound complexes was reduced in the presence of high concentration of unlabeled RNA **(Figure 23)**.

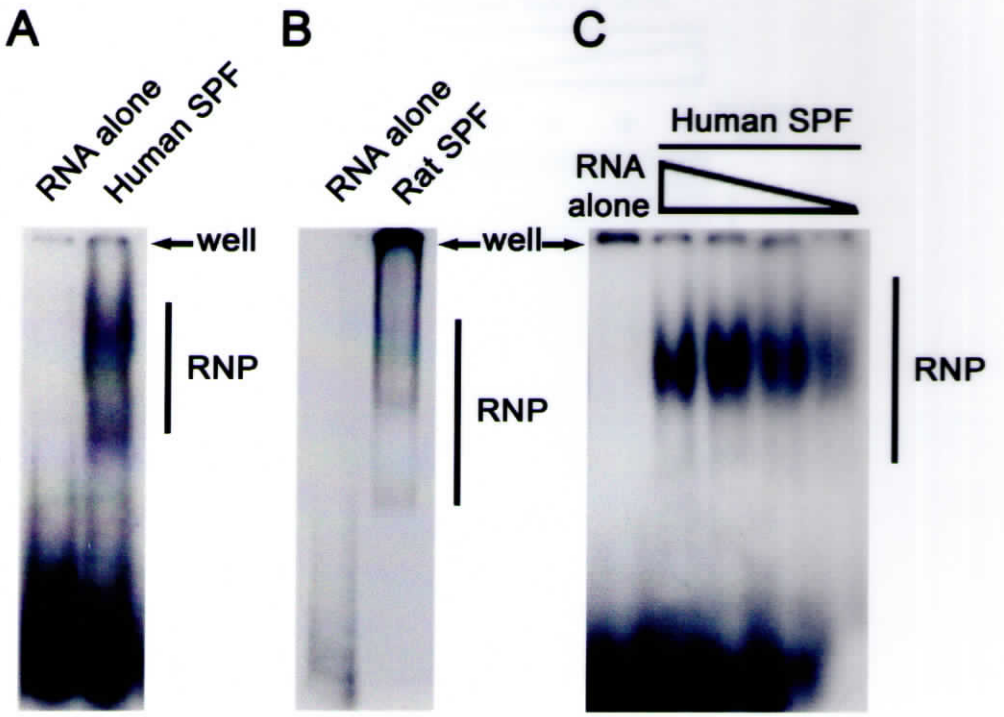

Figure 22: Syt I 3' UTR RNA can recognize the brain proteins. (A and B) The representative gels showing RNP formation with human and rat SPF with Syt I 3' UTR RNA (n=7). (C) The band intensity showed a gradual increase with the increasing protein concentration (0.5-3.0 μg).

UV-crosslinking assay was carried out to find out the molecular weights of the proteins in the RNP complex. The proteins in the RNP complex were estimated to be having approximately 47, 58 and 65 kDa in rat and 33, 47, 58, 65, 74 and 84 kDa in human **(Figure 24A)**, suggesting that a selective set of proteins recognized the Syt I 3' UTR RNA probe. As the post-translational glycosylated Syt I protein was having a molecular weight of 65 kDa (Perin, *et al.*, 1991a), we suspected that the native Syt I

protein in SPF could be the apparent candidate for this RNA-protein interaction.

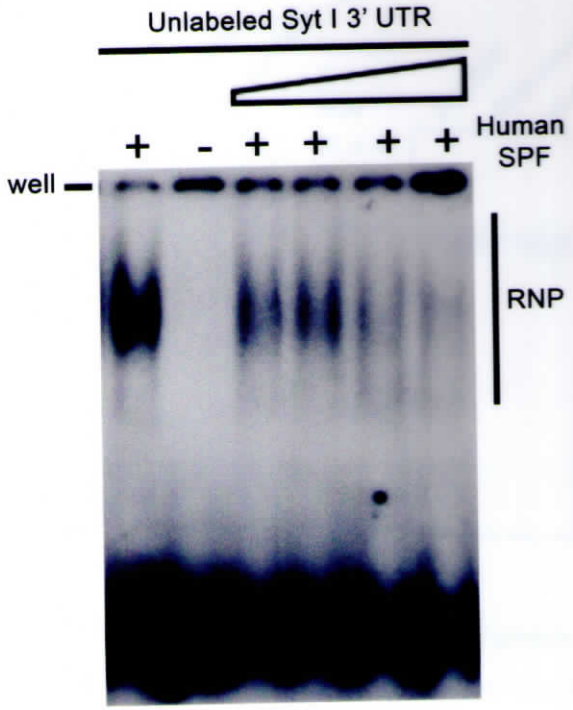

Figure 23: The specificity of RNA-protein interaction between Syt I 3' UTR RNA and human SPF protein was checked by competitive assay. The gel showed the competitive reduction in binding of protein with the labeled transcript as the concentration of unlabeled transcript is increased. The unlabeled transcript concentrations used were 0, 25, 50, 100 and 200%.

To check this hypothesis that Syt I protein can bind with its own RNA northwestern experiment was performed, but it failed to detect Syt I RNA-protein complex. The failure could be due to the heat or SDS sensitivity of Syt I protein in the SPF. However, a 65 kDa Syt I protein was detected in the UV cross-linked RNP complex when probed with Syt I polyclonal antibody **(Figure 24B)**. To confirm further, recombinant Syt I protein was synthesized for assaying its affinity for RNA interaction.

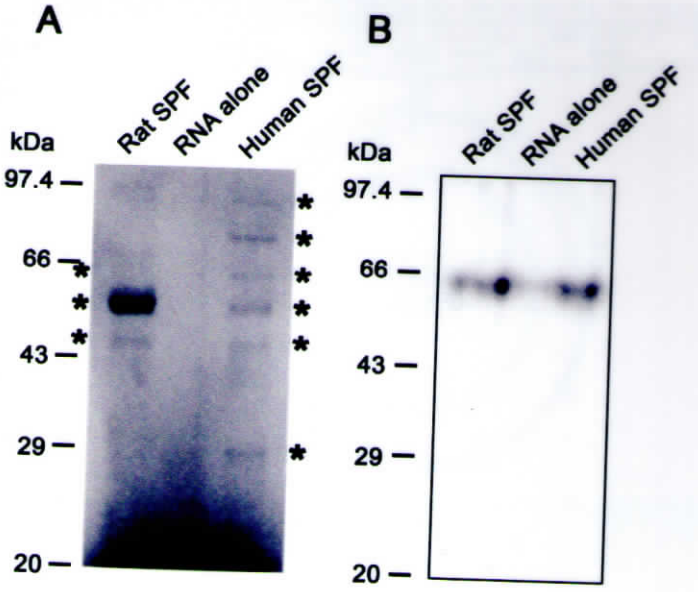

Figure 24: The Syt I 3' UTR RNA recognized Syt I protein in brain lysate (A) UV cross-linking assay gel showing the molecular weight of protein in rat and human SPF binding with the Syt I 3' UTR RNA. The representative gel shows a major band at 58 kDa in addition to 47 and 65 kDa bands in rat (n=3). Human SPF showed multiple protein bands compare to rat SPF (n=3). Asterisks indicate major protein bands. (B) Immunostaining of the gel after UV cross-linking assay detected the intact Syt I protein of 65 kDa in human and rat SPF.

4.5. RECOMBINANT SYT I PROTEIN PREPARATION

4.5.1. Cloning of Syt I gene

To synthesize the recombinant protein, the full coding region of the Syt I was PCR amplified from rat hippocampal mRNA **(Figure 25A)**, cloned in pTZ57R/T vector and sub-cloned into pGEX4T1 expression vector **(Figure 25B)**. The pTZ57R/T-Syt I was verified by restriction digestions with Rsa I and Xba I-Sal I **(Figure 26A and B and Table 8)** and confirmed by sequencing.

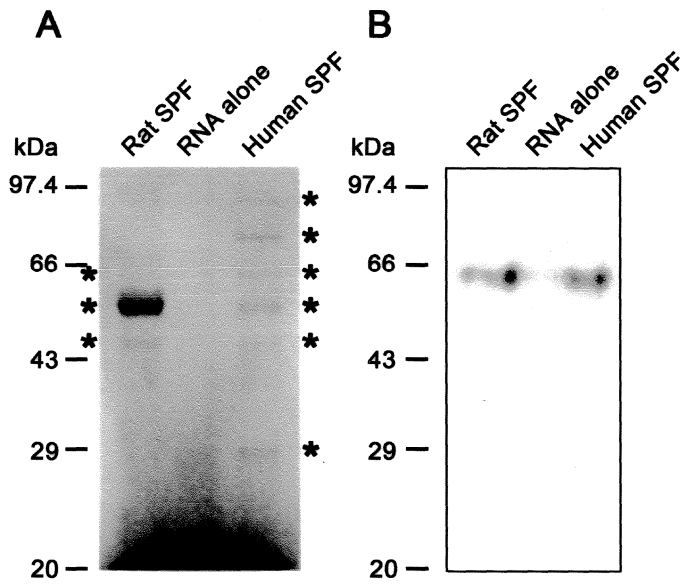

Figure 24: The Syt I 3' UTR RNA recognized Syt I protein in brain lysate (A) UV cross-linking assay gel showing the molecular weight of protein in rat and human SPF binding with the Syt I 3' UTR RNA. The representative gel shows a major band at 58 kDa in addition to 47 and 65 kDa bands in rat (n=3). Human SPF showed multiple protein bands compare to rat SPF (n=3). Asterisks indicate major protein bands. (B) Immunostaining of the gel after UV cross-linking assay detected the intact Syt I protein of 65 kDa in human and rat SPF.

4.5. RECOMBINANT SYT I PROTEIN PREPARATION

4.5.1. Cloning of Syt I gene

To synthesize the recombinant protein, the full coding region of the Syt I was PCR amplified from rat hippocampal mRNA **(Figure 25A)**, cloned in pTZ57R/T vector and sub-cloned into pGEX4T1 expression vector **(Figure 25B)**. The pTZ57R/T-Syt I was verified by restriction digestions with Rsa I and Xba I-Sal I **(Figure 26A and B and Table 8)** and confirmed by sequencing.

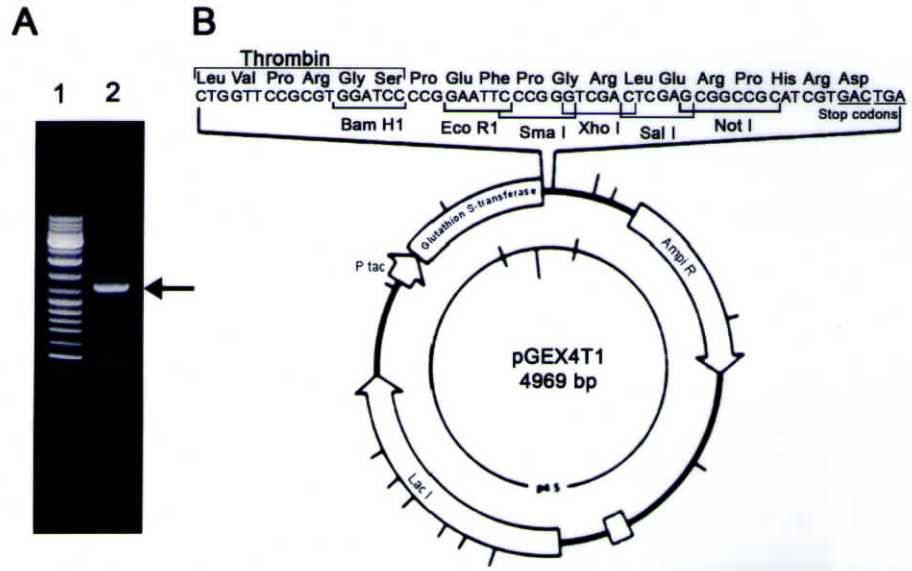

Figure 25: For recombinant Syt I protein expression, the gene was PCR amplified and cloned in expression vector, pGEX4T1. (A) PCR amplification of Syt I gene (lane 2). The arrow points Syt I PCR product at 1.2 kb position, an additional band at 500 bp also seen. (B) The map of pGEX4T1 vector showing restriction enzyme sites and multiple cloning sites.

The predicted amino acid sequence showed the following variations: Asp^{188}, Gly^{374} and Met^{393} **(Figure 27)** differing from the published rat Syt I sequence of Asp^{188}, Asp^{374} and Met^{393} (Perin, *et al.*, 1990) and Glu^{188}, Gly^{374} and Ile^{393} (Osborne, *et al.*, 1999). The sequence is deposited in GenBank (Accession No. DQ181550). It has been reported that the two forms of Syt I, with Asp^{374} or Gly^{374}, have distinct oligomerization properties. The Syt I-Asp^{374} failed to form self oligomerization (Desai, *et al.*, 2000). The sequence with Gly^{374} should have retained the self oligomerization property.

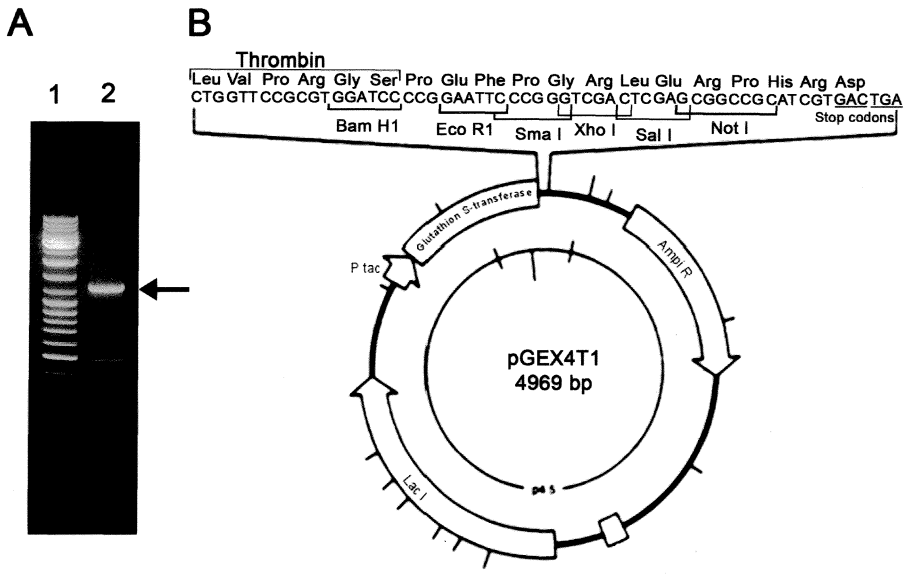

Figure 25: For recombinant Syt I protein expression, the gene was PCR amplified and cloned in expression vector, pGEX4T1. (A) PCR amplification of Syt I gene (lane 2). The arrow points Syt I PCR product at 1.2 kb position, an additional band at 500 bp also seen. (B) The map of pGEX4T1 vector showing restriction enzyme sites and multiple cloning sites.

The predicted amino acid sequence showed the following variations: Asp^{188}, Gly^{374} and Met^{393} **(Figure 27)** differing from the published rat Syt I sequence of Asp^{188}, Asp^{374} and Met^{393} (Perin, *et al.*, 1990) and Glu^{188}, Gly^{374} and Ile^{393} (Osborne, *et al.*, 1999). The sequence is deposited in GenBank (Accession No. DQ181550). It has been reported that the two forms of Syt I, with Asp^{374} or Gly^{374}, have distinct oligomerization properties. The Syt I-Asp^{374} failed to form self oligomerization (Desai, *et al.*, 2000). The sequence with Gly^{374} should have retained the self oligomerization property.

The gene was sub-cloned into pUC19 vector before cloning in pGEX4T vector to get the correct reading frame for protein expression. The pUC19 ar pGEX4T1 clones were confirmed by various restriction digestions **(Figure 26C an D and Table 8)**.

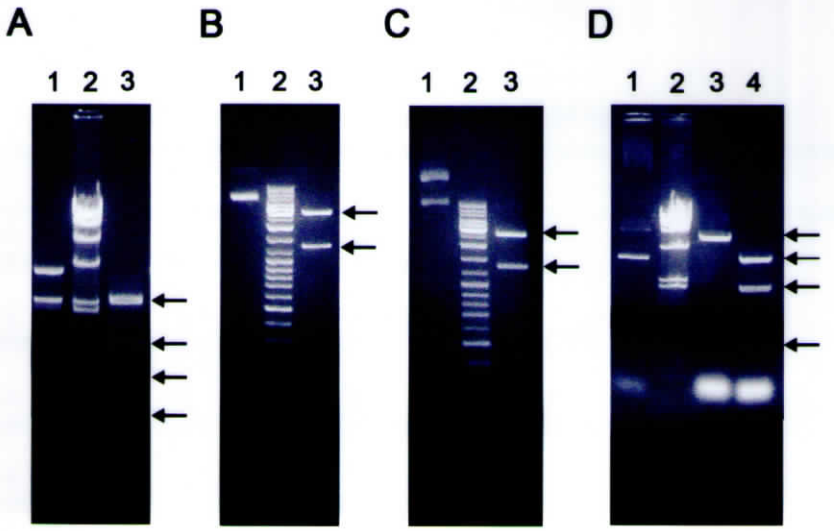

Figure 26: Restriction digestion pattern of Syt I gene in pTZ57R/T, pUC19 and pGEX4T1 vectors. (A) Rsa I digestion of pTZ57R/T-Syt I (lane 3) (B) Xba I-Sal I double digestion released Syt I gene from pTZ57R/T vector (lane 3). (C) The presence of Syt I gene in pUC19 vector is confirmed by Eco R1-Sal I double digestion (lane 3) (D) pGEX4T1-Syt I plasmid was confirmed by Kpn I and Xcm I digestions. All the gels contain undigested plasmid to compare the digestion pattern. The gels A and D contain Lambda DNA/Hind III marker (MBI Fermentas) and the gels B and C contain GeneRuler™ DNA ladder mix (MBI Fermentas) as molecular weight markers. The arrows indicate expected products.

The gene was sub-cloned into pUC19 vector before cloning in pGEX4T1 vector to get the correct reading frame for protein expression. The pUC19 and pGEX4T1 clones were confirmed by various restriction digestions **(Figure 26C and D and Table 8)**.

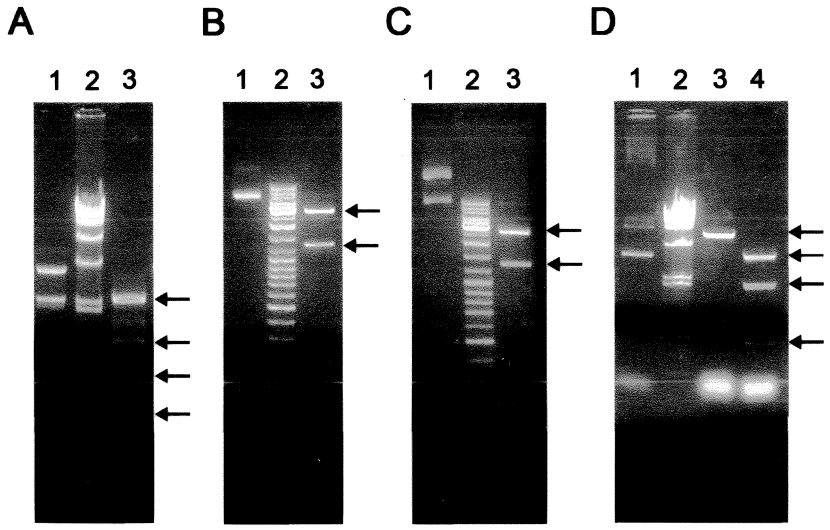

Figure 26: Restriction digestion pattern of Syt I gene in pTZ57R/T, pUC19 and pGEX4T1 vectors. (A) Rsa I digestion of pTZ57R/T-Syt I (lane 3) (B) Xba I-Sal I double digestion released Syt I gene from pTZ57R/T vector (lane 3). (C) The presence of Syt I gene in pUC19 vector is confirmed by Eco R1-Sal I double digestion (lane 3) (D) pGEX4T1-Syt I plasmid was confirmed by Kpn I and Xcm I digestions. All the gels contain undigested plasmid to compare the digestion pattern. The gels A and D contain Lambda DNA/Hind III marker (MBI Fermentas) and the gels B and C contain GeneRuler^{TM} DNA ladder mix (MBI Fermentas) as molecular weight markers. The arrows indicate expected products.

Table 8: Restriction digestion of Syt I gene in pTZ57R/T, pUC19 and pGEX4T1 vectors

Clone	Restriction enzymes	Expected products	Lane No.
pTZ57R/T-Syt I	Rsa I	2.3 kb, 1 kb, 621 bp and 116 bp	A-3
	Xba I-Sal I	2.8 kb 1.3 kb	B-3
pUC19-Syt I	Eco R1-Sal I	2.65 kb and 1.3 kb	C-3
pGEX4T1-Syt I	Kpn I	6.3 kb	D-3
	Xcm I	3.7 kb, 2.0 kb, 516 bp and 18 bp	D-4

```
 M   V   S   A   S   H   P   E   A   L   A   A   P   V   T      15
ATG GTG AGT GCC AGT CAT CCT GAG GCC CTG GCC GCC CCT GTC ACC      45

 T   V   A   T   L   V   P   H   N   A   T   E   P   A   S      30
ACT GTT GCG ACC CTT GTC CCA CAC AAT GCC ACT GAG CCA GCC AGT      90

 P   G   E   G   K   E   D   A   F   S   K   L   K   Q   K      45
CCT GGG GAA GGG AAG GAA GAT GCC TTT TCC AAG CTG AAG CAG AAG     135

 F   M   N   E   L   H   K   I   P   L   P   P   W   A   L      60
TTT ATG AAT GAG CTG CAT AAA ATT CCA TTG CCA CCG TGG GCC TTA     180

 I   A   I   A   I   V   A   V   L   L   V   V   T   C   C      75
ATA GCC ATA GCC ATA GTT GCG GTC CTT TTA GTC GTA ACC TGC TGC     225

 F   C   V   C   K   K   C   L   F   K   K   K   N   K   K      90
TTT TGT GTC TGT AAG AAA TGT TTG TTC AAA AAG AAA AAC AAG AAG     270

 K   G   K   E   K   G   G   K   N   A   I   N   M   K   D     105
AAG GGG AAG GAA AAG GGA GGA AAG AAC GCC ATT AAC ATG AAA GAC     315

 V   K   D   L   G   K   T   M   K   D   Q   A   L   K   D     120
GTG AAA GAC TTA GGG AAG ACC ATG AAG GAT CAG GCC CTT AAG GAT     360

 D   D   A   E   T   G   L   T   D   G   E   E   K   E   E     135
GAC GAT GCT GAA ACC GGA CTG ACT GAT GGA GAA GAA AAG GAA GAG     405
 P   K   E   E   E   K   L   G   K   L   Q   Y   S   L   D     150
CCC AAG GAA GAG GAG AAA CTG GGA AAG CTC CAA TAT TCA CTG GAC     450

 Y   D   F   Q   N   N   Q   L   L   V   G   I   I   Q   A     165
TAT GAC TTC CAG AAT AAC CAG CTG TTG GTG GGA ATC ATC CAG GCT     495

 A   E   L   P   A   L   D   M   G   G   T   S   D   P   Y     180
GCT GAA CTG CCC GCC CTG GAC ATG GGG GGT ACA TCC GAT CCA TAC     540

 V   K   V   F   L   L   P   D   K   K   K   K   F   E   T     195
GTC AAA GTC TTC CTG CTG CCT GAC AAA AAG AAG AAA TTT GAG ACT     585
```

```
 K   V   H   R   K   T   L   N   P   V   F   N   E   Q   F      210
AAA GTC CAC CGG AAA ACC CTC AAT CCA GTC TTC AAT GAA CAA TTT      630

 T   F   K   V   P   Y   S   E   L   G   G   K   T   L   V      225
ACT TTC AAG GTA CCC TAC TCG GAA TTA GGT GGC AAA ACC CTG GTG      675

 M   A   V   Y   D   F   D   R   F   S   K   H   D   I   I      240
ATG GCT GTG TAT GAC TTT GAT CGC TTC TCC AAG CAC GAC ATC ATC      720

 G   E   F   K   V   P   M   N   T   V   D   F   G   H   V      255
GGA GAG TTC AAA GTT CCT ATG AAC ACC GTG GAT TTT GGC CAT GTG      765

 T   E   E   W   R   D   L   Q   S   A   E   K   E   E   Q      270
ACC GAG GAG TGG CGT GAT CTC CAG AGC GCT GAG AAA GAA GAG CAA      810

 E   K   L   G   D   I   C   F   S   L   R   Y   V   P   T      285
GAG AAA CTG GGT GAC ATC TGC TTC TCC CTC CGC TAC GTC CCT ACT      855

 A   G   K   L   T   V   V   I   L   E   A   K   N   L   K      300
GCC GGC AAA CTG ACT GTT GTC ATT CTG GAA GCC AAG AAC CTG AAG      900

 K   M   D   V   G   G   L   S   D   P   Y   V   K   I   H      315
AAG ATG GAT GTG GGT GGC TTA TCT GAT CCC TAC GTG AAG ATT CAC      945

 L   M   Q   N   G   K   R   L   K   K   K   K   T   T   I      330
CTG ATG CAG AAC GGT AAG AGG CTG AAG AAG AAA AAG ACG ACG ATT      990

 K   K   N   T   L   N   P   Y   Y   N   E   S   F   S   F      345
AAG AAG AAC ACA CTC AAC CCC TAC TAC AAC GAG TCC TTC AGC TTT     1035

 E   V   P   F   E   Q   I   Q   K   V   Q   V   V   V   T      360
GAA GTT CCG TTC GAG CAA ATC CAG AAA GTG CAA GTG GTG GTA ACT     1080

 V   L   D   Y   D   K   I   G   K   N   D   A   I   G   K      375
GTT TTG GAC TAT GAC AAG ATT GGC AAG AAC GAC GCC ATC GGC AAA     1125

 V   F   V   G   Y   N   S   T   G   A   E   L   R   H   W      390
GTC TTC GTT GGT TAC AAC AGC ACT GGG GCG GAG CTG CGA CAC TGG     1170

 S   D   M   L   A   N   P   R   R   P   I   A   Q   W   H      405
TCA GAC ATG CTG GCC AAC CCC CGG CGA CCC ATC GCA CAG TGG CAC     1215

 T   L   Q   V   E   E   E   V   D   A   M   L   A   V   K      420
ACT CTG CAG GTA GAG GAG GAG GTT GAT GCC ATG CTG GCT GTC AAG     1260

 K   *                                                          422
AAG TAA                                                        1266
```

Figure 27: The deduced amino acid sequence from the Syt I gene used in this study revealed three amino acid variations from the known sequence. The amino acid sequence is shown on top of the nucleic acid sequences. The nucleic acid variation is shaded and the amino acid variation is indicated in red.

4.5.2. Purification of GST-Syt I protein

GST-Syt I fusion protein was expressed in BL21 *E. coli* strain **(Figure 28A** the 3 M urea soluble fraction **(Figure 28B)** is purified using MicroSpin purificatic column and confirmed by SDS-PAGE analysis **(Figure 28C)**.

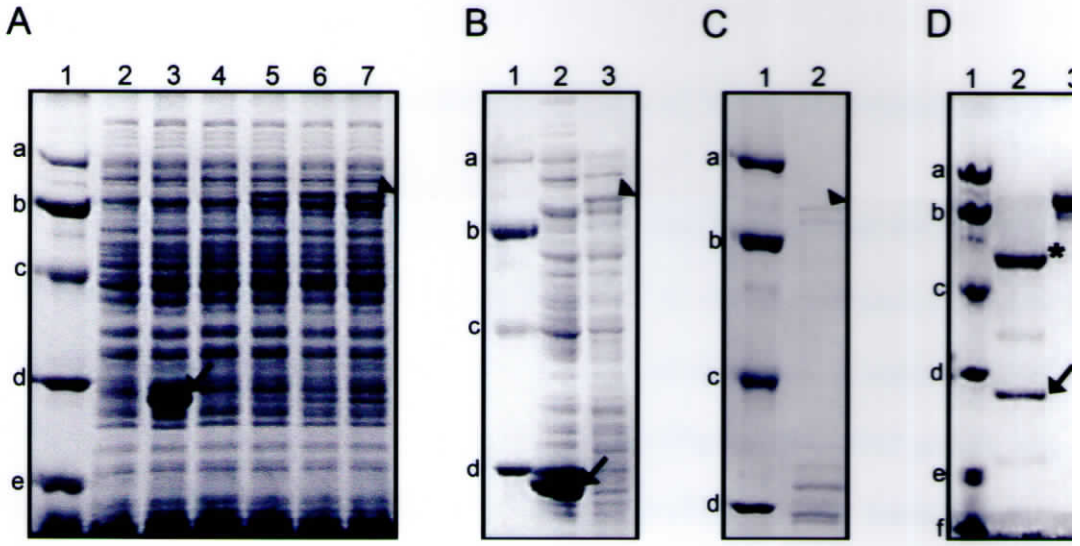

Figure 28: The recombinant GST-Syt I protein was expressed and affinity purified. (A) Lanes 2-7 represent proteins bands by loading 0.3 OD of the bacterial culture. Lanes 2 and 3 show 0^{th} hour (before IPTG induction) and 3^{rd} hour (after IPTG induction) of pGEX4T1 respectively. The arrow indicates GST protein. Lane 4 to 7 show the time period of GST-Syt I protein (arrow head) expression at 0^{th}, 1^{st}, 2^{nd} and 3^{rd} hour after IPTG induction. (B) Protein lysates showing GST (arrow) and GST-Syt I (arrow head) protein bands. (C) Purified GST-Syt I fusion protein (arrow head) 10 µg loaded. (D) Thrombin digestion of electro-eluted GST-Syt I protein. Lane 2 shows thrombin cleaved Syt I (asterisk) and GST (arrow) protein bands and lane 3 shows electro-eluted GST-Syt I (arrow head) protein. In all the gels, in lane 1 protein marker (PMWM medium range, Bangalore Genei, India) is loaded as a standard with bands at 97.4 (a), 66.0 (b), 43.0 (c), 29.0 (d), 20.1 (e) and 14.3 (f) kDa positions.

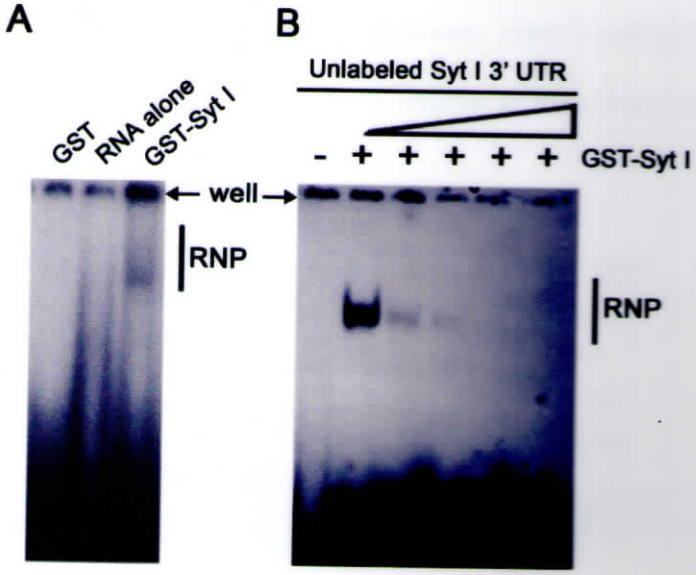

Figure 29: The Syt I protein interacts with its own RNA. (A) The interaction between recombinant GST-Syt I and labeled Syt I 3' UTR shows strong RNP formation (representative gel from nine independent experiments). GST protein was used as negative control which showed no affinity for RNA. (B) Syt I 3' UTR RNA - GST-Syt I protein interaction is highly specific. Competitive assay in the presence of unlabeled Syt I 3' UTR RNA precludes the binding of GST-Syt I with the labeled transcript in a concentration-dependent manner (n=3). The unlabeled probe concentrations used were 10, 25, 50 and 100%.

4.7. EFFECT OF PROTEIN BINDING SEQUENCES IN THE SYT I 3' UTR RNA

Since the Syt I protein can distinctively recognize its own RNA it was further wanted to characterize the sequence within the 3' UTR which is recognized by the protein for its interactive binding. For this smaller RNA constructs from the Syt I 3' UTR sequence were synthesized **(Figure 30)**. The Syt I 3' UTR smaller fragments (Syt I_{1-171}, Syt I_{1-101}, Syt I_{94-360} and Syt $I_{102-302}$) were prepared by digesting either the Syt I 3' UTR PCR product or pTZ57R/T-Syt I 3' UTR plasmid (see Materials and

4.5.2. Purification of GST-Syt I protein

GST-Syt I fusion protein was expressed in BL21 *E. coli* strain **(Figure 28A)**, the 3 M urea soluble fraction **(Figure 28B)** is purified using MicroSpin purification column and confirmed by SDS-PAGE analysis **(Figure 28C)**.

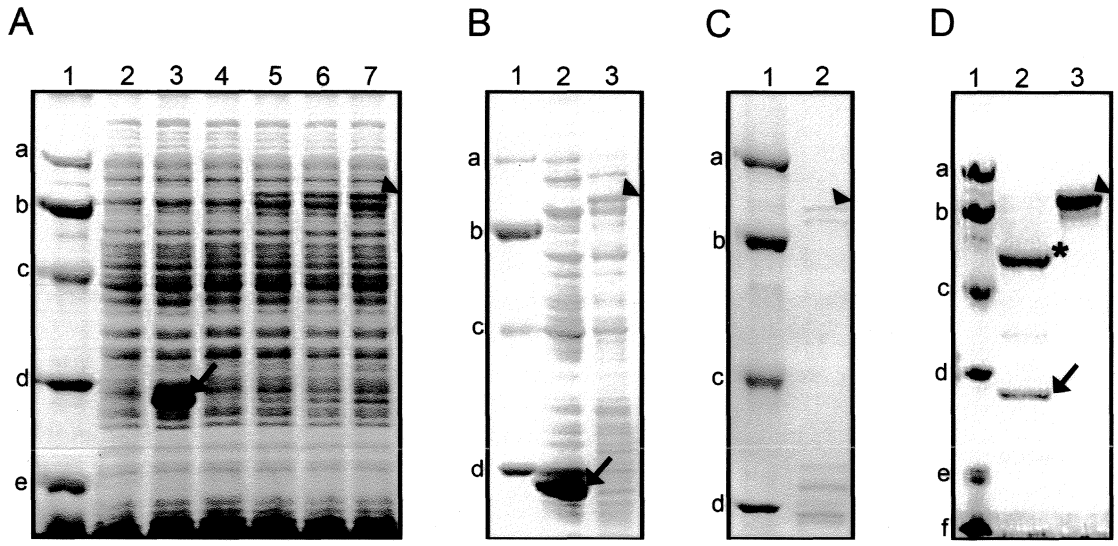

Figure 28: The recombinant GST-Syt I protein was expressed and affinity purified. (A) Lanes 2-7 represent proteins bands by loading 0.3 OD of the bacterial culture. Lanes 2 and 3 show 0^{th} hour (before IPTG induction) and 3^{rd} hour (after IPTG induction) of pGEX4T1 respectively. The arrow indicates GST protein. Lane 4 to 7 show the time period of GST-Syt I protein (arrow head) expression at 0^{th}, 1^{st}, 2^{nd} and 3^{rd} hour after IPTG induction. (B) Protein lysates showing GST (arrow) and GST-Syt I (arrow head) protein bands. (C) Purified GST-Syt I fusion protein (arrow head) 10 µg loaded. (D) Thrombin digestion of electro-eluted GST-Syt I protein. Lane 2 shows thrombin cleaved Syt I (asterisk) and GST (arrow) protein bands and lane 3 shows electro-eluted GST-Syt I (arrow head) protein. In all the gels, in lane 1 protein marker (PMWM medium range, Bangalore Genei, India) is loaded as a standard with bands at 97.4 (a), 66.0 (b), 43.0 (c), 29.0 (d), 20.1 (e) and 14.3 (f) kDa positions.

As the protein yield was very low (only in ng levels) to confirm the GST-Syt I band, protein bands from the corresponding region (around 73.5 kDa) was gel eluted and digested with thrombin. The digestion resulted in bands approximately at 47.5 kDa (Syt I – without post-translational modification) and at 26 kDa (GST protein) positions **(Figure 28D)**. The Syt I protein without GST moiety was used for raising polyclonal antibody in rabbit.

4.6. SYT I 3' UTR mRNA RECOGNIZES SYT I AND FORMS RNP COMPLEX

The recombinant GST-Syt I fusion protein and α-^{32}P-labeled Syt I 3' UTR RNA were incubated at 37°C in binding buffer for 30 minutes and analyzed for the formation of RNP complex by electrophoretic mobility shift assay. A substantial RNP formation was observed between the two molecules **(Figure 29A)**. GST protein was used as a negative control **(Figure 29A)**. The specificity of the interaction was confirmed by competitive assay using unlabeled Syt I 3' UTR RNA which showed a reduction in signal intensity with increasing amount of unlabeled RNA **(Figure 29B)**.

The human SPF showed a slower saturation **(Figure 23)** with the competitive probe (0-200% non-labeled probe) compared to the GST-Syt I, which showed a reduction in binding pattern with the labeled probe at a lower concentration (10%) of non-labeled probe **(Figure 29B)**. Reasons for the faster saturation in recombinant GST-Syt I protein might be because of its prokaryotic expression and folding variations compared to the native protein from the brain; besides the SPF will contain additional RNA binding proteins which could bind the RNA with different affinities.

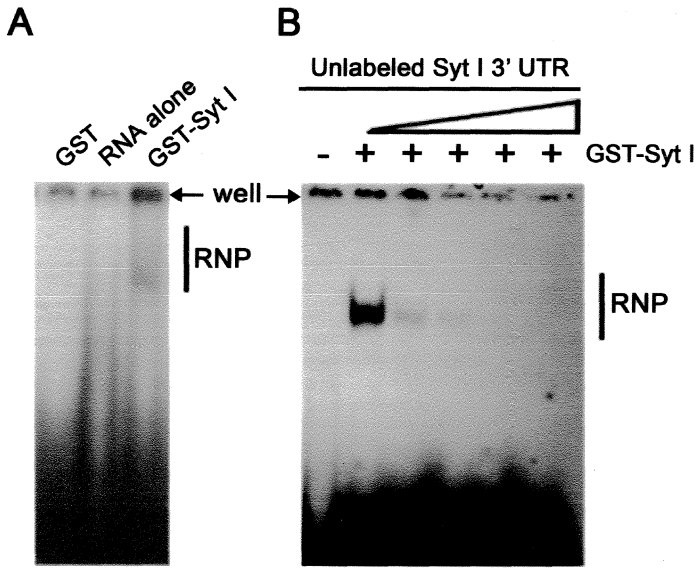

Figure 29: The Syt I protein interacts with its own RNA. (A) The interaction between recombinant GST-Syt I and labeled Syt I 3' UTR shows strong RNP formation (representative gel from nine independent experiments). GST protein was used as negative control which showed no affinity for RNA. (B) Syt I 3' UTR RNA - GST-Syt I protein interaction is highly specific. Competitive assay in the presence of unlabeled Syt I 3' UTR RNA precludes the binding of GST-Syt I with the labeled transcript in a concentration-dependent manner (n=3). The unlabeled probe concentrations used were 10, 25, 50 and 100%.

4.7. EFFECT OF PROTEIN BINDING SEQUENCES IN THE SYT I 3' UTR RNA

Since the Syt I protein can distinctively recognize its own RNA it was further wanted to characterize the sequence within the 3' UTR which is recognized by the protein for its interactive binding. For this smaller RNA constructs from the Syt I 3' UTR sequence were synthesized **(Figure 30)**. The Syt I 3' UTR smaller fragments (Syt I_{1-171}, Syt I_{1-101}, Syt I_{94-360} and Syt $I_{102-302}$) were prepared by digesting either the Syt I 3' UTR PCR product or pTZ57R/T-Syt I 3' UTR plasmid (see Materials and

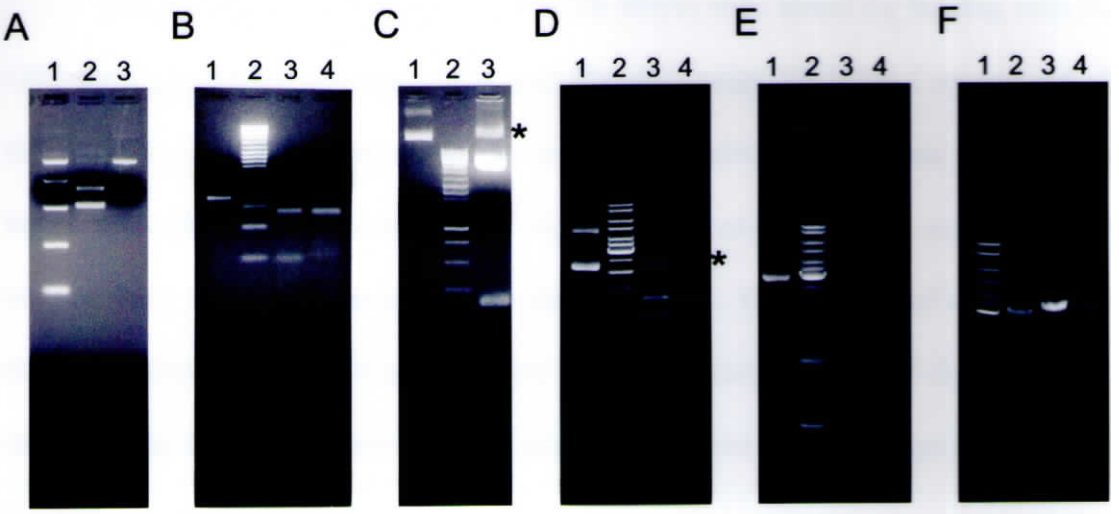

Figure 31: Restriction digestion of Syt I 3' UTR for creating smaller fragments. (A) Apa L1 digestion of pTZ57R/T-Syt I 3' UTR-Pvu II fragment for creating Syt I_{1-171} fragment. Lane 1 - marker (bands at 766, 500, 300, 150 and 50 bp, New England BioLabs, USA). Lane 2 and 3 contain Apa L1 digested and undigested (UD) Pvu II fragment respectively. (B) Hinf I and Ple I digestion of Syt I 3' UTR (360 bp) PCR product for creating Syt I_{1-101}, Syt I_{94-360} and Syt $I_{101-302}$ fragments. Lane 1- Syt I 3' UTR PCR product, lane 3 and 4 – Hinf I and Ple I digestion products respectively. (C) The Syt I_{1-101} fragment in pTZ57R/T vector is confirmed by double digestion with Eco R1 and Sal I (lane 3), UD plasmid (lane 1). (D) The presence and orientation of Syt I_{94-360} fragment was confirmed by Apa L1 digestion. Lane 1 – UD plasmid, lanes 3 and 4 – Apa L1 digested direct and reverse oriented plasmids of pTZ57R/T-Syt I_{94-360} respectively. For RNA synthesis using T7 promoter in pTZ57R/T vector, the reverse clone is required. The lane 1 contain UD plasmid (E) The pGEMT-Syt $I_{102-302}$ was confirmed by Apa L1 (lane 3) and Rsa I (lane 4) digestions. Lane 1 contains UD plasmid. (F) For the *in vitro* transcription of RNA the plasmids containing Syt I_{1-101}, Syt I_{94-360} and Syt $I_{102-302}$ were linearized and eluted. Lane 1- pTZ57R/T- Syt I_{1-101} – Xba I, lane 2- pTZ57R/T- Syt I_{94-360} – Xba I and lane 3 pGEMT-Syt $I_{102-302}$ – Sal I. B-F contain molecular weight markers (GeneRuler™ DNA ladder mix, MBI Fermentas). The asterisks indicate the UD form of DNA in the mixture.

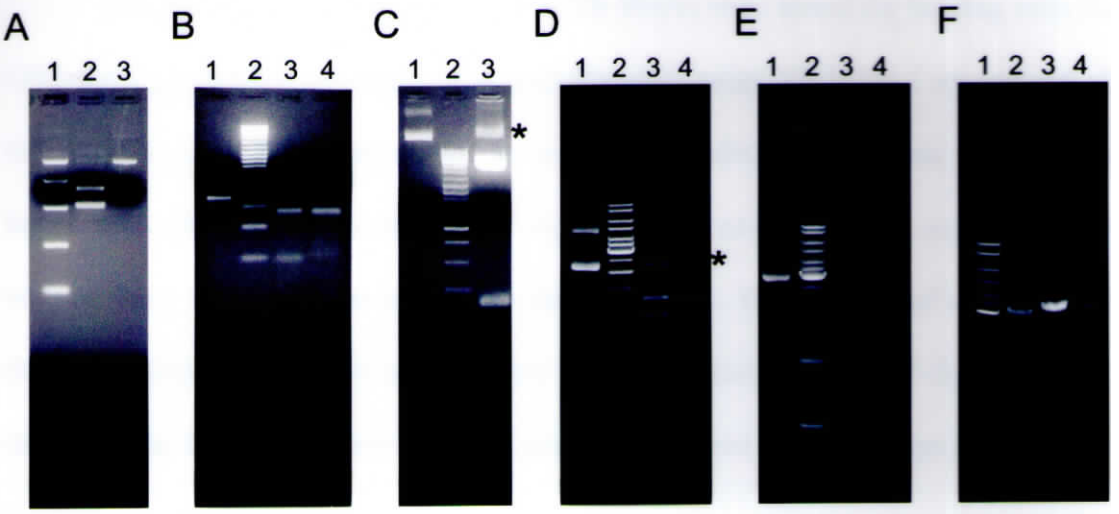

Figure 31: Restriction digestion of Syt I 3' UTR for creating smaller fragments. (A) Apa L1 digestion of pTZ57R/T-Syt I 3' UTR-Pvu II fragment for creating Syt I_{1-171} fragment. Lane 1 - marker (bands at 766, 500, 300, 150 and 50 bp, New England BioLabs, USA). Lane 2 and 3 contain Apa L1 digested and undigested (UD) Pvu II fragment respectively. (B) Hinf I and Ple I digestion of Syt I 3' UTR (360 bp) PCR product for creating Syt I_{1-101}, Syt I_{94-360} and Syt $I_{101-302}$ fragments. Lane 1- Syt I 3' UTR PCR product, lane 3 and 4 – Hinf I and Ple I digestion products respectively. (C) The Syt I_{1-101} fragment in pTZ57R/T vector is confirmed by double digestion with Eco R1 and Sal I (lane 3), UD plasmid (lane 1). (D) The presence and orientation of Syt I_{94-360} fragment was confirmed by Apa L1 digestion. Lane 1 – UD plasmid, lanes 3 and 4 – Apa L1 digested direct and reverse oriented plasmids of pTZ57R/T-Syt I_{94-360} respectively. For RNA synthesis using T7 promoter in pTZ57R/T vector, the reverse clone is required. The lane 1 contain UD plasmid (E) The pGEMT-Syt $I_{102-302}$ was confirmed by Apa L1 (lane 3) and Rsa I (lane 4) digestions. Lane 1 contains UD plasmid. (F) For the *in vitro* transcription of RNA the plasmids containing Syt I_{1-101}, Syt I_{94-360} and Syt $I_{102-302}$ were linearized and eluted. Lane 1- pTZ57R/T- Syt I_{1-101} – Xba I, lane 2- pTZ57R/T- Syt I_{94-360} – Xba I and lane 3 pGEMT-Syt $I_{102-302}$ – Sal I. B-F contain molecular weight markers (GeneRuler™ DNA ladder mix, MBI Fermentas). The asterisks indicate the UD form of DNA in the mixture.

Methods for details). The clones or fragments were confirmed by restriction digestions **(Figure 31A-F and Table 9)** and used for *in vitro* synthesis of RNA.

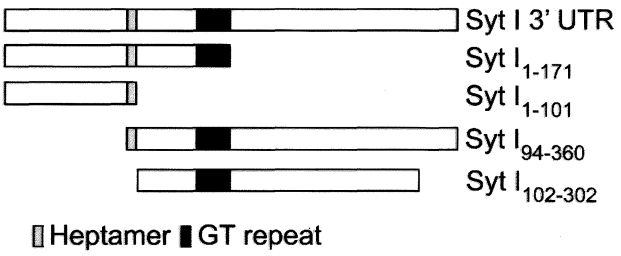

Figure 30: Schematic representation of Syt I 3' UTR RNA constructs.

Table 9: Restriction digestions for the Syt I 3' UTR smaller constructs

Clone/Gene	Restriction enzymes	Expected products	Lane No.
pTZ57R/T-Syt I 3' UTR – Pvu II fragment	Apa L1	421 bp and 314 bp	A-2
Syt I 3' UTR PCR product	Hinf I	259 bp and 93 bp	B-3
	Ple I	267 bp and 101 bp	B-4
pTZ57R/T-Syt I_{1-101}	Eco R1-Sal I	2.8 kb and 155 bp	C-3
	Xba I	2.98 kb	F-2
pTZ57R/T-Syt I_{94-360}	Apa L1	1.2 kb, 1.08 kb and 820 bp	D-4
	Xba I	3.2 kb	F-3
pGEMT-Syt $I_{102-302}$	Apa L1	1.25 kb, 968 bp and 931 bp	E-3
	Rsa I	1.9 kb and 1.37 kb	E-4
	Sal I	3.26 kb	F-4

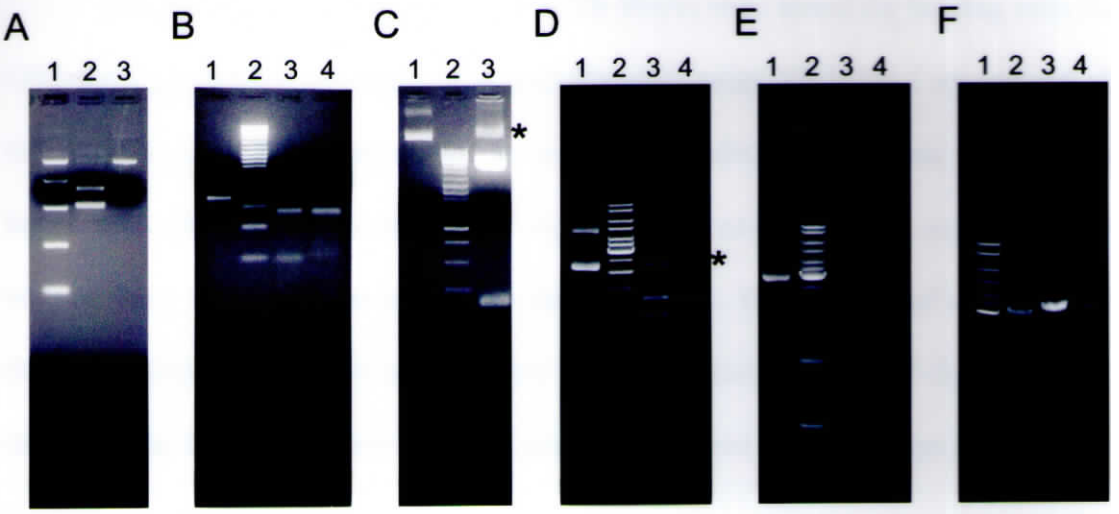

Figure 31: Restriction digestion of Syt I 3' UTR for creating smaller fragments. (A) Apa L1 digestion of pTZ57R/T-Syt I 3' UTR-Pvu II fragment for creating Syt I_{1-171} fragment. Lane 1 - marker (bands at 766, 500, 300, 150 and 50 bp, New England BioLabs, USA). Lane 2 and 3 contain Apa L1 digested and undigested (UD) Pvu II fragment respectively. (B) Hinf I and Ple I digestion of Syt I 3' UTR (360 bp) PCR product for creating Syt I_{1-101}, Syt I_{94-360} and Syt $I_{101-302}$ fragments. Lane 1- Syt I 3' UTR PCR product, lane 3 and 4 – Hinf I and Ple I digestion products respectively. (C) The Syt I_{1-101} fragment in pTZ57R/T vector is confirmed by double digestion with Eco R1 and Sal I (lane 3), UD plasmid (lane 1). (D) The presence and orientation of Syt I_{94-360} fragment was confirmed by Apa L1 digestion. Lane 1 – UD plasmid, lanes 3 and 4 – Apa L1 digested direct and reverse oriented plasmids of pTZ57R/T-Syt I_{94-360} respectively. For RNA synthesis using T7 promoter in pTZ57R/T vector, the reverse clone is required. The lane 1 contain UD plasmid (E) The pGEMT-Syt $I_{102-302}$ was confirmed by Apa L1 (lane 3) and Rsa I (lane 4) digestions. Lane 1 contains UD plasmid. (F) For the *in vitro* transcription of RNA the plasmids containing Syt I_{1-101}, Syt I_{94-360} and Syt $I_{102-302}$ were linearized and eluted. Lane 1- pTZ57R/T- Syt I_{1-101} – Xba I, lane 2- pTZ57R/T- Syt I_{94-360} – Xba I and lane 3 pGEMT-Syt $I_{102-302}$ – Sal I. B-F contain molecular weight markers (GeneRuler™ DNA ladder mix, MBI Fermentas). The asterisks indicate the UD form of DNA in the mixture.

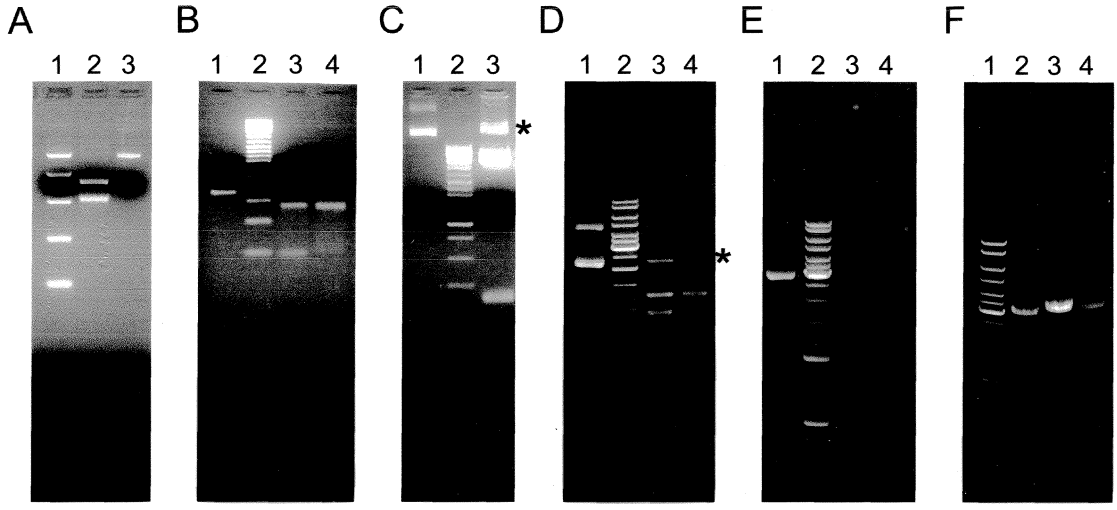

Figure 31: Restriction digestion of Syt I 3' UTR for creating smaller fragments. (A) Apa L1 digestion of pTZ57R/T-Syt I 3' UTR-Pvu II fragment for creating Syt $I_{1\text{-}171}$ fragment. Lane 1 - marker (bands at 766, 500, 300, 150 and 50 bp, New England BioLabs, USA). Lane 2 and 3 contain Apa L1 digested and undigested (UD) Pvu II fragment respectively. (B) Hinf I and Ple I digestion of Syt I 3' UTR (360 bp) PCR product for creating Syt $I_{1\text{-}101}$, Syt $I_{94\text{-}360}$ and Syt $I_{101\text{-}302}$ fragments. Lane 1- Syt I 3' UTR PCR product, lane 3 and 4 – Hinf I and Ple I digestion products respectively. (C) The Syt $I_{1\text{-}101}$ fragment in pTZ57R/T vector is confirmed by double digestion with Eco R1 and Sal I (lane 3), UD plasmid (lane 1). (D) The presence and orientation of Syt $I_{94\text{-}360}$ fragment was confirmed by Apa L1 digestion. Lane 1 – UD plasmid, lanes 3 and 4 – Apa L1 digested direct and reverse oriented plasmids of pTZ57R/T-Syt $I_{94\text{-}360}$ respectively. For RNA synthesis using T7 promoter in pTZ57R/T vector, the reverse clone is required. The lane 1 contain UD plasmid (E) The pGEMT-Syt $I_{102\text{-}302}$ was confirmed by Apa L1 (lane 3) and Rsa I (lane 4) digestions. Lane 1 contains UD plasmid. (F) For the *in vitro* transcription of RNA the plasmids containing Syt $I_{1\text{-}101}$, Syt $I_{94\text{-}360}$ and Syt $I_{102\text{-}302}$ were linearized and eluted. Lane 1- pTZ57R/T- Syt $I_{1\text{-}101}$ – Xba I, lane 2- pTZ57R/T- Syt $I_{94\text{-}360}$ – Xba I and lane 3 pGEMT-Syt $I_{102\text{-}302}$ – Sal I. B-F contain molecular weight markers (GeneRuler™ DNA ladder mix, MBI Fermentas). The asterisks indicate the UD form of DNA in the mixture.

The smaller constructs of Syt I 3' UTR RNAs were tested for binding with the GST-Syt I protein by electrophoretic mobility shift assay. GST-Syt I recognized all the Syt I 3' UTR RNA fragments; however, the binding affinity was significantly lower in the absence of heptamer or GT repeat sequences **(Figure 32)**, suggesting that both of these sequences are crucial for the interaction. The absence of either one of these domains in the RNA reduced the binding affinity with GST-Syt I protein, indicates that the Syt I protein detects a structural element within the Syt I 3' UTR for binding.

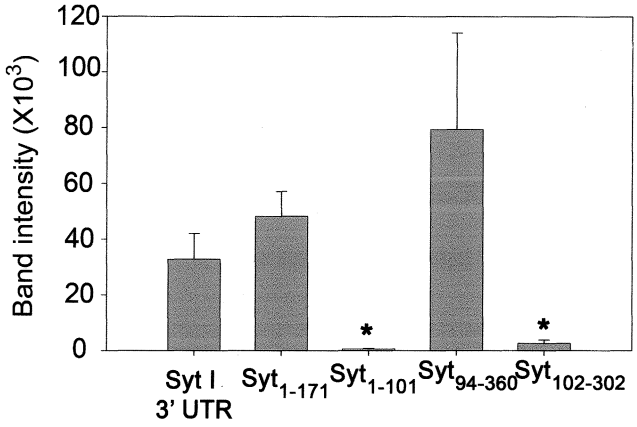

Figure 32: The smaller RNA fragments of Syt I 3' UTR were allowed to interact with GST-Syt I protein and the band intensities of RNP complexes on the native gel were measured densitometrically. Binding affinity of the Syt I 3' UTR RNA constructs with Syt I, represented in the graph (values were normalized to equal RNA and protein concentration), shows that both GU repeat and heptamer sequences are essential for protein recognition. Syt I_{1-101} without GU repeat and Syt $I_{102-302}$ without heptamer sequence showing less binding affinity for the protein. Data derived from three to nine independent experiments (± s.e.m.; *, $P<0.01$ compare to Syt I 3' UTR).

The smaller constructs of Syt I 3' UTR RNAs were tested for binding with the GST-Syt I protein by electrophoretic mobility shift assay. GST-Syt I recognized all the Syt I 3' UTR RNA fragments; however, the binding affinity was significantly lower in the absence of heptamer or GT repeat sequences **(Figure 32)**, suggesting that both of these sequences are crucial for the interaction. The absence of either one of these domains in the RNA reduced the binding affinity with GST-Syt I protein, indicates that the Syt I protein detects a structural element within the Syt I 3' UTR for binding.

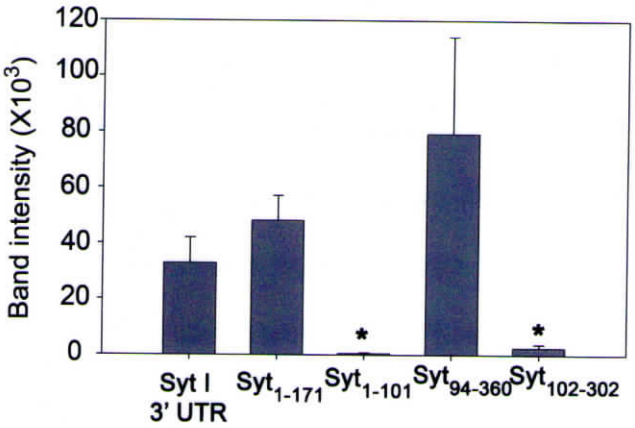

Figure 32: The smaller RNA fragments of Syt I 3' UTR were allowed to interact with GST-Syt I protein and the band intensities of RNP complexes on the native gel were measured densitometrically. Binding affinity of the Syt I 3' UTR RNA constructs with Syt I, represented in the graph (values were normalized to equal RNA and protein concentration), shows that both GU repeat and heptamer sequences are essential for protein recognition. Syt I_{1-101} without GU repeat and Syt $I_{102-302}$ without heptamer sequence showing less binding affinity for the protein. Data derived from three to nine independent experiments (± s.e.m.; *, $P<0.01$ compare to Syt I 3' UTR).

The heptamer sequence in human Syt I 3' UTR share similarity to CDEI element of yeast centromeres, which binds with nuclear proteins (Vidal, *et al.*, 1992). Variations in CDEI sequence reduce its protein binding but not totally abolishes it; mutated sequences like GTCAtATG and GTCACAcG could able to emulate protein binding at a higher concentration (Blangy, *et al.*, 1991). The CDEI element has been implicated mainly in maintaining a tight association between sister chromatids during meiosis in *S. cervisiae* (Bloom, *et al.*, 1989) as well as in transcriptional control in higher eukaryotes (Blangy, *et al.*, 1991).

The results in the present study suggest that the modified CDEI element, the heptamer sequence also has a protein binding ability. In addition, the GU_{15} repeat region immediately downstream to the heptamer sequence facilitates the specificity of this binding. Nucleo-protein complex formation with GT repeat has shown that the number of dinucleotide repeat is critical in protein binding affinity. For example GT_{17} competes for protein better than GT_{12} (Gao, *et al.*, 2004). These dinucleotide repeats are often localized in the promoter region of genes including human type I collagen alpha 2 (Akai, *et al.*, 1999), human growth factor hormone receptor (Hadjiyannakis, *et al.*, 2001) and STAT6 (Tamura, *et al.*, 2001). It is postulated that in DNA these GT repeats form non-B-form DNA conformation that differentially modulate the transcriptional element and in RNA the repeats regulate its stability and translation efficiency (Gao, *et al.*, 2004).

4.8. RNA BINDING DOMAIN OF SYT I PROTEIN

Although, Syt I protein has no known conserved RNA binding sites, the C2B domain binds to small nucleic acid fragments (Ubach, *et al.*, 2001) and alters the

biochemical properties including the Ca^{2+} triggered oligomerization and the membrane binding property of Syt I (Wu, *et al.*, 2003). Studies using ^{1}H-^{15}N HSQC spectra showed that Lys326 and Lys327 which corresponded to a poly basic region of strand 4 and the preceding loop were bound with polyacidic molecules, probably nucleic acids (Ubach, *et al.*, 2001).

There is a serious debate on whether the small nucleic acid fragments associated with C2B domain influence its function, because removal of these nucleic acids found to alter oligomerization property of Syt I proteins. However, the soluble portion of native Syt I (p39) forms large oligomers as a function of Ca^{2+} (Fukuda and Mikoshiba, 2000; Ubach, *et al.*, 2001) suggesting that not only the recombinant protein but also the native Syt I C2B have the intrinsic property to bind with short RNA molecules.

4.8.1. Recombinant proteins for Syt I C2 domains

To study the role of the Syt I C2A and C2B domains in Syt I 3' UTR RNA interaction, three recombinant fusion proteins were constructed: GST-C2 (containing both C2 domains), GST-C2A, and GST-C2B **(Figure 33)**. For this, the region corresponding to Syt I C2, Syt I C2A and Syt I C2B were PCR amplified from the pTZ57R/T-Syt I plasmid clone **(Figure 34)**, cloned in pTZ57R/T vector and sub-cloned in pGEX4T1 vector for protein expressions (see Materials and Methods for details). The clones were confirmed by restriction digestions **(Figure 34 and Table 10)**.

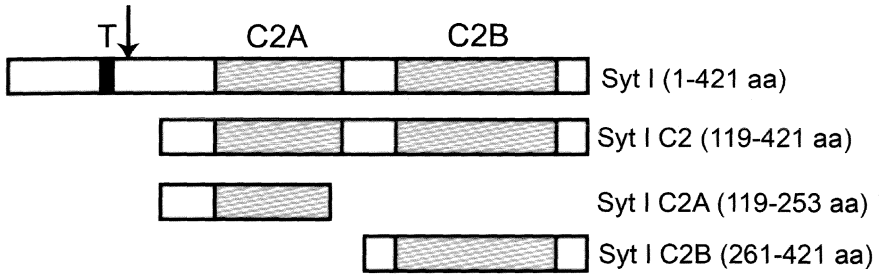

Figure 33: Structural domains of Syt I in the recombinant protein construct. Transmembrane [T] and C2A and C2B domains (shaded) are shown. The arrow indicates the hypersensitive proteolytic site in Syt I.

Table 10: Restriction digestions of Syt I C2, Syt I C2A and Syt I C2B clones in pTZ57R/T, pUC19 and pGEX4T1 vectors

Clone	Restriction enzymes	Expected products	Lane No.
pTZ57R/T-Syt I C2	Eco R1-Sal I	2.8 kb and 929 bp	4
	Kpn I	3.5 kb and 312 bp	5
pGEX4T1-Syt I C2	Bam H1	4.9 kb and 979 bp	8
pTZ57R/T-Syt I C2A	Eco R1-Sal I	2.8 kb and 460 bp	9
	Xba I-Hind III	2.8 kb and 452 bp	10
pUC19-Syt I C2A	Eco R1-Sal I	2.65 kb and 458 bp	13
pGEX4T1-Syt I C2A	Eco R1-Sal I	4.96 bp and 451 bp	15
pTZ57R/T-Syt I C2B	Bgl I	1.47 kb, 1.27 kb and 653 bp	16
	Xba I-Hind III	2.8 kb and 549 bp	18
pUC19-Syt I C2B	Eco R1-Sal I	2.65 kb and 555 bp	21
pGEX4T1-Syt I C2B	Pst I	4.53 kb and 1.05 kb	22

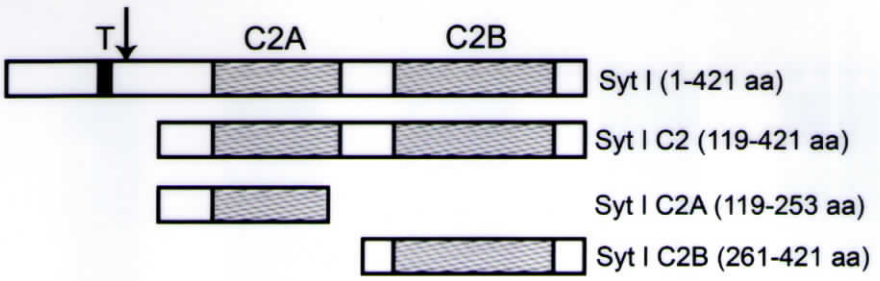

Figure 33: Structural domains of Syt I in the recombinant protein construct. Transmembrane [T] and C2A and C2B domains (shaded) are shown. The arrow indicates the hypersensitive proteolytic site in Syt I.

Table 10: Restriction digestions of Syt I C2, Syt I C2A and Syt I C2B clones in pTZ57R/T, pUC19 and pGEX4T1 vectors

Clone	Restriction enzymes	Expected products	Lane No.
pTZ57R/T-Syt I C2	Eco R1-Sal I	2.8 kb and 929 bp	4
	Kpn I	3.5 kb and 312 bp	5
pGEX4T1-Syt I C2	Bam H1	4.9 kb and 979 bp	8
pTZ57R/T-Syt I C2A	Eco R1-Sal I	2.8 kb and 460 bp	9
	Xba I-Hind III	2.8 kb and 452 bp	10
pUC19-Syt I C2A	Eco R1-Sal I	2.65 kb and 458 bp	13
pGEX4T1-Syt I C2A	Eco R1-Sal I	4.96 bp and 451 bp	15
pTZ57R/T-Syt I C2B	Bgl I	1.47 kb, 1.27 kb and 653 bp	16
	Xba I-Hind III	2.8 kb and 549 bp	18
pUC19-Syt I C2B	Eco R1-Sal I	2.65 kb and 555 bp	21
pGEX4T1-Syt I C2B	Pst I	4.53 kb and 1.05 kb	22

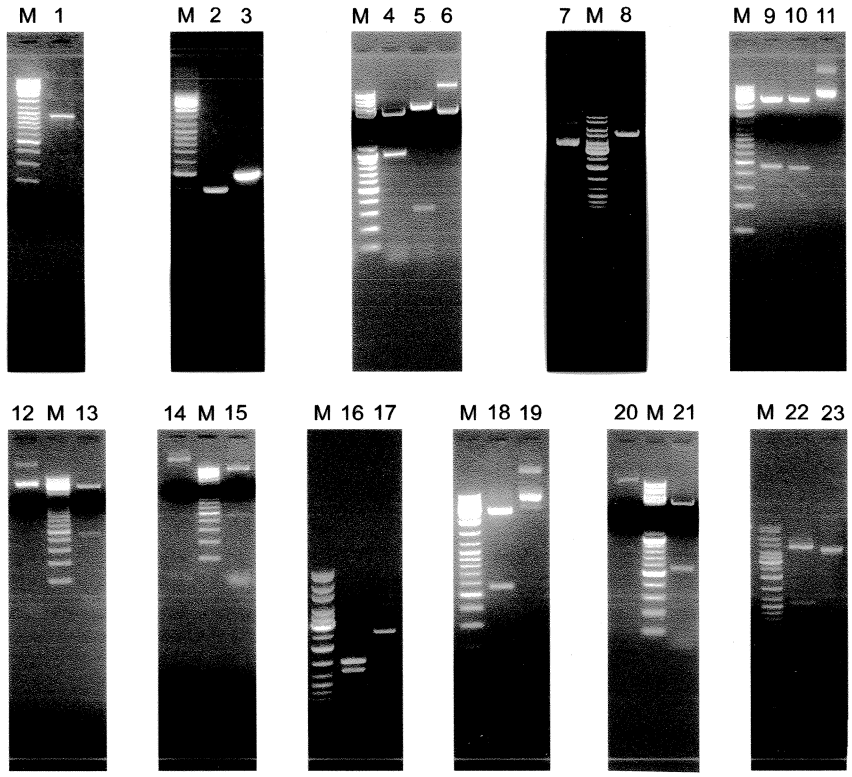

Figure 34: PCR for Syt I -C2, -C2A and -C2B domains and restriction digestion pattern of genes in pTZ57R/T, pUC19 and pGEX4T1 vectors. Lanes 1-23 represent: (1) Syt I C2 PCR, (2) Syt I C2A PCR, (3) Syt I C2B PCR, (4) pTZ57R/T-Syt I C2 - Eco R1-Sal I, (5) pTZ57R/T-Syt I C2 - Kpn I, (6) pTZ57R/T-Syt I C2 undigested (UD) plasmid, (7) pGEX4T1-Syt I C2 UD plasmid, (8) pGEX4T1-Syt I C2 - Bam H1, (9) pTZ57R/T-Syt I C2A - Xba I-Sal I, (10) pTZ57R/T-Syt I C2A - Xba I-Hind III, (11) pTZ57R/T-Syt I C2A UD plasmid, (12) pUC19-Syt I C2A UD plasmid, (13) pUC19-Syt I C2A - Eco R1-Sal I, (14) pGEX4T1-Syt I C2A UD plasmid, (15) pGEX4T1-Syt I C2A - Eco R1-Sal I, (16) pTZ57R/T-Syt I C2B - Bgl I, (17) pTZ57R/T-Syt I C2B UD plasmid, (18) pTZ57R/T-Syt I C2B - Xba I-Hind III, (19) pTZ57R/T-Syt I C2B UD plasmid, (20) pUC19-Syt I C2B UD plasmid, (21) pUC19-Syt I C2B - Eco R1-Sal I, (22) pGEX4T1-Syt I C2B - Pst I and (23) pGEX4T1-Syt I C2B UD plasmid. Lane M represent marker lane (GeneRuler^{TM} DNA ladder mix, MBI Fermentas) as a standard.

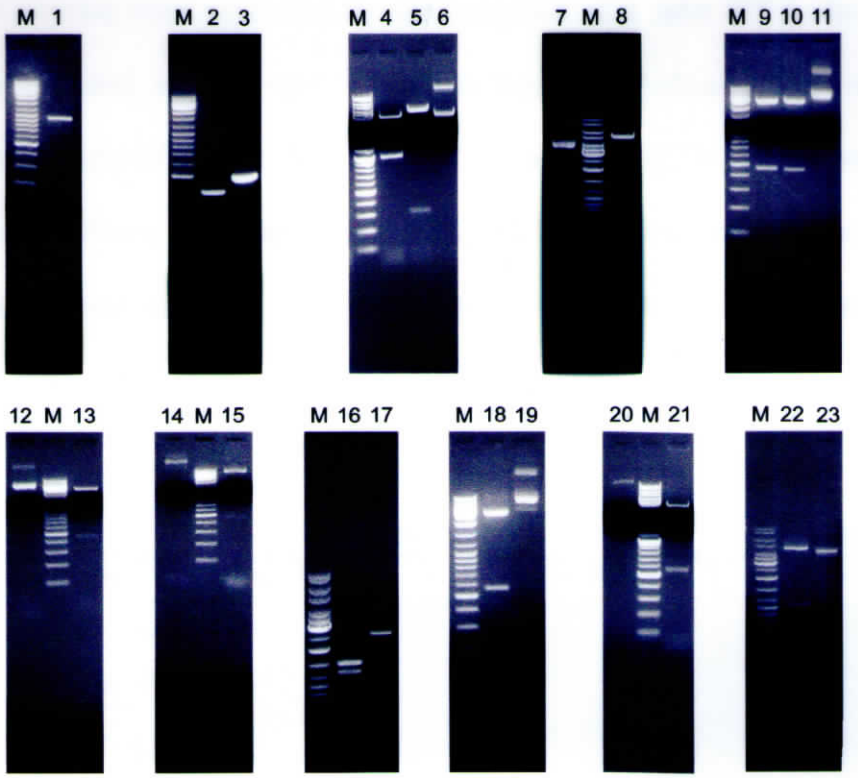

Figure 34: PCR for Syt I -C2, -C2A and -C2B domains and restriction digestion pattern of genes in pTZ57R/T, pUC19 and pGEX4T1 vectors. Lanes 1-23 represent: (1) Syt I C2 PCR, (2) Syt I C2A PCR, (3) Syt I C2B PCR, (4) pTZ57R/T-Syt I C2 - Eco R1-Sal I, (5) pTZ57R/T-Syt I C2 - Kpn I, (6) pTZ57R/T-Syt I C2 undigested (UD) plasmid, (7) pGEX4T1-Syt I C2 UD plasmid, (8) pGEX4T1-Syt I C2 - Bam H1, (9) pTZ57R/T-Syt I C2A - Xba I-Sal I, (10) pTZ57R/T-Syt I C2A - Xba I-Hind III, (11) pTZ57R/T-Syt I C2A UD plasmid, (12) pUC19-Syt I C2A UD plasmid, (13) pUC19-Syt I C2A - Eco R1-Sal I, (14) pGEX4T1-Syt I C2A UD plasmid, (15) pGEX4T1-Syt I C2A - Eco R1-Sal I, (16) pTZ57R/T-Syt I C2B - Bgl I, (17) pTZ57R/T-Syt I C2B UD plasmid, (18) pTZ57R/T-Syt I C2B - Xba I-Hind III, (19) pTZ57R/T-Syt I C2B UD plasmid, (20) pUC19-Syt I C2B UD plasmid, (21) pUC19-Syt I C2B - Eco R1-Sal I, (22) pGEX4T1-Syt I C2B - Pst I and (23) pGEX4T1-Syt I C2B UD plasmid. Lane M represent marker lane (GeneRuler^{TM} DNA ladder mix, MBI Fermentas) as a standard.

The proteins were expressed by the induction of 1 mM IPTG, the protein lysates were prepared, purified using MicroSpin purification columns and confirmed by SDS-PAGE analysis **(Figure 35)**. The GST-C2 and GST-C2B proteins were also purified using affinity chromatography with AKTA protein purification system (Amersham Biosciences, USA). The protein peaks were observed in chromatogram **(Figure 36)** and further confirmed by SDS-PAGE analysis.

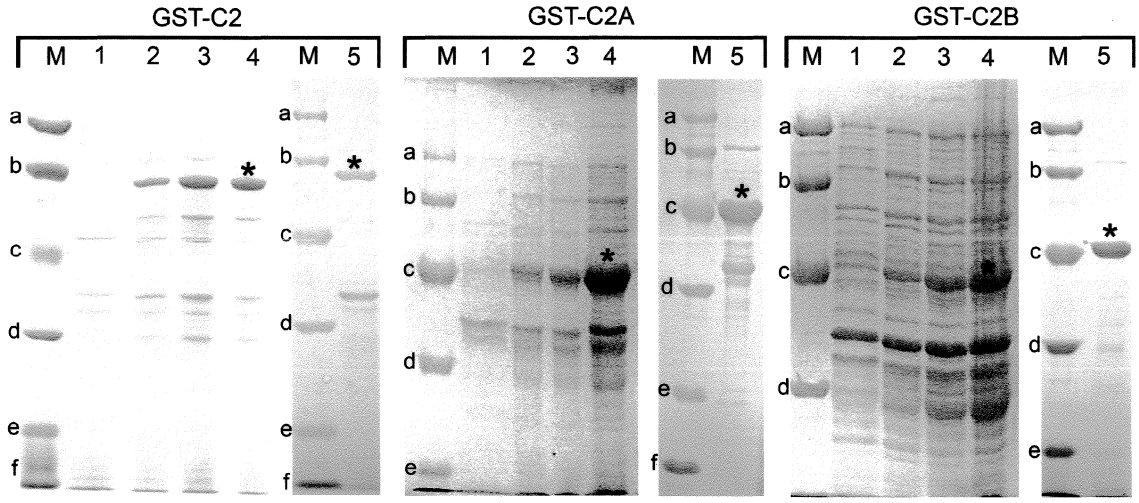

Figure 35: SDS-PAGE showing the expression of GST-C2, -C2A and -C2B proteins. Lanes 1-4 represent protein bands by loading 0.3 OD of the bacterial culture - Lane 1, 0th hour (pre-IPTG induction), lane 2, 1st hour, lane 3, 2nd hour and lane 4, 3rd hour after IPTG induction. Lane 5 represents the purified GST fusion proteins (10 µg) using MicroSpin columns (Amersham Bioscciences, USA), marked by asterisks. Lane M show protein marker (PMWM medium range, Bangalore Genei, India) with bands at 97.4 (a), 66.0 (b), 43.0 (c), 29.0 (d), 20.1 (e) and 14.3 (f) kDa positions.

The proteins were expressed by the induction of 1 mM IPTG, the protein lysates were prepared, purified using MicroSpin purification columns and confirmed by SDS-PAGE analysis **(Figure 35)**. The GST-C2 and GST-C2B proteins were also purified using affinity chromatography with AKTA protein purification system (Amersham Biosciences, USA). The protein peaks were observed in chromatogram **(Figure 36)** and further confirmed by SDS-PAGE analysis.

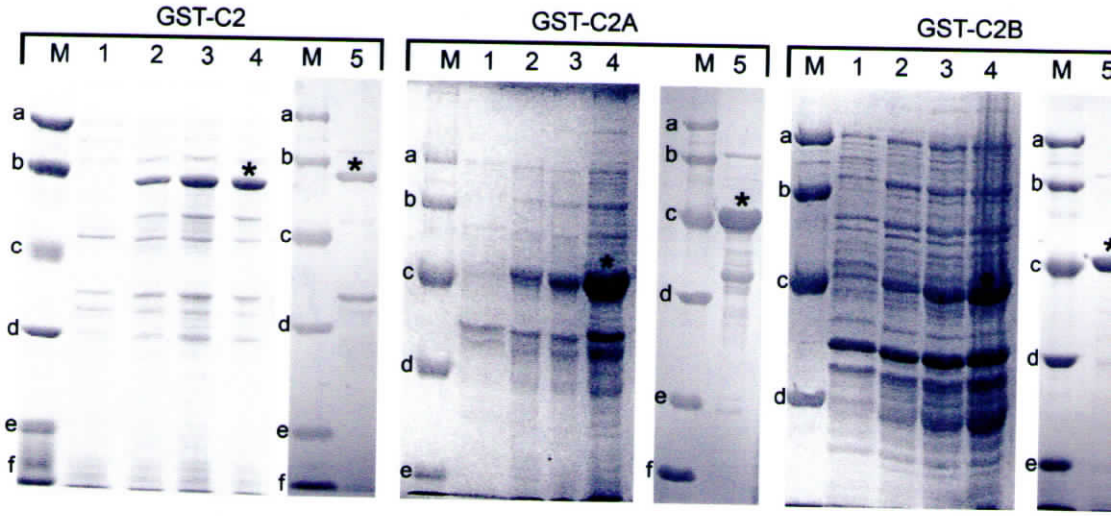

Figure 35: SDS-PAGE showing the expression of GST-C2, -C2A and -C2B proteins. Lanes 1-4 represent protein bands by loading 0.3 OD of the bacterial culture - Lane 1, 0th hour (pre-IPTG induction), lane 2, 1st hour, lane 3, 2nd hour and lane 4, 3rd hour after IPTG induction. Lane 5 represents the purified GST fusion proteins (10 µg) using MicroSpin columns (Amersham Bioscciences, USA), marked by asterisks. Lane M show protein marker (PMWM medium range, Bangalore Genei, India) with bands at 97.4 (a), 66.0 (b), 43.0 (c), 29.0 (d), 20.1 (e) and 14.3 (f) kDa positions.

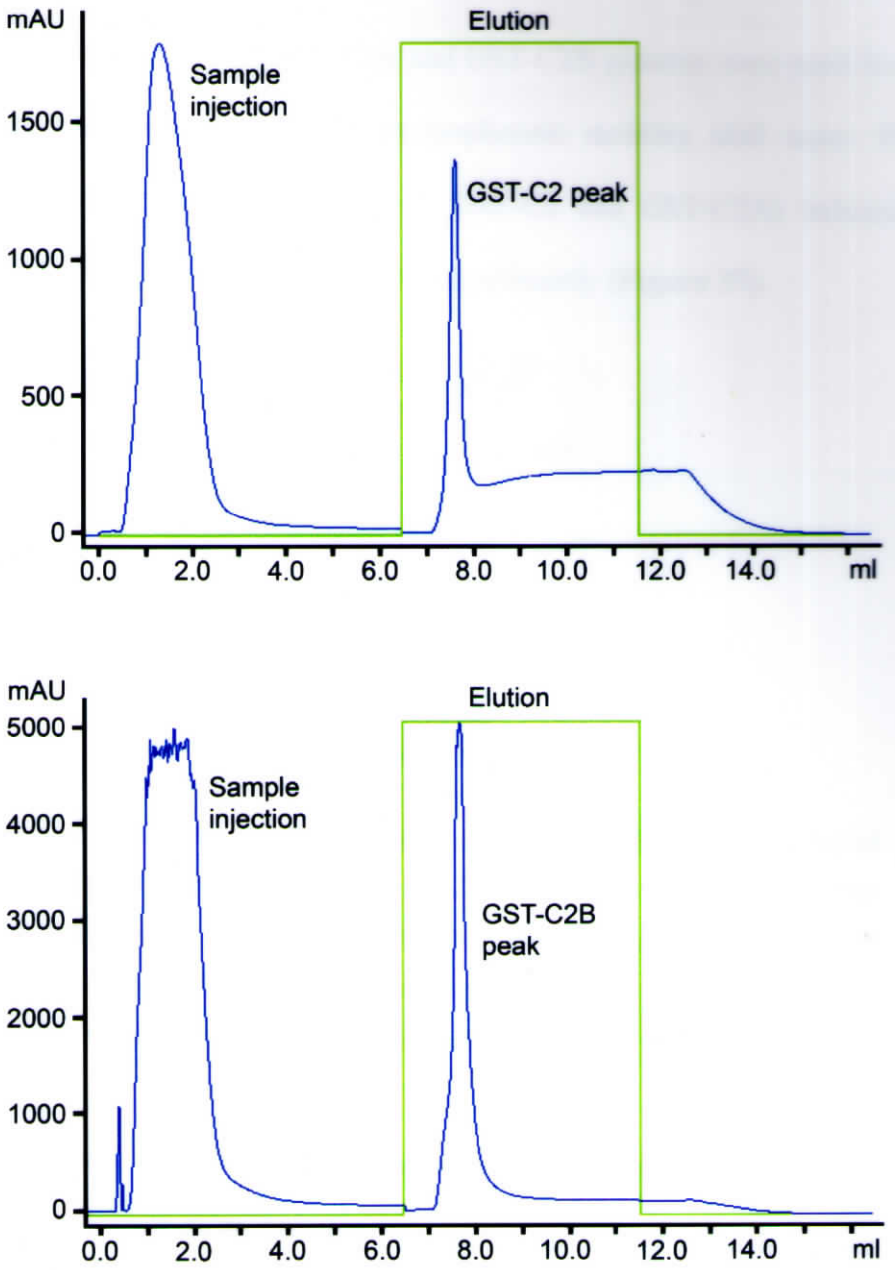

Figure 36: Chromatograms showing the purification of GST-C2 and GST-C2B proteins using GSTrap HP columns with AKTA purifier (GE Healthcare, USA).

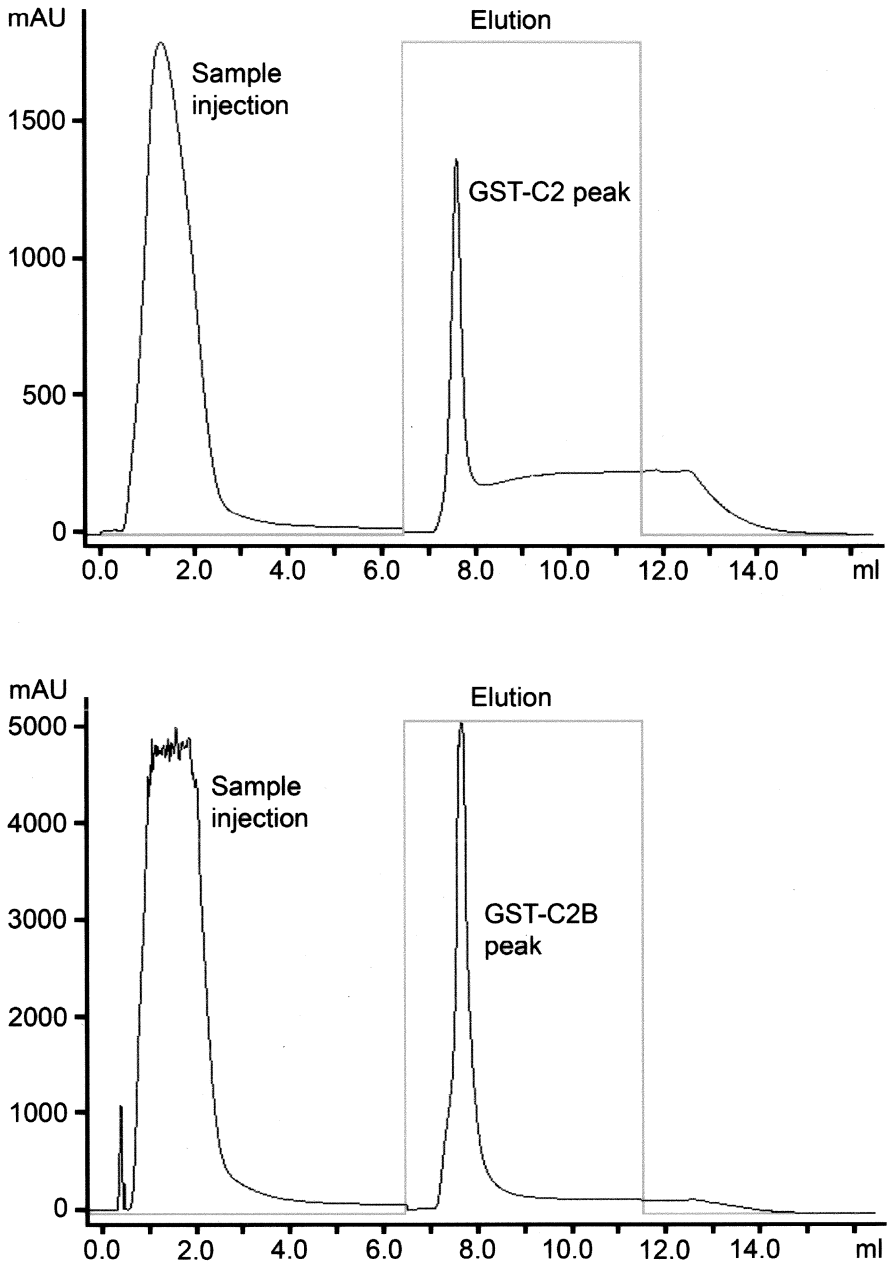

Figure 36: Chromatograms showing the purification of GST-C2 and GST-C2B proteins using GSTrap HP columns with AKTA purifier (GE Healthcare, USA).

4.8.2. C2A domain of Syt I is essential in RNP complex formation

The purified GST-C2, GST-C2A and GST-C2B proteins were used for RNA-protein interaction and analyzed by electrophoretic mobility shift assay. Proteins containing the C2A domain (GST-Syt I, GST-C2 and GST-C2A) induced RNP formation, but GST-C2B did not bind RNA significantly **(Figure 37)**.

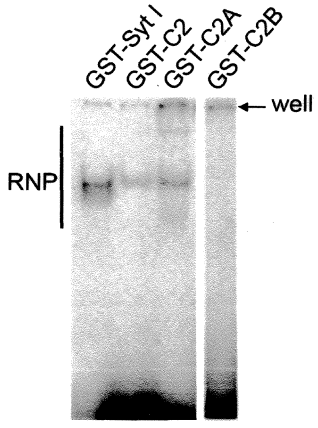

Figure 37: Electrophoretic mobility shift assay gel showing the interaction of Syt I 3' UTR RNA with GST-Syt I, -C2, -C2A and -C2B proteins. The proteins containing C2A domain recognized the RNA probe, whereas C2B domain showed significantly lower affinity for the probe as shown in the gel (n=7). For the assay, equal concentrations of protein were used.

We avoided the RNase treatment of the recombinant proteins so that the nucleic acid probe used in the binding assay will not interact non-specifically to the C2B domain. The recombinant proteins with the C2B domain, GST-Syt I, GST-C2 and GST-C2B, shown high values for the 260/280 ratio compared to GST and GST-C2A proteins **(Figure 38)** confirming the presence of nucleic acids. In the present study, absence of RNA binding to the C2B domain also give evidence that the domain is pre-saturated with small nucleic acid fragments. The C2A domain in the

4.8.2. C2A domain of Syt I is essential in RNP complex formation

The purified GST-C2, GST-C2A and GST-C2B proteins were used for RNA protein interaction and analyzed by electrophoretic mobility shift assay. Protein containing the C2A domain (GST-Syt I, GST-C2 and GST-C2A) induced RNP formation, but GST-C2B did not bind RNA significantly **(Figure 37)**.

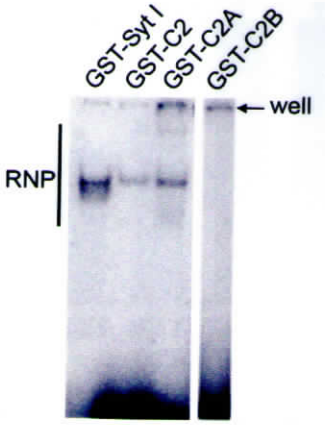

Figure 37: Electrophoretic mobility shift assay gel showing the interaction of Syt I 3' UTR RNA with GST-Syt I, -C2, -C2A and -C2B proteins. The proteins containing C2A domain recognized the RNA probe, whereas C2B domain showed significantly lower affinity for the probe as shown in the gel (n=7). For the assay, equal concentrations of protein were used.

We avoided the RNase treatment of the recombinant proteins so that the nucleic acid probe used in the binding assay will not interact non-specifically to the C2B domain. The recombinant proteins with the C2B domain, GST-Syt I, GST-C2 and GST-C2B, shown high values for the 260/280 ratio compared to GST and GST-C2A proteins **(Figure 38)** confirming the presence of nucleic acids. In the present study, absence of RNA binding to the C2B domain also give evidence that the domain is pre-saturated with small nucleic acid fragments. The C2A domain in the

protein is sufficient for the RNA binding but compared to the GST-Syt I protein, the RNP complex intensity was comparatively less in GST-C2 and GST-C2A proteins. From the above qualitative experiments, it was presumed that C2A would be acting as the RNA interacting domain in Syt I.

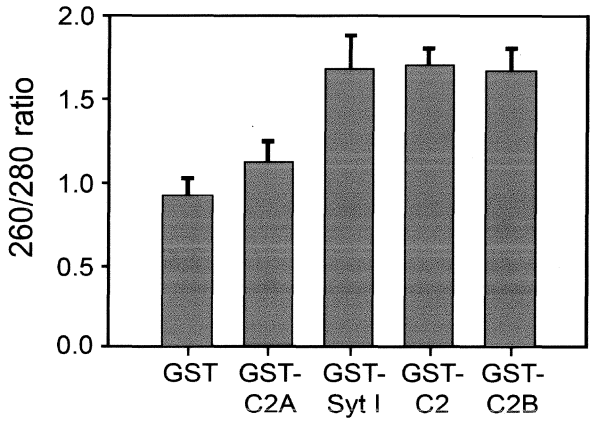

Figure 38: Quantitation of 260/280 ratio of GST-Syt fusion proteins shows significant nucleic acid presence in proteins containing C2B domain – GST-Syt I, -C2 and -C2B. The proteins containing only the C2A domain showed values similar to the GST protein. The data derived from 4 to 5 independent protein preparations, mean±s.e.m.

4.9. KINETICS OF RNA-PROTEIN INTERACTION

To measure the concentration-dependent affinity of the protein for the RNA filter-binding assay was conducted as a quantitative experiment (Baumann, *et al.*, 1996). The band intensities on the Nylon membranes were measured and the RNA bound to the protein was calculated by subtracting the normalized probe intensity in nylon membrane in presence of protein from the total probe added. The results showed that the GST-C2 protein has a saturation level for RNA affinity at 10 pMol

while GST-C2A has a slower linear kinetics for RNA binding even at 100 pMol (n=5) **(Figure 39)**.

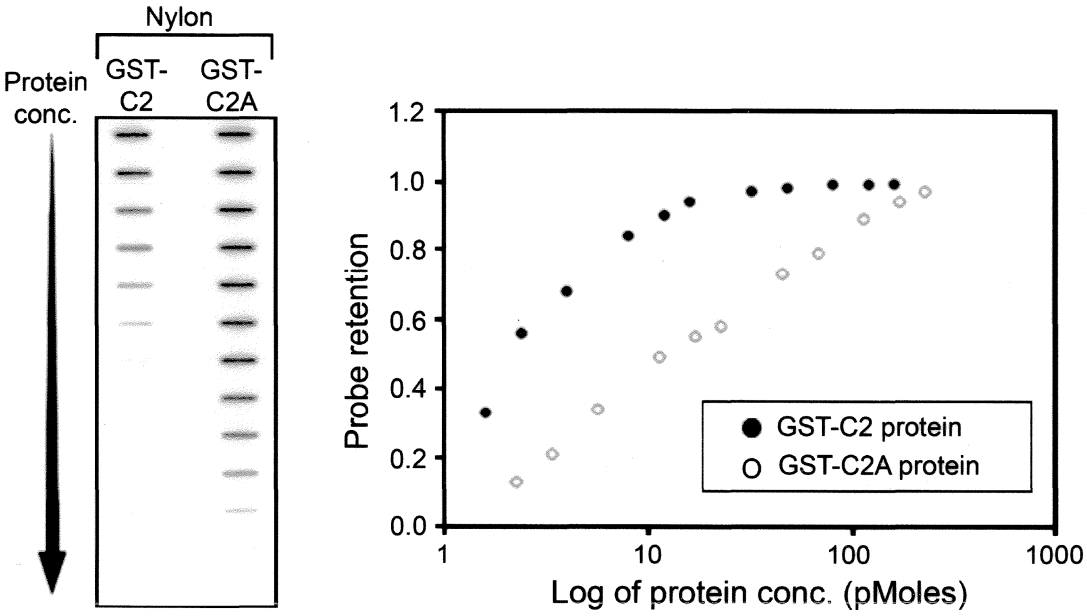

Figure 39: Kinetics of RNA interaction of GST -C2 and -C2A were measured by filter binding assay (n=5 for each). The RNA retained on the nylon membrane was quantitated and plotted against the log of protein concentration. The arrow indicates increasing concentration of protein.

This differing kinetics shown by the two proteins could be due to structural variations and/or co-operative role of C2A and C2B in RNA binding. The structural conformational changes occurring in presence of both C2A and C2B domains must be enhancing RNA recognition of GST-C2 protein. For example, in membrane fusion and oligomerization of Syt I, a complementary functional interlink between the two C2 domains is critical (Wu, *et al.*, 2003). Moreover, The variation in binding kinetics observed between C2 and C2A proteins for Syt I RNA indicates that the C2B domain

can play a partial role in the RNA binding affinity of C2A domain but not in the specificity of binding because C2B domain alone does not have an affinity for Syt I mRNA.

4.10. NEGATIVE CONTROLS FOR RNA-PROTEIN INTERACTION

To confirm the specificity of interaction of the Syt I protein with RNA, the control RNAs like antisense Syt I 3' UTR RNA (360 bases) and β-actin RNA (691 bases) were used for binding with GST-C2 and GST-C2A proteins. The antisense Syt I 3' UTR RNA contained CA_{15} repeats and totally degenerated sequence CAUUGAC at the heptamer position while β-actin RNA contained neither dinucleotide repeats nor heptamer sequence. Both the RNAs, antisense Syt I 3' UTR and β-actin RNA did not show affinity for GST-C2 and GST-C2A proteins suggesting that the interaction between Syt I 3' UTR RNA and Syt I protein was highly sequence specific **(Figure 40A)**. In addition, heat denaturation of GST-C2A protein abolished the RNA-protein interaction indicating that structural integrity of the protein is critical in the interaction with mRNA sequence **(Figure 40B)**.

4.11. EFFECT OF PHOSPHOLIPIDS IN RNA-PROTEIN INTERACTION

The signal intensity in gel retardation assay for GST-Syt I was always observed to be stronger than that of GST-C2 and -C2A **(Figure 37)**. To rule out whether the discrepancy in binding affinity of these proteins is owed to multiple binding sites within the GST-Syt I, phospholipids were included in the binding reaction to block the transmembrane domain. The intensity of binding showed

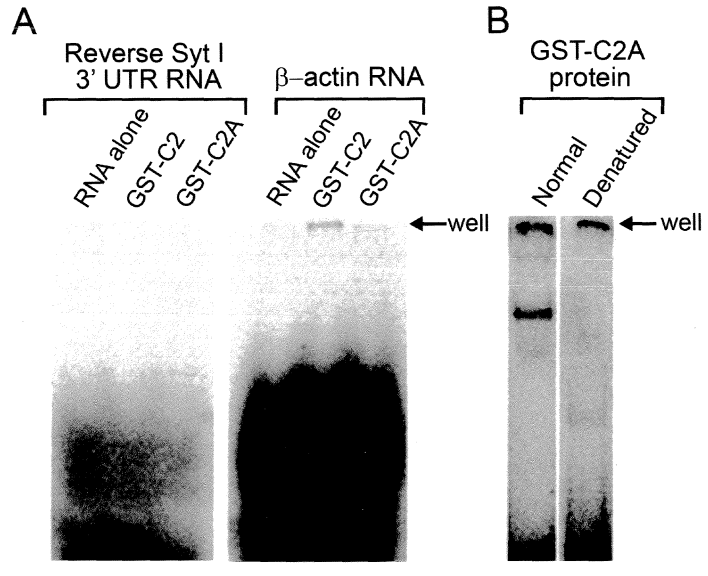

Figure 40: RNA-protein interaction is sequence and structure specific. (A) Control experiments using *in vitro* transcribed reverse Syt I 3' UTR RNA and β-actin RNA probes with GST-C2 and -C2A proteins did not show any interaction. The reverse Syt I 3' UTR probe contains CA_{15} repeat and totally degenerated heptamer sequence while β-actin mRNA do not contain both dinucleotide repeat and heptamer sequence. (B) Heat denaturation abolished the RNA binding property of GST-C2A protein.

decrease in the presence of phospholipids for GST-Syt I but remained unaffected for GST-C2 and GST-C2A proteins **(Figure 41)**. This implied an additional RNA binding site in the transmembrane domain of the full length Syt I. The GST-C2B protein remained unbound with RNA even in the presence of phospholipids **(Figure 41)**. Though the C2A domain has a Ca^{2+}-phospholipid-binding site (Sutton, *et al.*, 1995), presence of phospholipids and Ca^{2+} did not affect its RNA recognition property suggesting multiple functional sites within C2A domain for molecular interactions.

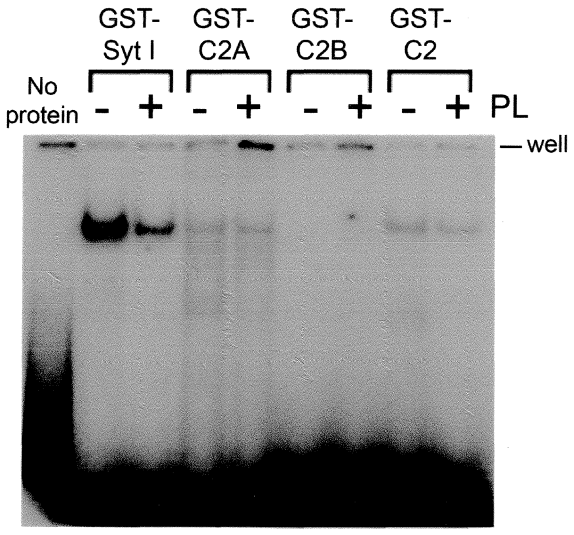

Figure 41: Phospholipids (PL) were incubated in the presence of 50 mM $CaCl_2$ in the RNA-protein binding assay. No significant variation in RNP formation was observed for GST-C2 and -C2A. GST-Syt I showed a significant reduction in binding with RNA in the presence of PL, indicating additional RNA binding site than the C2A domain within this protein (n=3).

4.12. PRESENCE OF 3' UTR DOWNREGULATES THE SYT I TRANSLATION

It was further wanted to test whether the RNP formation results in translational regulation of the Syt I protein using *in vitro* transcription-translation coupled rabbit reticulocyte lysate expression system. This assay allows both transcription and translation occur in the same reaction mixture and hence if RNA-protein interaction happens the protein synthesis will block after a certain level of translation. For the reaction we constructed two clones, one having Syt I full coding region alone (S) and another one containing 3' UTR (360 bp) immediately downstream to the coding region (S+U) **(Figure 42A)**.

4.12.1. Cloning of Syt I constructs with and without 3' UTR

The Syt I coding region and Syt I coding with 3' UTR were cloned in pGEMT vector (see Materials and methods for details). Briefly, the Syt I gene in pTZ57R/T vector was released by Eco R1-Sal I double digestion and cloned in pGEMT vector. The pGEMT-Syt I clone (S) was confirmed by restriction digestions. For the pGEMT-Syt I 3' UTR clone (S+U), the Syt I 3' UTR fragment was ligated to the full length coding region of Syt I gene in pGEMT vector (see Materials and methods for details).

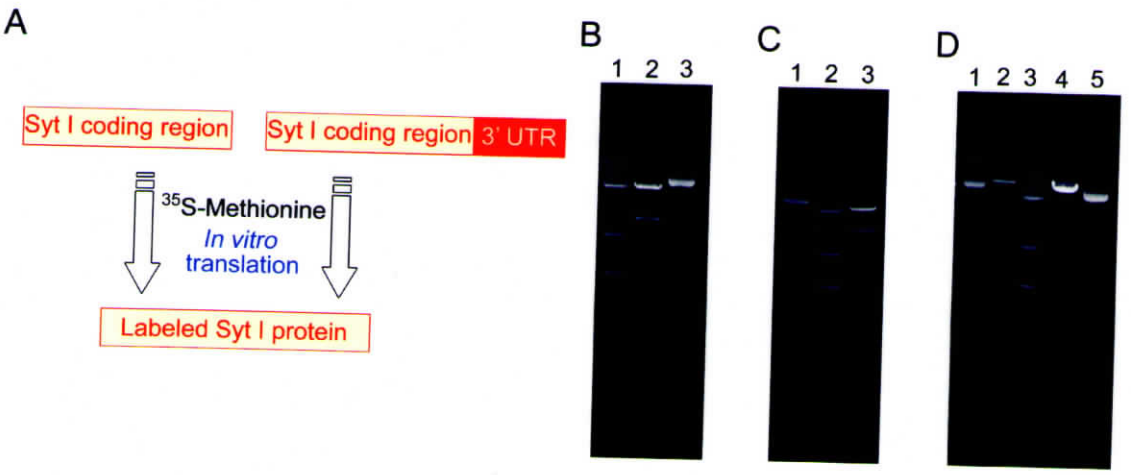

Figure 42: Cloning of Syt I gene with and without 3' UTR (360 bp) for *in vitro* translation assay. (A) Schematic representation of Syt I clones with/without 3' UTR. (B) Restriction digestion of pGEMT-Syt I with Eco R1-Sal I double digestion, in lane 2 digestion product and in lane 3 undigested (UD) plasmid is loaded. (C) Restriction digestion of pGEMT-Syt I 3' UTR with Eco R1, in lane 1 UD plasmid and in lane 3 digestion product is loaded. (D) The pGEMT-Syt I and -Syt I 3' UTR plasmids were linearized with Sal I enzyme for *in vitro* translation. Lanes 1 and 5 contain undigested plasmid and lanes 2 and 4 contain digestion products of pGEMT-Syt I 3' UTR and pGEMT-Syt I respectively. In all the gels marker (GeneRuler™ DNA ladder mix, MBI Fermentas) was included as a standard.

The digestion patterns and expected products were shown **(Figure 42B and C and Table 11)**. For *in vitro* translation assay both the plasmids were linearized with Sal I enzyme **(Figure 42D and Table 11)**.

Table 11: Restriction digestion pattern of Syt I with/without 3' UTR in pGEMT vector

Clone	Restriction enzymes	Expected products	Lane No.
pGEMT-Syt I	Eco R1- Sal I	3.0 kb and 1.3 kb	A-2
pGEMT-Syt I	Sal I	4.3 kb	C-4
pGEMT-Syt I 3' UTR	Eco R1	3.0 kb and 1.7 kb	B-3
pGEMT-Syt I 3' UTR	Sal I	4.66 kb	C-2

4.12.2. *In vitro* translation assay

For the translation assay with TNT T7 Quick Master Mix system (Promega, USA) equal concentrations of DNA (750 ng) were used. An aliquot of the translated [^{35}S] labeled proteins were resolved electrophoretically on SDS-polyacrylamide gel and bands were observed approximately at 47.5 kDa positions. The molecular weight of the translated protein was matching with non-glycosylated Syt I protein (Perin, *et al.*, 1991b). The band intensity in S and S+U were quantitated densitometrically. The translation efficiency of the 3' UTR-containing clone was reduced ~50% compared to the clone lacking the 3' UTR **(Figure 43)**.

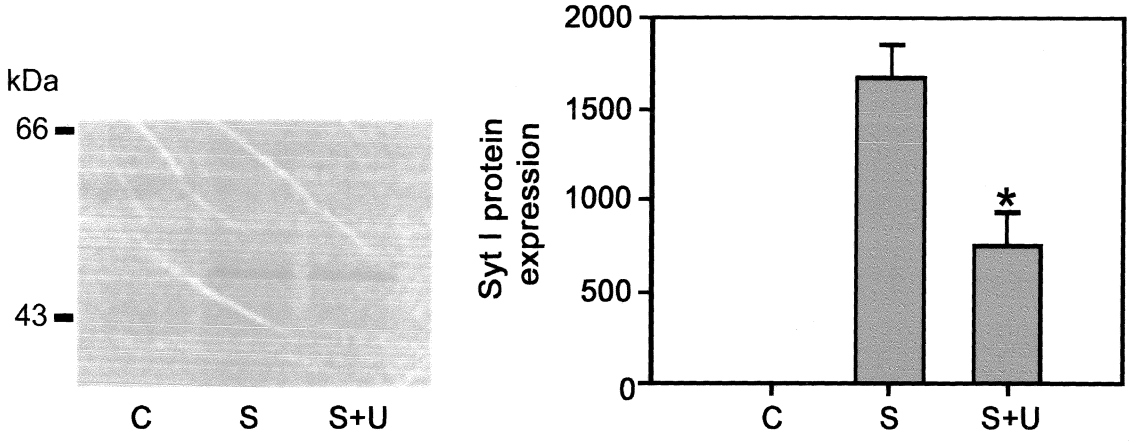

Figure 43: Translation of Syt I protein is regulated by 3' UTR of its own mRNA. Syt I gene constructs with and without the 360 bp 3' UTR were *in vitro* transcribed and translated. Reactions lacking DNA served as negative controls (C). S, Syt I gene construct without the 3' UTR; S+U, Syt I gene construct with the 3' UTR. A significant reduction in protein expression was observed in constructs with 3' UTR. The graph represents values from three independent experiments (± s.e.m; *, $P<0.008$).

The presence of 3' UTR had a significant effect on rate of Syt I translation. Together, these observations suggest to the compelling possibility that Syt I level in neurons changes through RNA-protein interaction, which consequently allows a translation control system.

Chapter 5

SUMMARY, CONCLUSIONS AND FUTURE PROSPECTS

5.1. SUMMARY AND CONCLUSIONS

Although it is well established that Syt family of proteins has a critical role in neurotransmitter release and synaptic vesicle endocytosis pathway, the regulation of their expression is controversial. In neonatal sympathetic neurons membrane depolarization induced by cyclic AMP results in parallel increase in Syt I level (Greif, 2001) and it is critical to have a normal postnatal expression of Syt I for synaptic activity (Greif and Trenchard, 1988). The results in the present study suggest that during seizure a rapid reduction in Syt I protein level in hippocampus occurs without altering the Syt I mRNA level. This attenuation of Syt I protein level in neurons can be due to autoregulation through its sequence-specific interaction with the 3' UTR of its own mRNA.

This study also bring evidences that in the protein, the C2A domain, and in the mRNA, a heptamer and GU repeat sequence in its 3' UTR are essential for this interaction. The presence of two C2 domains found to increase the affinity for its RNA binding while the C2B domain alone did not recognize Syt I transcript. The RNA-protein interaction is highly sequence specific as the negative controls like

antisense Syt I 3' UTR RNA and β-actin RNA have no affinity for the C2A domain. Besides, phospholipids has no influence in regulating the RNA-protein interaction mediated through the C2A domain, however, the structural integrity of the protein is very essential for this interaction.

The level of proteins at the presynaptic terminal alters through a different pathway compare to the postsynaptic terminal where the local protein expression depends on targeted transport of mRNA. The autoregulation of Syt I may act as a defensive mechanism against hyperactivation of neurons because low Syt I level at synapse impairs the neurotransmitter release. Conversely, a selective downregulation of Syt I within inhibitory neurons may result in seizure phenotype by allowing the excitatory neurons to dominate.

The soluble Syt I peptides in cytoplasm could act as a signal to regulate the translation and maintain a constant Syt I level at the synapse **(Figure 44)**. The hypersensitivity of Syt I to proteolysis might play a critical role in this regulatory pathway by allowing the release of the soluble cytoplasmic domain of the protein, thus set stage for RNA-protein complex to form. Syt I has a protease hypersensitive site immediately after its transmembrane domain, which on protease cleavage releases soluble p39 Syt I (Perin, *et al.*, 1991a). During seizure excessive protease activity sets in (Bi, *et al.*, 1996) which could increase the level of soluble p39 Syt I in the cell. Calpain protease gets activated during seizure (Bi, *et al.*, 1996) and has a strong affinity for Syt I (Liu, *et al.*, 2006). In addition, seizure associated stress response might induce the Met113 initiation codon and allow the synthesis of soluble p40 Syt I (Bagala, *et al.*, 2003). Both p39 and p40 Syts were found to be stable (Bagala, *et al.*,

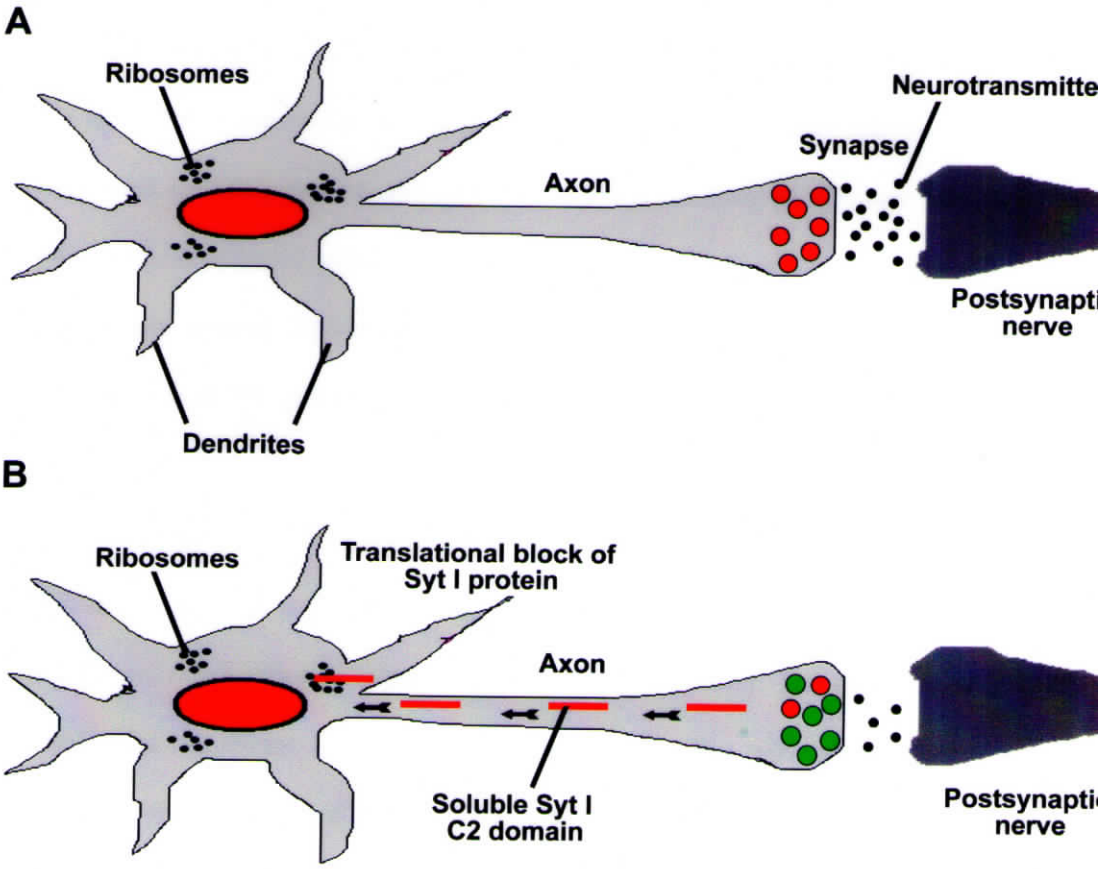

Figure 44: Functional model for Syt I protein regulation. The model indicates that Syt I protein level is maintained in a constant level in neurons. (A) Syt I is needed for the neurotransmitter release. The red circles represent synaptic vesicles with Syt I protein. The proteins synthesized by ribosomes were transported in an anterograde manner through the axon to the nerve terminals. (B) During the conditions like seizure, by the excessive proteolytic action as well by alternate translation initiation, the soluble form of Syt I protein level increases in the neuron. These soluble Syt I C2 domains are transported to ribosomes in a retrograde manner and block the further translation of Syt I protein. The green circles represent synaptic vesicles devoid of Syt I protein. Neurotransmitter release is blocked due to the absence of Syt I protein.

2003) and distributed both in cell body and axons. Both these forms can interact with the Syt I RNA present at the cell body. It is also possible that seizure initiates the ribosomal shunting process (Bagala, *et al.*, 2003) resulting in alternate translation of p40 Syt I. Significant reduction in p65 Syt I observed in seizure brain, suggest that there is an activity-dependent variation in the protein level. Thus the presence of soluble Syt I in the system can act as feed back loop to regulate the further translation of Syt I protein.

Besides, the Syt I cDNA constructs with and without 3' UTR, coding for the full-length protein, modeling the *in vivo* transcripts, were used to investigate their translation efficiencies in rabbit reticulocyte lysate system. The presence of 3' UTR resulted in significant reduction in Syt I translation. The reduced protein expression levels in the presence of the 3' UTR reiterates that there is a checkpoint in Syt I translation through the direct interaction between Syt I 3' UTR RNA and Syt I protein. These observations bring evidence to the possibility that the translation of Syt I mRNA in brain can be highly restrained in an autoregulatory manner by its own protein.

5.2. FUTURE PROSPECTS

The results presented in this work suggest a novel mechanism of regulation of Syt I expression in neurons in an activity dependent manner at the presynaptic terminal. Further evidences using *in vivo* experiments may give additional insights into the mechanism of regulation. Especially, experiments using slice physiology may be ideal to investigate functional regulation of Syt I in an activity dependent manner. *In vivo* studies are also needed to check how the autoregulation pathway activated

during seizure and how the blockage is removed after prolonged activation of neurons. Besides, further evidences are needed to confirm that during seizure, in which types of neurons - excitatory or inhibitory - the translational downregulation of Syt I protein is taking place. Possible localization of Syt I-RNA complex formation within neurons will be critical in establishing this pathway. FRET analysis could be one of the methods to prove this concept. More over, it will be interesting to check the translation efficiency of Syt I protein with the 3' UTR RNA after creating mutations in the C2A domain of the protein as well the GU repeat and Heptamer sequences in the 3' UTR. Further studies on this unique pathway may provide important insight into the functional adaptation between molecules in the most dynamic cellular pathway.

Chapter 6

REFERENCES

1. Abe R, Yamamoto K and Sakamoto H. Target specificity of neuronal RNA-binding protein, Mel-N1: direct binding to the 3' untranslated region of its own mRNA. Nucleic Acids Res 1996; 24 (11): 2011-6.

2. Adolfsen B and Littleton JT. Genetic and molecular analysis of the synaptotagmin family. Cell Mol Life Sci 2001; 58 (3): 393-402.

3. Adolfsen B, Saraswati S, Yoshihara M and Littleton JT. Synaptotagmins are trafficked to distinct subcellular domains including the postsynaptic compartment. J Cell Biol 2004; 166 (2): 249-60.

4. Akai J, Kimura A and Hata RI. Transcriptional regulation of the human type I collagen alpha2 (COL1A2) gene by the combination of two dinucleotide repeats. Gene 1999; 239 (1): 65-73.

5. Arac D, Chen X, Khant HA, Ubach J, Ludtke SJ, Kikkawa M, Johnson AE, Chiu W, Sudhof TC and Rizo J. Close membrane-membrane proximity induced by Ca(2+)-dependent multivalent binding of synaptotagmin-1 to phospholipids. Nat Struct Mol Biol 2006; 13 (3): 209-17.

6. Augustine GJ, Burns ME, DeBello WM, Hilfiker S, Morgan JR, Schweizer FE, Tokumaru H and Umayahara K. Proteins involved in synaptic vesicle trafficking. J Physiol 1999; 520 Pt 1: 33-41.

7. Babity JM, Armstrong JN, Plumier JC, Currie RW and Robertson HA. A novel seizure-induced synaptotagmin gene identified by differential display. Proc Natl Acad Sci U S A 1997; 94 (6): 2638-41.

8. Bagala C, Kolev V, Mandinova A, Soldi R, Mouta C, Graziani I, Prudovsky I and Maciag T. The alternative translation of synaptotagmin 1 mediates the non-classical release of FGF1. Biochem Biophys Res Commun 2003; 310 (4): 1041-7.

9. Bai J, Wang P and Chapman ER. C2A activates a cryptic Ca(2+)-triggered membrane penetration activity within the C2B domain of synaptotagmin I. Proc Natl Acad Sci U S A 2002; 99 (3): 1665-70.

10. Bai J, Tucker WC and Chapman ER. PIP2 increases the speed of response of synaptotagmin and steers its membrane-penetration activity toward the plasma membrane. Nat Struct Mol Biol 2004a; 11 (1): 36-44.

11. Bai J, Wang CT, Richards DA, Jackson MB and Chapman ER. Fusion pore dynamics are regulated by synaptotagmin*t-SNARE interactions. Neuron 2004b; 41 (6): 929-42.

12. Bajjalieh SM. Synaptic vesicle docking and fusion. Curr Opin Neurobiol 1999; 9 (3): 321-8.

13. Banerjee A, Kowalchyk JA, DasGupta BR and Martin TF. SNAP-25 is required for a late postdocking step in Ca2+-dependent exocytosis. J Biol Chem 1996; 271 (34): 20227-30.

14. Baumann C, Otridge J and Gollnick P. Kinetic and thermodynamic analysis of the interaction between TRAP (trp RNA-binding attenuation protein) of Bacillus subtilis and trp leader RNA. J Biol Chem 1996; 271 (21): 12269-74.

15. Becker AJ, Chen J, Zien A, Sochivko D, Normann S, Schramm J, Elger CE, Wiestler OD and Blumcke I. Correlated stage- and subfield-associated hippocampal gene expression patterns in experimental and human temporal lobe epilepsy. Eur J Neurosci 2003; 18 (10): 2792-802.

16. Ben-Ari Y and Cossart R. Kainate, a double agent that generates seizures: two decades of progress. Trends Neurosci 2000; 23 (11): 580-7.

17. Bi X, Chang V, Siman R, Tocco G and Baudry M. Regional distribution and time-course of calpain activation following kainate-induced seizure activity in adult rat brain. Brain Res 1996; 726 (1-2): 98-108.

18. Blangy A, Leopold P, Vidal F, Rassoulzadegan M and Cuzin F. Recognition of the CDEI motif GTCACATG by mouse nuclear proteins and interference with the early development of the mouse embryo. Nucleic Acids Res 1991; 19 (25): 7243-50.

19. Bliss TV and Collingridge GL. A synaptic model of memory: long-term potentiation in the hippocampus. Nature 1993; 361 (6407): 31-9.

20. Bloom K, Hill A, Kenna M and Saunders M. The structure of a primitive kinetochore. Trends Biochem Sci 1989; 14 (6): 223-7.

21. Bommert K, Charlton MP, DeBello WM, Chin GJ, Betz H and Augustine GJ. Inhibition of neurotransmitter release by C2-domain peptides implicates synaptotagmin in exocytosis. Nature 1993; 363 (6425): 163-5.

22. Bowen ME, Weninger K, Ernst J, Chu S and Brunger AT. Single-molecule studies of synaptotagmin and complexin binding to the SNARE complex. Biophys J 2005; 89 (1): 690-702.

23. Brachya G, Yanay C and Linial M. Synaptic proteins as multi-sensor devices of neurotransmission. BMC Neurosci 2006; 7 Suppl 1: S4.

24. Bradford MM. A rapid and sensitive method for the quantitation of microgram quantities of protein utilizing the principle of protein-dye binding. Anal Biochem 1976; 72: 248-54.

25. Broadie KS and Richmond JE. Establishing and sculpting the synapse in Drosophila and C. elegans. Curr Opin Neurobiol 2002; 12 (5): 491-8.

26. Brose N, Petrenko AG, Sudhof TC and Jahn R. Synaptotagmin: a calcium sensor on the synaptic vesicle surface. Science 1992; 256 (5059): 1021-5.

27. Burre J and Volknandt W. The synaptic vesicle proteome. J Neurochem 2007; 101 (6): 1448-62.

28. Catterall WA. Interactions of presynaptic Ca2+ channels and snare proteins in neurotransmitter release. Ann N Y Acad Sci 1999; 868: 144-59.

29. Cavalheiro EA, Leite JP, Bortolotto ZA, Turski WA, Ikonomidou C and Turski L. Long-term effects of pilocarpine in rats: structural damage of the brain triggers kindling and spontaneous recurrent seizures. Epilepsia 1991; 32 (6): 778-82.

30. Ceccarelli B and Hurlbut WP. Vesicle hypothesis of the release of quanta of acetylcholine. Physiol Rev 1980; 60 (2): 396-441.

31. Chapman ER, Hanson PI, An S and Jahn R. Ca2+ regulates the interaction between synaptotagmin and syntaxin 1. J Biol Chem 1995; 270 (40): 23667-71.

32. Chapman ER, An S, Edwardson JM and Jahn R. A novel function for the second C2 domain of synaptotagmin. Ca2+- triggered dimerization. J Biol Chem 1996; 271 (10): 5844-9.

33. Chapman ER and Davis AF. Direct interaction of a Ca2+-binding loop of synaptotagmin with lipid bilayers. J Biol Chem 1998; 273 (22): 13995-4001.

34. Chapman ER, Desai RC, Davis AF and Tornehl CK. Delineation of the oligomerization, AP-2 binding, and synprint binding region of the C2B domain of synaptotagmin. J Biol Chem 1998; 273 (49): 32966-72.

35. Chapman ER. Synaptotagmin: a Ca(2+) sensor that triggers exocytosis? Nat Rev Mol Cell Biol 2002; 3 (7): 498-508.

36. Charvin N, L'Eveque C, Walker D, Berton F, Raymond C, Kataoka M, Shoji-Kasai Y, Takahashi M, De Waard M and Seagar MJ. Direct interaction of the calcium sensor protein synaptotagmin I with a cytoplasmic domain of the alpha1A subunit of the P/Q-type calcium channel. EMBO J 1997; 16 (15): 4591-6.

37. Chieregatti E, Chicka MC, Chapman ER and Baldini G. SNAP-23 functions in docking/fusion of granules at low Ca2+. Mol Biol Cell 2004; 15 (4): 1918-30.

38. Chomczynski P and Sacchi N. Single-step method of RNA isolation by acid guanidinium thiocyanate- phenol-chloroform extraction. Anal Biochem 1987; 162 (1): 156-9.

39. Craxton M. Genomic analysis of synaptotagmin genes. Genomics 2001; 77 (1-2): 43-9.

40. Craxton M. Synaptotagmin gene content of the sequenced genomes. BMC Genomics 2004; 5 (1): 43.

41. Crowder KM, Gunther JM, Jones TA, Hale BD, Zhang HZ, Peterson MR, Scheller RH, Chavkin C and Bajjalieh SM. Abnormal neurotransmission in mice lacking synaptic vesicle protein 2A (SV2A). Proc Natl Acad Sci U S A 1999; 96 (26): 15268-73.

42. Dai H, Shin OH, Machius M, Tomchick DR, Sudhof TC and Rizo J. Structural basis for the evolutionary inactivation of Ca2+ binding to synaptotagmin 4. Nat Struct Mol Biol 2004; 11 (9): 844-9.

43. Daly C and Ziff EB. Post-transcriptional regulation of synaptic vesicle protein expression and the developmental control of synaptic vesicle formation. J Neurosci 1997; 17 (7): 2365-75.

44. Damer CK and Creutz CE. Calcium-dependent self-association of synaptotagmin I. J Neurochem 1996; 67 (4): 1661-8.

45. Davis AF, Bai J, Fasshauer D, Wolowick MJ, Lewis JL and Chapman ER. Kinetics of synaptotagmin responses to Ca2+ and assembly with the core SNARE complex onto membranes. Neuron 1999; 24 (2): 363-76.

46. Davletov BA and Sudhof TC. A single C2 domain from synaptotagmin I is sufficient for high affinity Ca2+/phospholipid binding. J Biol Chem 1993; 268 (35): 26386-90.

47. Davletov BA and Sudhof TC. Ca(2+)-dependent conformational change in synaptotagmin I. J Biol Chem 1994; 269 (46): 28547-50.

48. Desai RC, Vyas B, Earles CA, Littleton JT, Kowalchyck JA, Martin TF and Chapman ER. The C2B domain of synaptotagmin is a Ca(2+)-sensing module essential for exocytosis. J Cell Biol 2000; 150 (5): 1125-36.

49. Deutch AY and Roth RH. Neurotransmitters. In: Zigmond M, Bloom, FE, Landis, SC, Roberts, JL, Squire, LR, editor. Fundamental Neuroscience. California: Academic Press, 1999:193-233.

50. DiAntonio A and Schwarz TL. The effect on synaptic physiology of synaptotagmin mutations in Drosophila. Neuron 1994; 12 (4): 909-20.

51. Dodge FA, Jr. and Rahamimoff R. Co-operative action a calcium ions in transmitter release at the neuromuscular junction. J Physiol 1967; 193 (2): 419-32.

52. Eccles JC. The synapse: from electrical to chemical transmission. Annu Rev Neurosci 1982; 5: 325-39.

53. Engel J and Pedley TA. Epilepsy: A Comprehensive Textbook. Philadelphia: Lippincott-Raven 1997.

54. Ernst JA and Brunger AT. High resolution structure, stability, and synaptotagmin binding of a truncated neuronal SNARE complex. J Biol Chem 2003; 278 (10): 8630-6.

55. Fasshauer D, Antonin W, Subramaniam V and Jahn R. SNARE assembly and disassembly exhibit a pronounced hysteresis. Nat Struct Biol 2002; 9 (2): 144-51.

56. Feany MB and Buckley KM. The synaptic vesicle protein synaptotagmin promotes formation of filopodia in fibroblasts. Nature 1993; 364 (6437): 537-40.

57. Ferguson GD, Thomas DM, Elferink LA and Herschman HR. Synthesis degradation, and subcellular localization of synaptotagmin IV, a neuronal immediate early gene product. J Neurochem 1999; 72 (5): 1821-31.

58. Fernandez-Chacon R, Konigstorfer A, Gerber SH, Garcia J, Matos MF, Stevens CF, Brose N, Rizo J, Rosenmund C and Sudhof TC. Synaptotagmin I

functions as a calcium regulator of release probability. Nature 2001; 410 (6824): 41-9.

59. Fesce R, Grohovaz F, Valtorta F and Meldolesi J. Neurotransmitter release: fusion or 'kiss-and-run'? Trends Cell Biol 1994; 4 (1): 1-4.

60. Folch J. Brain cephalin, a mixture of phosphatides. Separation from it of phosphatidyl serine, phosphatidyl ethanolamine, and fraction containing an inositol phosphatide. J. Biol. Chem. 1942; 146: 35-44.

61. Fukuda M, Aruga J, Niinobe M, Aimoto S and Mikoshiba K. Inositol-1,3,4,5-tetrakisphosphate binding to C2B domain of IP4BP/synaptotagmin II. J Biol Chem 1994; 269 (46): 29206-11.

62. Fukuda M, Moreira JE, Lewis FM, Sugimori M, Niinobe M, Mikoshiba K and Llinas R. Role of the C2B domain of synaptotagmin in vesicular release and recycling as determined by specific antibody injection into the squid giant synapse preterminal. Proc Natl Acad Sci U S A 1995; 92 (23): 10708-12.

63. Fukuda M, Kanno E and Mikoshiba K. Conserved N-terminal cysteine motif is essential for homo- and heterodimer formation of synaptotagmins III, V, VI, and X. J Biol Chem 1999; 274 (44): 31421-7.

64. Fukuda M, Kabayama H and Mikoshiba K. Drosophila AD3 mutation of synaptotagmin impairs calcium-dependent self-oligomerization activity. FEBS Lett 2000a; 482 (3): 269-72.

65. Fukuda M and Mikoshiba K. Calcium-dependent and -independent hetero-oligomerization in the synaptotagmin family. J Biochem (Tokyo) 2000; 128 (4): 637-45.

66. Fukuda M, Moreira JE, Liu V, Sugimori M, Mikoshiba K and Llinas RR. Role of the conserved WHXL motif in the C terminus of synaptotagmin in synaptic vesicle docking. Proc Natl Acad Sci U S A 2000b; 97 (26): 14715-9.

67. Fukuda M, Kanno E, Ogata Y and Mikoshiba K. Mechanism of the SDS-resistant synaptotagmin clustering mediated by the cysteine cluster at the interface between the transmembrane and spacer domains. J Biol Chem 2001; 276 (43): 40319-25.

68. Fukuda M. Molecular cloning, expression, and characterization of a novel class of synaptotagmin (Syt XIV) conserved from Drosophila to humans. J Biochem 2003a; 133 (5): 641-9.

69. Fukuda M. Molecular cloning and characterization of human, rat, and mouse synaptotagmin XV. Biochem Biophys Res Commun 2003b; 306 (1): 64-71.

70. Gao PS, Heller NM, Walker W, Chen CH, Moller M, Plunkett B, Roberts MH, Schleimer RP, Hopkin JM and Huang SK. Variation in dinucleotide (GT) repeat sequence in the first exon of the STAT6 gene is associated with atopic asthma and differentially regulates the promoter activity in vitro. J Med Genet 2004; 41 (7): 535-9.

71. Geppert M, Goda Y, Hammer RE, Li C, Rosahl TW, Stevens CF and Sudhof TC. Synaptotagmin I: a major Ca2+ sensor for transmitter release at a central synapse. Cell 1994; 79 (4): 717-27.

72. Giraudo CG, Eng WS, Melia TJ and Rothman JE. A clamping mechanism involved in SNARE-dependent exocytosis. Science 2006; 313 (5787): 676-80.

73. Granseth B, Odermatt B, Royle SJ and Lagnado L. Clathrin-mediated endocytosis is the dominant mechanism of vesicle retrieval at hippocampal synapses. Neuron 2006; 51 (6): 773-86.

74. Grass I, Thiel S, Honing S and Haucke V. Recognition of a basic AP-2 binding motif within the C2B domain of synaptotagmin is dependent on multimerization. J Biol Chem 2004; 279 (52): 54872-80.

75. Greif KF and Trenchard H. Neonatal deafferentation prevents normal expression of synaptic vesicle antigens in the developing rat superior cervical ganglion. Synapse 1988; 2 (1): 1-6.

76. Greif KF. 3',5'-cyclic adenosine monophosphate regulates expression of synaptotagmin in neonatal sympathetic ganglia in vitro. J Neurobiol 2001; 46 (4): 281-8.

77. Hadjiyannakis S, Zheng H, Hendy GN and Goodyer CG. GT repeat polymorphism in the 5' flanking region of the human growth hormone receptor gene. Mol Cell Probes 2001; 15 (4): 239-42.

78. Hagler DJ, Jr. and Goda Y. Properties of synchronous and asynchronous release during pulse train depression in cultured hippocampal neurons. J Neurophysiol 2001; 85 (6): 2324-34.

79. Hall KB KJ. Nitrocellulose filter binding for determination of dissociation constants. Methods Mol Biol 1999; 118 105-114.

80. Han W, Rhee JS, Maximov A, Lao Y, Mashimo T, Rosenmund C and Sudhof TC. N-glycosylation is essential for vesicular targeting of synaptotagmin 1. Neuron 2004; 41 (1): 85-99.

81. Hanna MM, Bentsen L, Lucido M and Sapre A. RNA-protein cross linking with photoreactive nucleotide analogs. Methods Mol Biol 1999; 118: 21-33.

82. Harlow E and Lane D. Antibodies: a laboratory manual. Cold Spring Harbor: Cold Spring Harbor Laboratory., 1988.

83. He L and Wu LG. The debate on the kiss-and-run fusion at synapses. Trends Neurosci 2007; 30 (9): 447-55.

84. Heidelberger R, Heinemann C, Neher E and Matthews G. Calcium dependence of the rate of exocytosis in a synaptic terminal. Nature 1994; 371 (6497): 513-5.

85. Heuser JE and Reese TS. Evidence for recycling of synaptic vesicle membrane during transmitter release at the frog neuromuscular junction. J Cell Biol 1973; 57 (2): 315-44.

86. Hirokawa N and Takemura R. Molecular motors and mechanisms of directional transport in neurons. Nat Rev Neurosci 2005; 6 (3): 201-14.

87. Hirokawa N. mRNA transport in dendrites: RNA granules, motors, and tracks. J Neurosci 2006; 26 (27): 7139-42.

88. Itakura M, Misawa H, Sekiguchi M, Takahashi S and Takahashi M. Transfection analysis of functional roles of complexin I and II in the exocytosis of two different types of secretory vesicles. Biochem Biophys Res Commun 1999; 265 (3): 691-6.

89. Jahn R, Lang T and Sudhof TC. Membrane fusion. Cell 2003; 112 (4): 519-33.

90. Jarousse N and Kelly RB. Endocytotic mechanisms in synapses. Curr Opin Cell Biol 2001; 13 (4): 461-9.

91. Jorgensen EM, Hartwieg E, Schuske K, Nonet ML, Jin Y and Horvitz HR. Defective recycling of synaptic vesicles in synaptotagmin mutants of Caenorhabditis elegans. Nature 1995; 378 (6553): 196-9.

92. Kang R, Swayze R, Lise MF, Gerrow K, Mullard A, Honer WG and El-Husseini A. Presynaptic trafficking of synaptotagmin I is regulated by protein palmitoylation. J Biol Chem 2004; 279 (48): 50524-36.

93. Kato K, Katoh-Semba R, Takeuchi IK, Ito H and Kamei K. Responses of heat shock proteins hsp27, alphaB-crystallin, and hsp70 in rat brain after kainic acid-induced seizure activity. J Neurochem 1999; 73 (1): 229-36.

94. Katz B. The Release of Neural Transmitter Substances Liverpool: Liverpool University Press, 1969.

95. Kim DK and Catterall WA. Ca2+-dependent and -independent interactions of the isoforms of the alpha1A subunit of brain Ca2+ channels with presynaptic SNARE proteins. Proc Natl Acad Sci U S A 1997; 94 (26): 14782-6.

96. Koenig E and Giuditta A. Protein-synthesizing machinery in the axon compartment. Neuroscience 1999; 89 (1): 5-15.

97. Krasnov PA and Enikolopov G. Targeting of synaptotagmin to neurite terminals in neuronally differentiated PC12 cells. J Cell Sci 2000; 113 (Pt 8): 1389-404.

98. Krauss M, Kinuta M, Wenk MR, De Camilli P, Takei K and Haucke V. ARF6 stimulates clathrin/AP-2 recruitment to synaptic membranes by activating phosphatidylinositol phosphate kinase type Igamma. J Cell Biol 2003; 162 (1): 113-24.

99. LaVallee TM, Tarantini F, Gamble S, Mouta Carreira C, Jackson A and Maciag T. Synaptotagmin-1 is required for fibroblast growth factor-1 release. J Biol Chem 1998; 273 (35): 22217-23.

100. Lazzell DR, Belizaire R, Thakur P, Sherry DM and Janz R. SV2B regulates synaptotagmin 1 by direct interaction. J Biol Chem 2004; 279 (50): 52124-31.

101. Li C, Ullrich B, Zhang JZ, Anderson RG, Brose N and Sudhof TC. Ca(2+)-dependent and -independent activities of neural and non-neural synaptotagmins. Nature 1995; 375 (6532): 594-9.

102. Li L, Shin OH, Rhee JS, Arac D, Rah JC, Rizo J, Sudhof T and Rosenmund C. Phosphatidylinositol phosphates as co-activators of Ca2+ binding to C2 domains of synaptotagmin 1. J Biol Chem 2006; 281 (23): 15845-52.

103. Lin RC and Scheller RH. Mechanisms of synaptic vesicle exocytosis. Annu Rev Cell Dev Biol 2000; 16: 19-49.

104. Littleton JT, Stern M, Schulze K, Perin M and Bellen HJ. Mutational analysis of Drosophila synaptotagmin demonstrates its essential role in Ca(2+)-activated neurotransmitter release [see comments]. Cell 1993; 74 (6): 1125-34.

105. Littleton JT, Stern M, Perin M and Bellen HJ. Calcium dependence of neurotransmitter release and rate of spontaneous vesicle fusions are altered in Drosophila synaptotagmin mutants. Proc Natl Acad Sci U S A 1994; 91 (23): 10888-92.

106. Littleton JT, Serano TL, Rubin GM, Ganetzky B and Chapman ER. Synaptic function modulated by changes in the ratio of synaptotagmin I and IV. Nature 1999; 400 (6746): 757-60.

107. Littleton JT, Bai J, Vyas B, Desai R, Baltus AE, Garment MB, Carlson SD, Ganetzky B and Chapman ER. Synaptotagmin mutants reveal essential functions for the C2B domain in Ca2+-triggered fusion and recycling of synaptic vesicles in vivo. J Neurosci 2001; 21 (5): 1421-33.

108. Liu MC, Akle V, Zheng W, Dave JR, Tortella FC, Hayes RL and Wang KK. Comparing calpain- and caspase-3-mediated degradation patterns in traumatic brain injury by differential proteome analysis. Biochem J 2006; 394 (Pt 3): 715-25.

109. Livak KJ and Schmittgen TD. Analysis of relative gene expression data using real-time quantitative PCR and the 2(-Delta Delta C(T)) Method. Methods 2001; 25 (4): 402-8.

110. Llinas R, Steinberg IZ and Walton K. Presynaptic calcium currents in squid giant synapse. Biophys J 1981; 33 (3): 289-321.

111. Llinas R, Sugimori M and Silver RB. Microdomains of high calcium concentration in a presynaptic terminal. Science 1992; 256 (5057): 677-9.

112. Lou XJ and Bixby JL. Patterns of presynaptic gene expression define two stages of synaptic differentiation. Mol Cell Neurosci 1995; 6 (3): 252-62.

113. Lyubimova A, Bershadsky AD and Ben-Ze'ev A. Autoregulation of actin synthesis requires the 3'-UTR of actin mRNA and protects cells from actin overproduction. J Cell Biochem 1999; 76 (1): 1-12.

114. Machado HB, Liu W, Vician LJ and Herschman HR. Synaptotagmin IV overexpression inhibits depolarization-induced exocytosis in PC12 cells. J Neurosci Res 2004; 76 (3): 334-41.

115. Mackler JM, Drummond JA, Loewen CA, Robinson IM and Reist NE. The C(2)B Ca(2+)-binding motif of synaptotagmin is required for synaptic transmission in vivo. Nature 2002; 418 (6895): 340-4.

116. Mahata SK, Marksteiner J, Sperk G, Mahata M, Gruber B, Fischer-Colbrie R and Winkler H. Temporal lobe epilepsy of the rat: differential expression of mRNAs of chromogranin B, secretogranin II, synaptin/synaptophysin and p65 in subfield of the hippocampus. Brain Res Mol Brain Res 1992; 16 (1-2): 1-12.

117. Majores M, Eils J, Wiestler OD and Becker AJ. Molecular profiling of temporal lobe epilepsy: comparison of data from human tissue samples and animal models. Epilepsy Res 2004; 60 (2-3): 173-8.

118. Marek KW and Davis GW. Transgenically encoded protein photoinactivation (FlAsH-FALI): acute inactivation of synaptotagmin I. Neuron 2002; 36 (5): 805-13.

119. Marqueze B, Berton F and Seagar M. Synaptotagmins in membrane traffic: which vesicles do the tagmins tag? Biochimie 2000; 82 (5): 409-20.

120. McKeown MJ and McNamara JO. When do epileptic seizures really begin? Neuron 2001; 30 (1): 1-3.

121. McMahon HT, Missler M, Li C and Sudhof TC. Complexins: cytosolic proteins that regulate SNAP receptor function. Cell 1995; 83 (1): 111-9.

122. Mello LE, Cavalheiro EA, Tan AM, Kupfer WR, Pretorius JK, Babb TL and Finch DM. Circuit mechanisms of seizures in the pilocarpine model of chronic epilepsy: cell loss and mossy fiber sprouting. Epilepsia 1993; 34 (6): 985-95.

123. Morimoto T, Wang XH and Poo MM. Overexpression of synaptotagmin modulates short-term synaptic plasticity at developing neuromuscular junctions. Neuroscience 1998; 82 (4): 969-78.

124. Mousavi SA, Malerod L, Berg T and Kjeken R. Clathrin-dependent endocytosis. Biochem J 2004; 377 (Pt 1): 1-16.

125. Mundigl O, Matteoli M, Daniell L, Thomas-Reetz A, Metcalf A, Jahn R and De Camilli P. Synaptic vesicle proteins and early endosomes in cultured hippocampal neurons: differential effects of Brefeldin A in axon and dendrites. J Cell Biol 1993; 122 (6): 1207-21.

126. Murthy VN and De Camilli P. Cell biology of the presynaptic terminal. Annu Rev Neurosci 2003; 26: 701-28.

127. Myers SJ, Huang Y, Genetta T and Dingledine R. Inhibition of glutamate receptor 2 translation by a polymorphic repeat sequence in the 5'-untranslated leaders. J Neurosci 2004; 24 (14): 3489-99.

128. Nicholson-Tomishima K and Ryan TA. Kinetic efficiency of endocytosis at mammalian CNS synapses requires synaptotagmin I. Proc Natl Acad Sci U S A 2004; 101 (47): 16648-52.

129. Nonet ML, Grundahl K, Meyer BJ and Rand JB. Synaptic function is impaired but not eliminated in C. elegans mutants lacking synaptotagmin. Cell 1993; 73 (7): 1291-305.

130. Ono S, Baux G, Sekiguchi M, Fossier P, Morel NF, Nihonmatsu I, Hirata K, Awaji T, Takahashi S and Takahashi M. Regulatory roles of complexins in

neurotransmitter release from mature presynaptic nerve terminals. Eur J Neurosci 1998; 10 (6): 2143-52.

131. Osborne SL, Herreros J, Bastiaens PI and Schiavo G. Calcium-dependent oligomerization of synaptotagmins I and II. Synaptotagmins I and II are localized on the same synaptic vesicle and heterodimerize in the presence of calcium. J Biol Chem 1999; 274 (1): 59-66.

132. Pabst S, Margittai M, Vainius D, Langen R, Jahn R and Fasshauer D. Rapid and selective binding to the synaptic SNARE complex suggests a modulatory role of complexins in neuroexocytosis. J Biol Chem 2002; 277 (10): 7838-48.

133. Pang ZP, Shin OH, Meyer AC, Rosenmund C and Sudhof TC. A gain-of-function mutation in synaptotagmin-1 reveals a critical role of Ca2+-dependent soluble N-ethylmaleimide-sensitive factor attachment protein receptor complex binding in synaptic exocytosis. J Neurosci 2006; 26 (48): 12556-65.

134. Perin MS, Fried VA, Mignery GA, Jahn R and Sudhof TC. Phospholipid binding by a synaptic vesicle protein homologous to the regulatory region of protein kinase C. Nature 1990; 345 (6272): 260-3.

135. Perin MS, Brose N, Jahn R and Sudhof TC. Domain structure of synaptotagmin (p65). J Biol Chem 1991a; 266 (1): 623-9.

136. Perin MS, Johnston PA, Ozcelik T, Jahn R, Francke U and Sudhof TC. Structural and functional conservation of synaptotagmin (p65) in Drosophila and humans. J Biol Chem 1991b; 266 (1): 615-22.

137. Porter BE, Cui XN and Brooks-Kayal AR. Status epilepticus differentially alters AMPA and kainate receptor subunit expression in mature and immature dentate granule neurons. Eur J Neurosci 2006; 23 (11): 2857-63.

138. Reim K, Mansour M, Varoqueaux F, McMahon HT, Sudhof TC, Brose N and Rosenmund C. Complexins regulate a late step in Ca2+-dependent neurotransmitter release. Cell 2001; 104 (1): 71-81.

139. Reist NE, Buchanan J, Li J, DiAntonio A, Buxton EM and Schwarz TL. Morphologically docked synaptic vesicles are reduced in synaptotagmin mutants of Drosophila. J Neurosci 1998; 18 (19): 7662-73.

140. Rhee JS, Li LY, Shin OH, Rah JC, Rizo J, Sudhof TC and Rosenmund C. Augmenting neurotransmitter release by enhancing the apparent Ca2+ affinity of synaptotagmin 1. Proc Natl Acad Sci U S A 2005; 102 (51): 18664-9.

141. Rice AC and DeLorenzo RJ. NMDA receptor activation during status epilepticus is required for the development of epilepsy. Brain Res 1998; 782 (1-2): 240-7.

142. Rickman C and Davletov B. Mechanism of calcium-independent synaptotagmin binding to target SNAREs. J Biol Chem 2003; 278 (8): 5501-4.

143. Rickman C, Archer DA, Meunier FA, Craxton M, Fukuda M, Burgoyne RD and Davletov B. Synaptotagmin interaction with the syntaxin/SNAP-25 dimer is mediated by an evolutionarily conserved motif and is sensitive to inositol hexakisphosphate. J Biol Chem 2004; 279 (13): 12574-9.

144. Rizo J and Sudhof TC. C2-domains, structure and function of a universal Ca2+-binding domain. J Biol Chem 1998; 273 (26): 15879-82.

145. Robinson IM, Ranjan R and Schwarz TL. Synaptotagmins I and IV promote transmitter release independently of Ca(2+) binding in the C(2)A domain. Nature 2002; 418 (6895): 336-40.

146. Ryan TA and Smith SJ. Vesicle pool mobilization during action potential firing at hippocampal synapses. Neuron 1995; 14 (5): 983-9.

147. Ryan TA. Inhibitors of myosin light chain kinase block synaptic vesicle pool mobilization during action potential firing. J Neurosci 1999; 19 (4): 1317-23.

148. Sabatini BL and Regehr WG. Timing of neurotransmission at fast synapses in the mammalian brain. Nature 1996; 384 (6605): 170-2.

149. Sambrook J and Russel DW. Molecular cloning a laboratory manual. 3 ed. New York: Cold Spring Harbor Laboratory Press, 2001.

150. Samson ML. Evidence for 3' untranslated region-dependent autoregulation of the Drosophila gene encoding the neuronal nuclear RNA-binding protein ELAV. Genetics 1998; 150 (2): 723-33.

151. Sandberg R, Yasuda R, Pankratz DG, Carter TA, Del Rio JA, Wodicka L, Mayford M, Lockhart DJ and Barlow C. Regional and strain-specific gene expression mapping in the adult mouse brain. Proc Natl Acad Sci U S A 2000; 97 (20): 11038-43.

152. Schaub JR, Lu X, Doneske B, Shin YK and McNew JA. Hemifusion arrest by complexin is relieved by Ca2+-synaptotagmin I. Nat Struct Mol Biol 2006; 13 (8): 748-50.

153. Schiavo G, Stenbeck G, Rothman JE and Sollner TH. Binding of the synaptic vesicle v-SNARE, synaptotagmin, to the plasma membrane t-SNARE, SNAP-

25, can explain docked vesicles at neurotoxin-treated synapses. Proc Natl Acad Sci U S A 1997; 94 (3): 997-1001.

154. Schuldiner S, Shirvan A and Linial M. Vesicular neurotransmitter transporters: from bacteria to humans. Physiol Rev 1995; 75 (2): 369-92.

155. Setzer DR. Measuring equilibrium and kinetic constants using gel retardation assays. Methods Mol Biol 1999; 118: 115-128.

156. Sheng M and Greenberg ME. The regulation and function of c-fos and other immediate early genes in the nervous system. Neuron 1990; 4 (4): 477-85.

157. Sheng ZH, Yokoyama CT and Catterall WA. Interaction of the synprint site of N-type Ca2+ channels with the C2B domain of synaptotagmin I. Proc Natl Acad Sci U S A 1997; 94 (10): 5405-10.

158. Sollner T, Bennett MK, Whiteheart SW, Scheller RH and Rothman JE. A protein assembly-disassembly pathway in vitro that may correspond to sequential steps of synaptic vesicle docking, activation, and fusion. Cell 1993; 75 (3): 409-18.

159. Stevens CF and Sullivan JM. The synaptotagmin C2A domain is part of the calcium sensor controlling fast synaptic transmission. Neuron 2003; 39 (2): 299-308.

160. Sudhof TC. The synaptic vesicle cycle: a cascade of protein-protein interactions. Nature 1995; 375 (6533): 645-53.

161. Sudhof TC and Rizo J. Synaptotagmins: C2-domain proteins that regulate membrane traffic. Neuron 1996; 17 (3): 379-88.

162. Sudhof TC. Synaptotagmins: why so many? J Biol Chem 2002; 277 (10): 7629-32.

163. Sudhof TC. The synaptic vesicle cycle. Annu Rev Neurosci 2004; 27: 509-47.

164. Sugita S, Hata Y and Sudhof TC. Distinct Ca(2+)-dependent properties of the first and second C2-domains of synaptotagmin I. J Biol Chem 1996; 271 (3): 1262-5.

165. Sutton RB, Davletov BA, Berghuis AM, Sudhof TC and Sprang SR. Structure of the first C2 domain of synaptotagmin I: a novel Ca2+/phospholipid-binding fold. Cell 1995; 80 (6): 929-38.

166. Sutula TP. Secondary epileptogenesis, kindling, and intractable epilepsy: a reappraisal from the perspective of neural plasticity. Int Rev Neurobiol 2001; 45: 355-86.

167. Tamura K, Arakawa H, Suzuki M, Kobayashi Y, Mochizuki H, Kato M, Tokuyama K and Morikawa A. Novel dinucleotide repeat polymorphism in the first exon of the STAT-6 gene is associated with allergic diseases. Clin Exp Allergy 2001; 31 (10): 1509-14.

168. Tang J, Maximov A, Shin OH, Dai H, Rizo J and Sudhof TC. A complexin/synaptotagmin 1 switch controls fast synaptic vesicle exocytosis. Cell 2006; 126 (6): 1175-87.

169. Ting JT, Kelley BG and Sullivan JM. Synaptotagmin IV does not alter excitatory fast synaptic transmission or fusion pore kinetics in mammalian CNS neurons. J Neurosci 2006; 26 (2): 372-80.

170. Tocco G, Bi X, Vician L, Lim IK, Herschman H and Baudry M. Two synaptotagmin genes, Syt1 and Syt4, are differentially regulated in adult brain and during postnatal development following kainic acid-induced seizures. Brain Res Mol Brain Res 1996; 40 (2): 229-39.

171. Tsang VC, Peralta JM and Simons AR. Enzyme-linked immunoelectrotransfer blot techniques (EITB) for studying the specificities of antigens and antibodies separated by gel electrophoresis. Methods Enzymol 1983; 92: 377-91.

172. Tsirka SE, Gualandris A, Amaral DG and Strickland S. Excitotoxin-induced neuronal degeneration and seizure are mediated by tissue plasminogen activator. Nature 1995; 377 (6547): 340-4.

173. Tucker WC and Chapman ER. Role of synaptotagmin in Ca2+-triggered exocytosis. Biochem J 2002; 366 (Pt 1): 1-13.

174. Tucker WC, Edwardson JM, Bai J, Kim HJ, Martin TF and Chapman ER. Identification of synaptotagmin effectors via acute inhibition of secretion from cracked PC12 cells. J Cell Biol 2003; 162 (2): 199-209.

175. Ubach J, Lao Y, Fernandez I, Arac D, Sudhof TC and Rizo J. The C2B domain of synaptotagmin I is a Ca2+-binding module. Biochemistry 2001; 40 (20): 5854-60.

176. Ullrich B, Li C, Zhang JZ, McMahon H, Anderson RG, Geppert M and Sudhof TC. Functional properties of multiple synaptotagmins in brain. Neuron 1994; 13 (6): 1281-91.

177. Vician L, Lim IK, Ferguson G, Tocco G, Baudry M and Herschman HR. Synaptotagmin IV is an immediate early gene induced by depolarization in PC12 cells and in brain. Proc Natl Acad Sci U S A 1995; 92 (6): 2164-8.

178. Vidal F, Blangy A, Rassoulzadegan M and Cuzin F. A murine sequence-specific DNA binding protein shows extensive local similarities to the amyloid precursor protein. Biochem Biophys Res Commun 1992; 189 (3): 1336-41.

179. von Poser C, Ichtchenko K, Shao X, Rizo J and Sudhof TC. The evolutionary pressure to inactivate. A subclass of synaptotagmins with an amino acid substitution that abolishes Ca2+ binding. J Biol Chem 1997; 272 (22): 14314-9.

180. Walz R, Amaral OB, Rockenbach IC, Roesler R, Izquierdo I, Cavalheiro EA, Martins VR and Brentani RR. Increased sensitivity to seizures in mice lacking cellular prion protein. Epilepsia 1999; 40 (12): 1679-82.

181. Wang CT, Grishanin R, Earles CA, Chang PY, Martin TF, Chapman ER and Jackson MB. Synaptotagmin modulation of fusion pore kinetics in regulated exocytosis of dense-core vesicles. Science 2001; 294 (5544): 1111-5.

182. Wang H and Chong S. Visualization of coupled protein folding and binding in bacteria and purification of the heterodimeric complex. Proc Natl Acad Sci U S A 2003; 100 (2): 478-83.

183. Wilkie GS, Dickson KS and Gray NK. Regulation of mRNA translation by 5'- and 3'-UTR-binding factors. Trends Biochem Sci 2003; 28 (4): 182-8.

184. Wu Y, He Y, Bai J, Ji SR, Tucker WC, Chapman ER and Sui SF. Visualization of synaptotagmin I oligomers assembled onto lipid monolayers. Proc Natl Acad Sci U S A 2003; 100 (4): 2082-7.

185. Yang JW, Czech T, Felizardo M, Baumgartner C and Lubec G. Aberrant expression of cytoskeleton proteins in hippocampus from patients with mesial temporal lobe epilepsy. Amino Acids 2006; 30 (4): 477-93.

186. Yoshihara M, Ueda A, Zhang D, Deitcher DL, Schwarz TL and Kidokoro Y. Selective effects of neuronal-synaptobrevin mutations on transmitter release evoked by sustained versus transient Ca2+ increases and by cAMP. J Neurosci 1999; 19 (7): 2432-41.

187. Yoshihara M and Littleton JT. Synaptotagmin I functions as a calcium sensor to synchronize neurotransmitter release. Neuron 2002; 36 (5): 897-908.

188. Yoshihara M and Montana ES. The synaptotagmins: calcium sensors for vesicular trafficking. Neuroscientist 2004; 10 (6): 566-74.

189. Zehner ZE, Shepherd RK, Gabryszuk J, Fu TF, Al-Ali M and Holmes WM. RNA-protein interactions within the 3 ' untranslated region of vimentin mRNA. Nucleic Acids Res 1997; 25 (16): 3362-70.

190. Zhang JZ, Davletov BA, Sudhof TC and Anderson RG. Synaptotagmin I is a high affinity receptor for clathrin AP-2: implications for membrane recycling. Cell 1994; 78 (5): 751-60.

191. Zhen M and Jin Y. Presynaptic terminal differentiation: transport and assembly. Curr Opin Neurobiol 2004; 14 (3): 280-7.

192. Ziv NE and Garner CC. Cellular and molecular mechanisms of presynaptic assembly. Nat Rev Neurosci 2004; 5 (5): 385-99.